GEOLOGICAL SURVEY OF CANADA
OPEN FILE 7143

Assessment of Telluric Activity in Mackenzie Valley Area

L. Trichtchenko and P. Fernberg

2012

Natural Resources Canada | Ressources naturelles Canada

Canada

GEOLOGICAL SURVEY OF CANADA
OPEN FILE 7143

Assessment of Telluric Activity in Mackenzie Valley Area

L. Trichtchenko and P. Fernberg

2012

doi:10.4095/291562

This publication is available from the Geological Survey of Canada Bookstore
(http://gsc.nrcan.gc.ca/bookstore_e.php).
It can also be downloaded free of charge from GeoPub (http://geopub.nrcan.gc.ca/).

Recommended citation:
Trichtchenko, L. and Fernberg P., 2012, Assessment of Telluric Activity in Mackenzie Valley Area,
Geological Survey of Canada, Open File 7143, 127 p. doi:10.4095/291562

Publications in this series have not been edited; they are released as submitted by the authors.

For more information related to this document please contact

Larisa Trichtchenko
Research Scientist
Geomagnetic Laboratory
2617 Anderson Road
Ottawa, ON
K1A 0E7

Tel: 613-837-9452
Fax: 613-824-9803
Email: ltrichtc@nrcan.gc.ca

Table of Contents

Executive Summary

E 1. Introduction

Pipelines are affected by telluric currents that cause variations of pipe-to-soil potentials, disrupting close-interval surveys and compromising the performance of cathodic protection. Telluric activity is associated with (produced by) geomagnetic variations which are more intense in the Northern Canada, thus the importance of this assessment for planned pipeline in the Mackenzie Valley area.
There are three factors contributing to the telluric effects on variations of pipe-to-soil potential: geomagnetic activity, ground resistivity and pipeline electrical properties and topology (Fig. E1). The report is concerned with the geomagnetic and telluric activity as characteristics of the natural environment and only briefly mentioned the pipeline modeling.

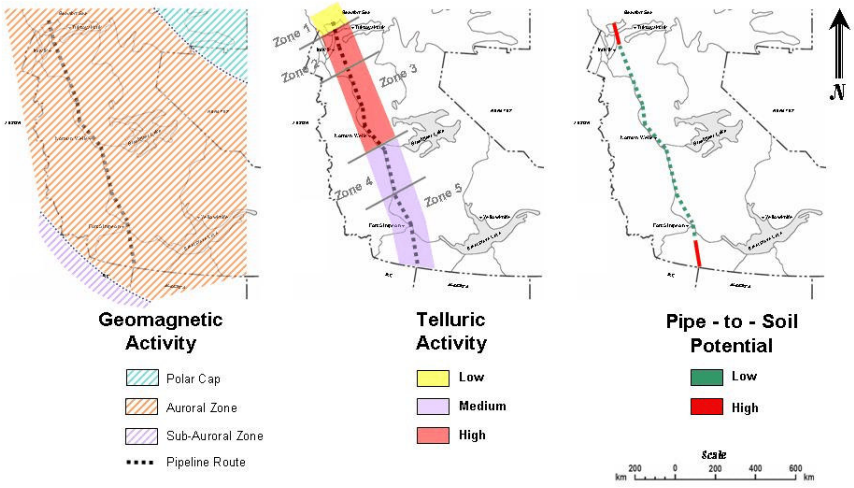

Fig. E1. Methodology of the telluric impact assessment on pipeline in Mackenzie area
Pipe-to-soil potential evaluations are not included in this report.

E 2. Geomagnetic Climatology

To analyse the occurrence of geomagnetic activity in the Mackenzie Valley we have used hourly ranges of the geomagnetic field variations recorded at the nearby Yellowknife Magnetic Observatory. We have examined the occurrence of the hourly ranges in 20 nano-Tesla (nT) bins for 30 years:1975 to 2004 (Chapter 2). These results show that the occurrence patterns are very similar each year with higher occurrence rates at low hourly range values and the occurrence rate falling off with increasing size of the hourly range value (Fig. E2).

To illustrate that greater geomagnetic activity occurs in the auroral zone we also analysed hourly range values for 2004 from Ottawa Magnetic Observatory in the sub-auroral zone. The results from Ottawa show that most of the time (95%) the magnetic activity is low with hourly ranges less than 40 nT. In contrast, at the auroral zone (Yellowknife) the "95%" level occurs at 300 nT while acvity is lower than 40 nT only about 40% of the year. Thus for the significant part of the time (55%) the geomagnetic activity in Yellowknife and surrounding area is in the "moderate" category with hourly range values between 40 nT and 300 nT.

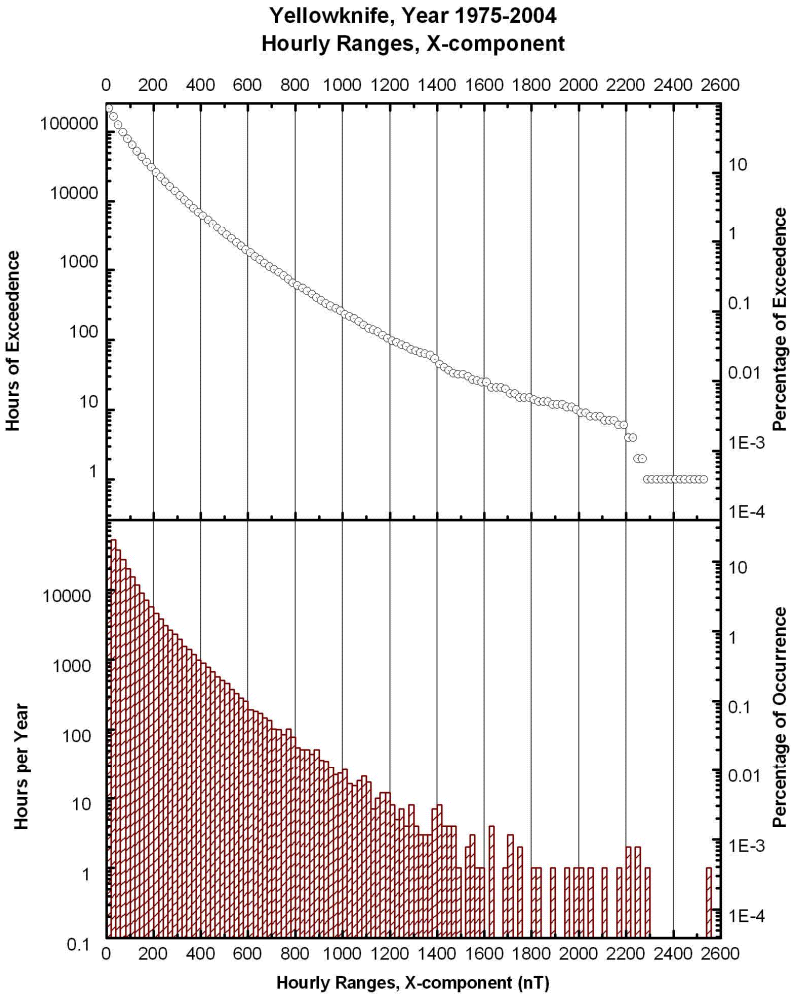

Fig. E2. Histogram and hours of exceedence of HRX in Yellowknife in 1975-2004.

E 3. Earth Conductivity Structure

To develop earth conductivity models for different areas along the pipeline route we reviewed the published literature concerning the geology of the area and resistivity of different layers. This study extended to the conductivities of the deeper crust and mantle of the earth because of the deep penetration of the low frequency geomagnetic variations. A particular feature of the work was also an investigation of the permafrost along the pipeline route.

The resistivity structure along the pipeline route was divided into five zones (Chapter 3), based initially on the extent of permafrost, however deeper structural differences between zones were also found. Zone 1, at the northern part, is characterized by a thick layer of surficial sediments beneath surface permafrost. Zone 2 is a region of continuous permafrost overlying the sedimentary layer. Zone 3 consists of extensive discontinuous permafrost, which became thinner moving to zone 4. Zone 5 at the southern part of the area, is virtually free of permafrost. At depth there is a conducting region due to the ancient subducted oceanic crust. An example of layered earth conductivity model is shown in Fig. E. 3.

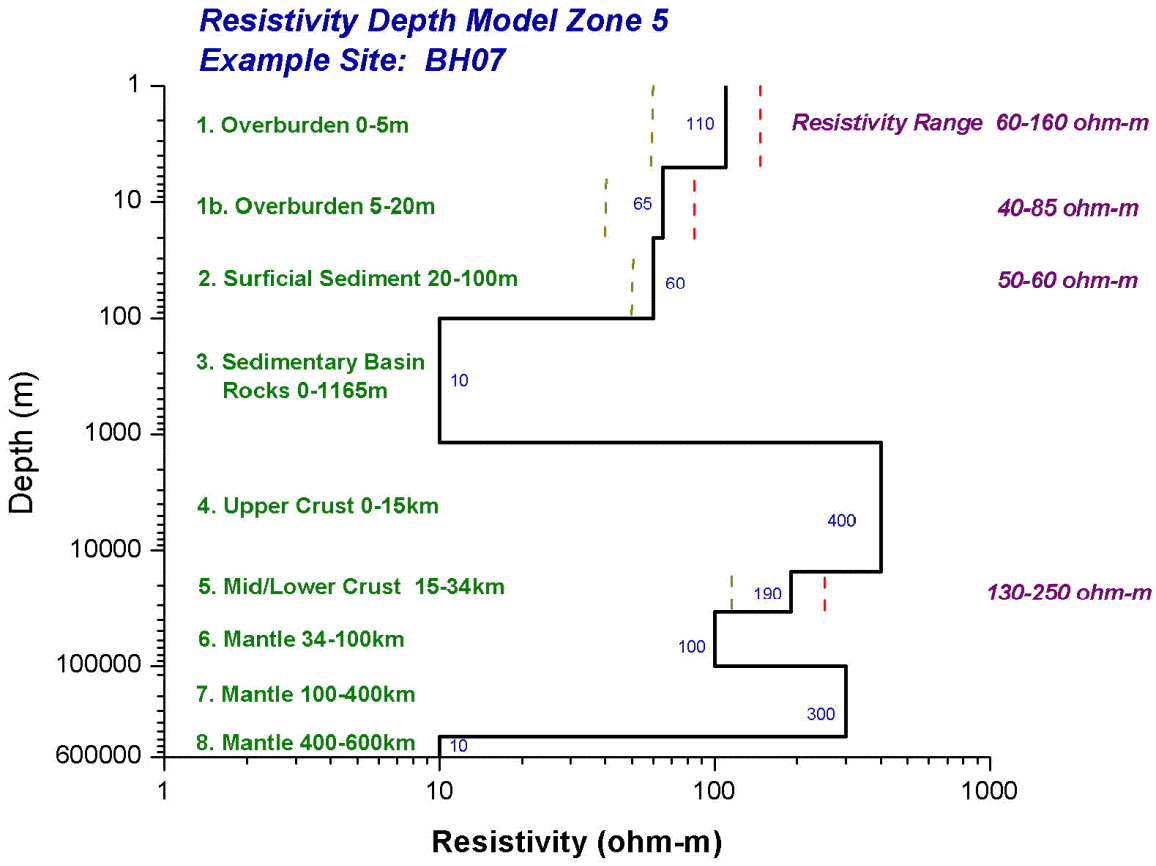

Fig. E3. Example of the earth resistivity model (Zone 5).

E 4. Geo-electric field and telluric activity

Northwards (Ex) and Eastwards (Ey) electric fields were calculated from Yellowknife geomagnetic data using the different earth resistivity models for five different zones along the pipeline route. Examples of the electric fields produced by different levels of geomagnetic activity and statistical analysis of telluric activity based on geoelectric field calculations are presented in Chapter 4. Statistical analysis has been done by using two newly developed indices of telluric activity, such as hourly maximum amplitude (HMA) of the electric field and the hourly standard deviation. The former is characterizing the maximum absolute electric field in one hour, while the latter characterizes the distribution of the fluctuations in each hour. These indices were calculated for every hour in a typical year (2004) and also for years representing solar minimum (1996) and solar maximum (2003). Fig. E.4 shows the occurrence of HMA values during solar maximum year 2003 for the North (Zone 1), middle (Zones 2 and 3) and south (Zones 4 and 5) areas of the planned pipeline route.

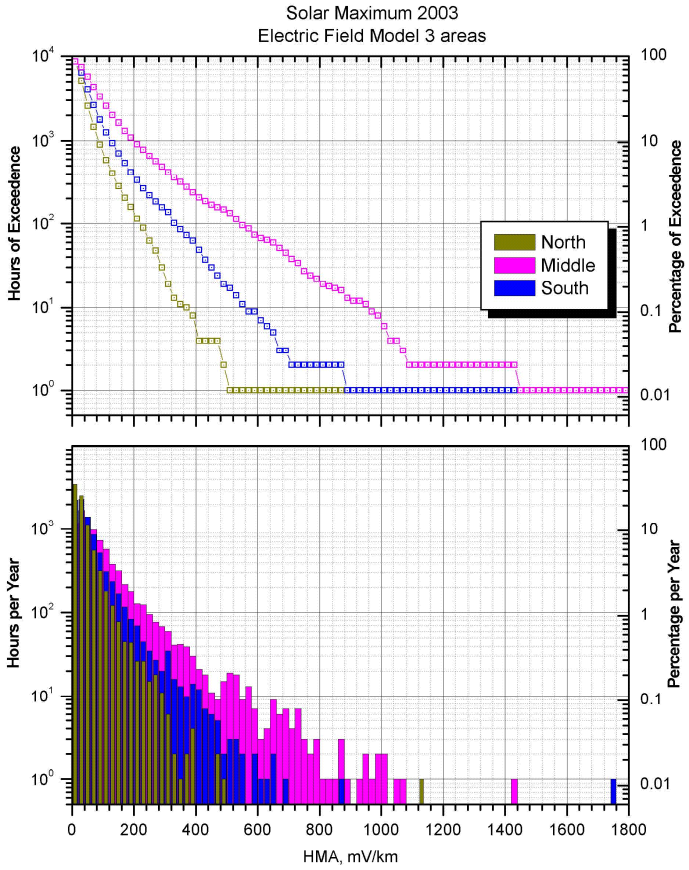

Fig. E4. Histogram (bottom) and hours of exceedence of HMA (top) in year 2003.

Chapter 1

Introduction

1.1. Location

The proposed pipeline along the Mackenzie Valley will be located in the auroral zone, the most active region for telluric currents in the world (see Fig 1.1). Therefore special consideration needs to be taken of telluric currents in the design of cathodic protection for the pipeline. The work described in this report is intended to assess the impact of telluric current to the proposed pipeline and to provide information that can be used to design a cathodic protection system that can ameliorate the telluric current effects. This introductory chapter provides background information on the causes of telluric currents, the history of these effects, previous assessments made for the Canadian power industry and explains the development of the pipeline modelling, before giving an outline of the work described in the subsequent chapters.

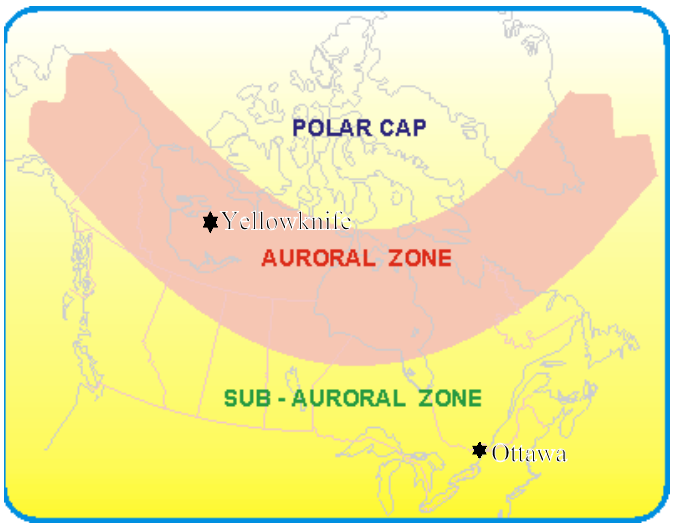

Fig 1.1 Map of Canada showing geomagnetic activity zones. Also shown are magnetic observatories at Yellowknife and Ottawa

1.2. Cause of Telluric Currents

Telluric currents in pipelines are caused by variations in the Earth`s magnetic field. These geomagnetic field variations are produced by electric currents in the ionosphere, 100 km above the Earth`s surface and drive electric currents in any long conductors. In pipelines these `telluric currents`give rise to variations in pipe-to-soil potentials as shown in Fig. 1.2.

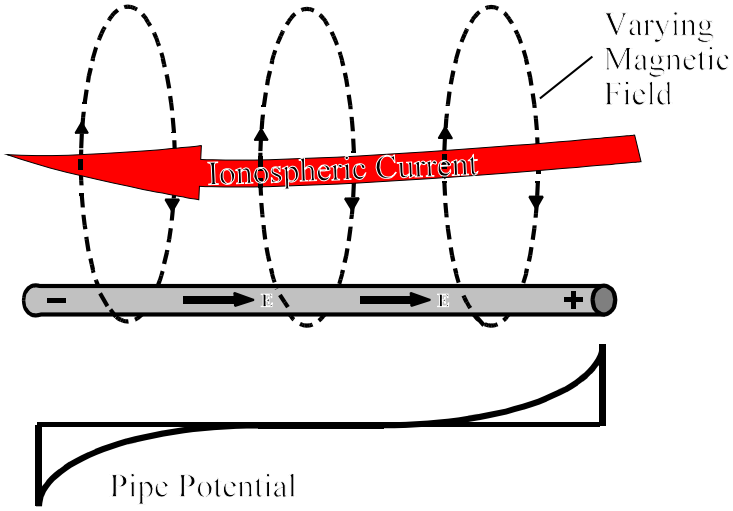

Figure 1.2. Geomagnetic field variations drive `telluric` electric currents which give rise to variations in pipe-to-soil potential.

The sequence of phenomena that give rise to geomagnetic disturbances and telluric currents originates on the Sun. The Sun constantly radiates particles out into space. This `solar wind` compresses the Earth`s magnetic field on the day-side and draws it out into a tail on the night-side forming a region, the magnetosphere, where the geomagnetic field shields the Earth from the solar particles.

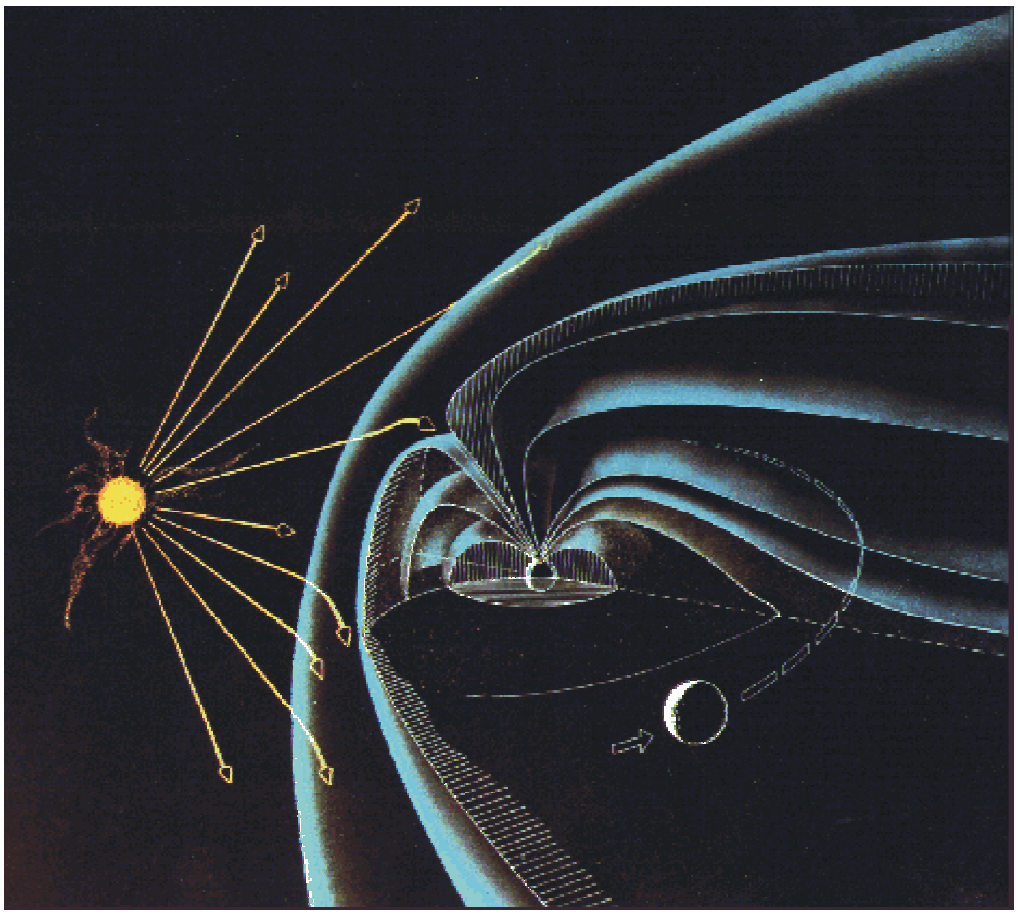

Fig. 1.3. Interaction of the Solar Wind with the Earth`s Magnetosphere.

However, solar particles can penetrate this shield in a narrow region around the magnetic poles. The particles are guided down the magnetic field lines into the upper atmosphere where they create the aurora (northern lights). Strong electric currents are also produced and flow down to the ionosphere in the auroral zones where an intense east-west current is produced called the auroral electrojet. The magnetic disturbances observed at high latitudes are the magnetic field of this auroral electrojet, and are the principal cause of telluric currents in arctic pipelines. An illustration of this phenomenon is shown in Figure 1.4. The top part of the figure shows a satellite picture of the aurora produced an intense solar eruption. Superimposed on this picture are arrows indicating the location and direction of the electric currents, the auroral electrojets, flowing in the ionosphere. The bottom part of the figure shows the magnetic disturbance produced by the auroral electrojet, plus pipe-to-soil potential variations recorded at the same time.

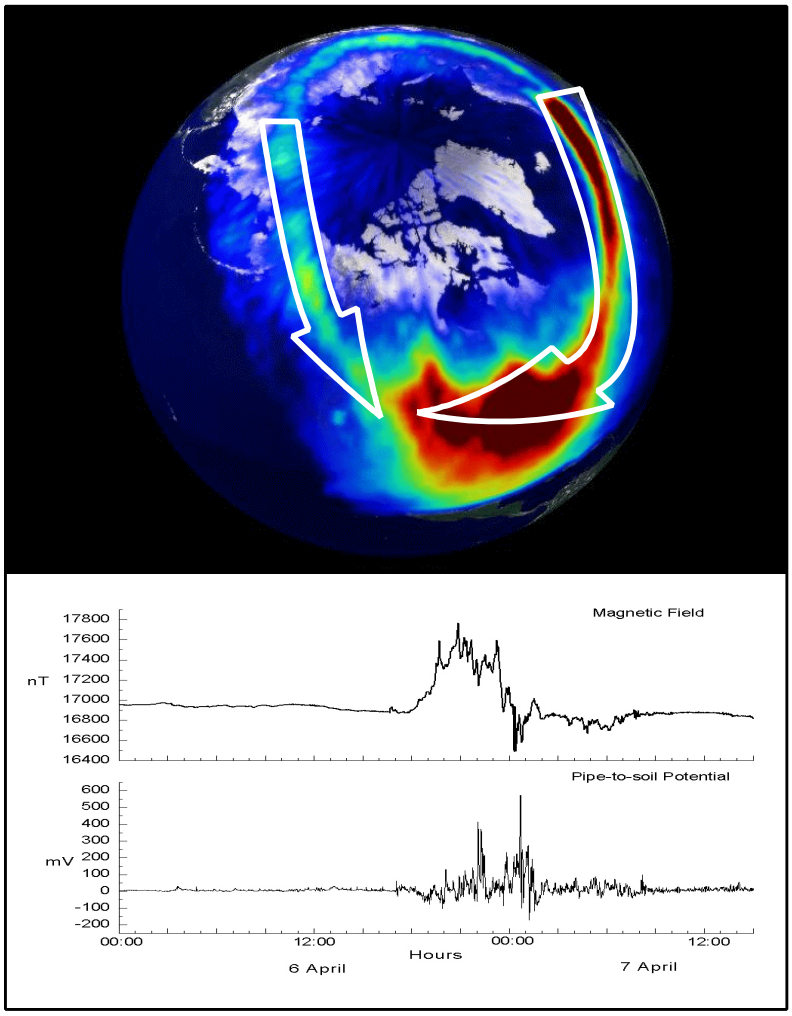

Figure 1.4. Schematic of the electric currents associated with the aurora plus associated geomagnetic field and pipe-to-soil potential variations.

1.3. History of Geomagnetic Effects

The history of geomagnetic effects on electrical systems extends back to the early days of the telegraph (Barlow, 1849). From the earliest accounts there is a recognition of the simultaneous occurrence of the earth currents on the telegraph system and fluctuations of compass needles and sightings of the aurora. Prescott (1866), in an early review, reported the appearance of the aurora on Nov 17, 1848, coincided with effects on the electric telegraph between Florence and Pisa. In 1851, Prescott (1866) reports, there was

> *"a remarkable aurora, which took complete possession of all the telegraph lines in New England, and prevented any business from being transacted during its continuance".*

In 1859, a magnetic storm from August 28 to September 2 produced widespread effects on the telegraph system in Europe and North America. Mr O. S. Wood, Superintendent of the Canadian telegraph lines, reported (see Prescott, 1866):

> *"I never, in my experience of fifteen years in the working of telegraph lines, witnessed anything like the extraordinary effect of the aurora borealis, between Quebec and Father's Point, last night. The line was in most perfect order, and well-skilled operators worked incessantly from eight o'clock last evening till one o'clock this morning, to get over, in even a tolerably intelligible form, about four hundred words of the steamer Indian's report for the press; but at the latter hour, so completely were the wires under the influence of the aurora borealis, that it was found utterly impossible to communicate between the telegraph stations, and the line was closed for the night."*

Problems were experienced by many telegraph operators in North America and Europe (Prescott, 1866). Telegraph problems recurred many times during the nineteenth century and were found to follow the 11 -year cycle of solar activity which affects the number of geomagnetic disturbances (see Figure 1.5).

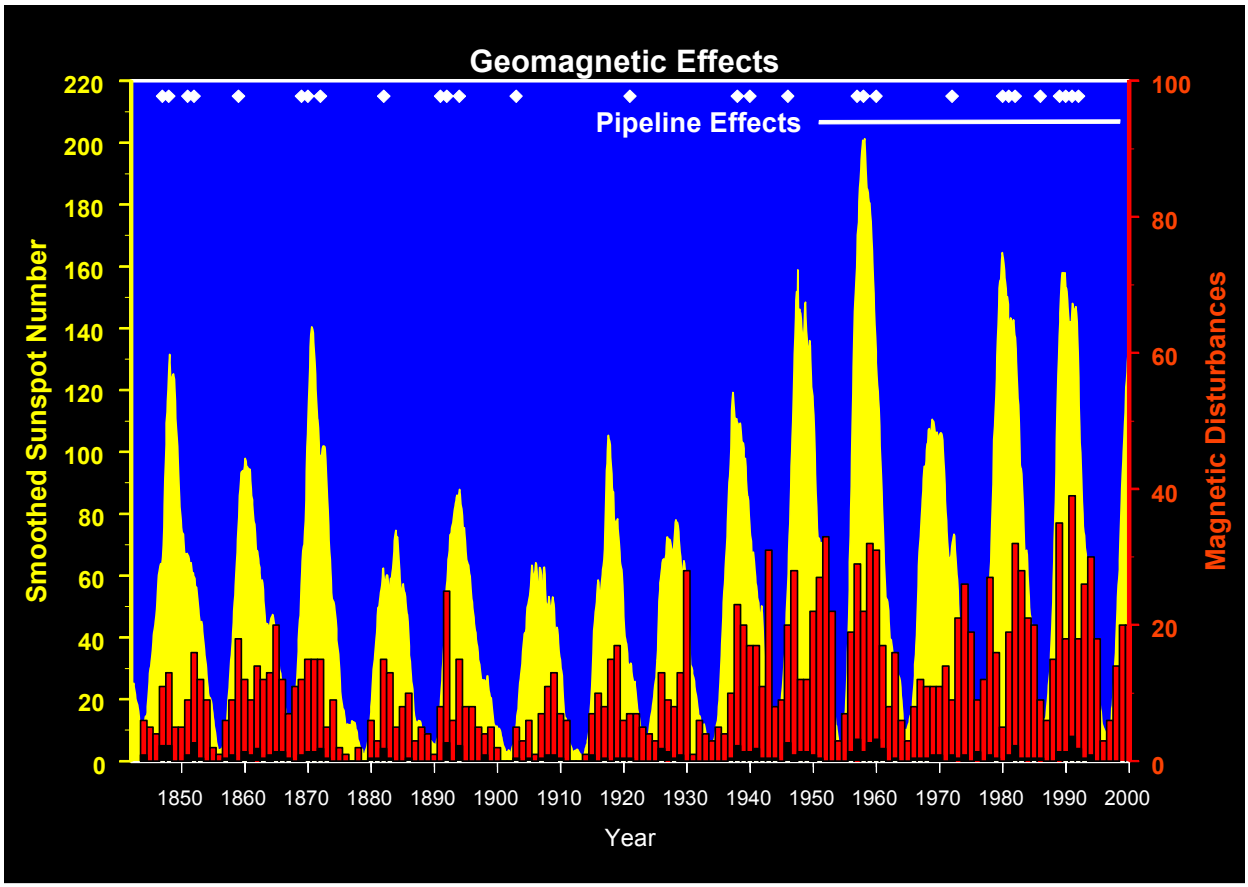

Figure 1.5 Variations of solar and geomagnetic activity for the last 150 years. White diamonds show disruption of telegraph, phone and power systems. White line shows when telluric effects seen on pipelines.

Pipelines are also long electrical conductors, often stretching thousands of kilometres across the Earth's surface. Early work on a pipeline in Canada noted the existence of stray currents that could not be accounted for by any of the usual sources and considered a possible association with magnetic disturbances (Allison and Huddleston, 1952). Telluric currents have been an ongoing problem for engineers setting up cathodic protection systems and the variations in pipe-to-soil potential (PSP) produced by telluric currents often make pipeline surveys difficult (Proctor, 1974; Peabody, 1979). Construction of the Trans-Alaska Pipeline in the auroral zone prompted considerable work on the currents that might be induced (Campbell, 1978) (Figure 1.6) and has required special monitoring techniques to be developed (Degerstedt et al, 1995).

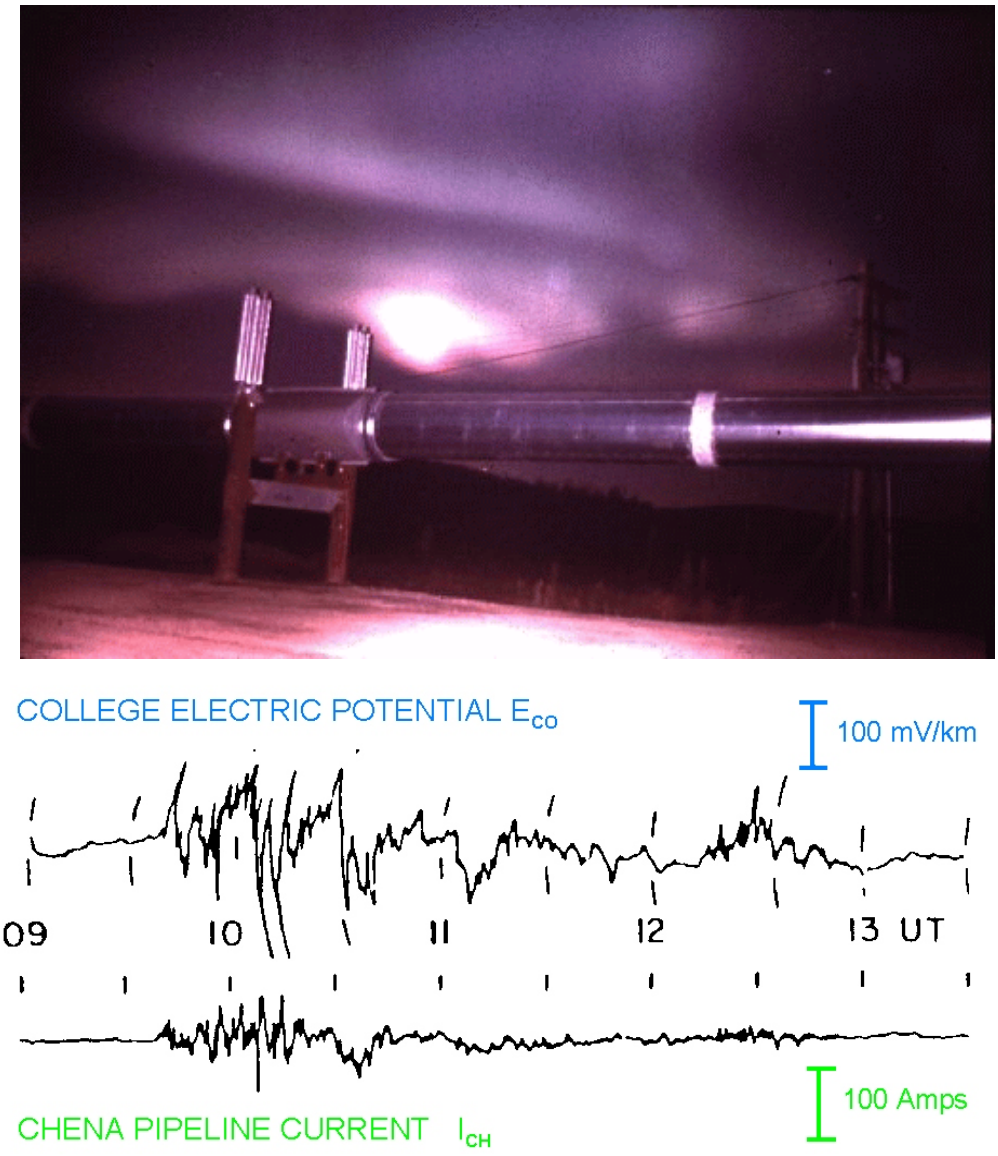

Figure 1.6. a) Aurora above the Alaska pipeline
b) Example of electric fields and telluric currents in the pipeline.

1.4. Development of Pipeline Modelling

For examining the impact of geomagnetic disturbances on pipelines, we have developed methods for modelling telluric currents in pipelines and their effects on pipe-to-soil potentials. The electrical characteristics of the pipeline are modelled as a lossy transmission line and the induced electric field is represented by voltage sources distributed along the line. This distributed source transmission line (DSTL) theory was used by Taflove and Dabkowski (1979) to examine AC induction in pipelines and was later adapted for geomagnetic induction in pipelines (Boteler and Cookson, 1986). Boteler (1997) extended the theory so that the modelling could be used for multi-section pipelines. This enabled the modelling to make predictions about the pipe-to-soil potentials that would be expected in different situations and showed that the telluric PSP variations changed with position on the pipeline.

Measurements of telluric effects that could be compared with the modeling results were scarce because of the difficulty of monitoring pipe-to-soil potentials varying both in time and place. However, by leapfrogging two potential recorders by helicopter along the Norman Wells - Zama pipeline, W.H. Seager was able to examine the phase relationship of the telluric variations on the pipeline. Also, by comparing the pipeline potential recordings to the magnetic recordings from the Yellowknife Magnetic Observatory, Seager was able to construct a schematic picture of how the amplitude of telluric fluctuations varied along the pipe (Figure 1.7a). Additional tests were conducted at Wrigley Station (Kilometre Point 335) where an insulating flange, normally shorted by a bond wire, was located. When the bond was opened the telluric potential increased substantially on both sides and a phase reversal of the telluric potentials on opposite sides of the insulating flange was noted.

Model calculations of the potential profile along the Norman Wells - Zama pipeline have been made for comparison with the observations (Boteler and Seager, 1998). Figure 1.7b shows the potential profile for an electric field of 1 V/km parallel to the pipeline. This figure also shows the calculated potential profile for the pipeline with an insulating flange at KP 335. The calculated potential profile (Figure 1.7b agrees very well with the potential profile derived from observations (Figure 1.7a). They both show the characteristic S shape profile with potential variations at one end of the pipeline having the opposite sign to those at the other end that is characteristic of an "electrically-long" pipeline. Both the model results and the observations show that the maximum voltages occur at the ends of the pipeline. They also both show that large voltage variations are produced either side of an insulating flange.

Further tests of the DSTL modeling were made as part of an international study, led by the Geological Survey of Canada, involving pipeline companies from Canada, Norway, Sweden and Finland (Boteler and Trichtchenko, 2000). In this study the first comprehensive set of simultaneous multi-site recordings were made of telluric PSP variations. These were used to construct PSP profiles for pipelines in a variety of locations. Recordings on the Norman Wells - Zama pipeline further illustrate the effect of an insulating flange (Figure 1.7c). Results from other Canadian and Scandinavian pipelines confirmed the validity of the DSTL modeling.

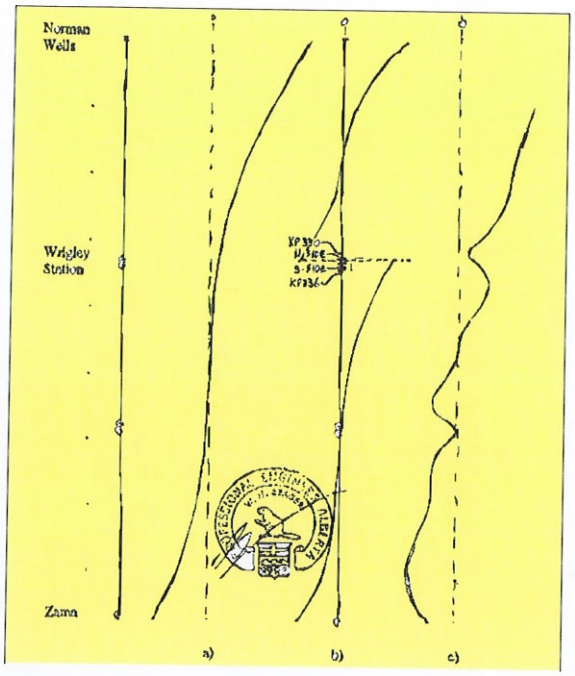

a)

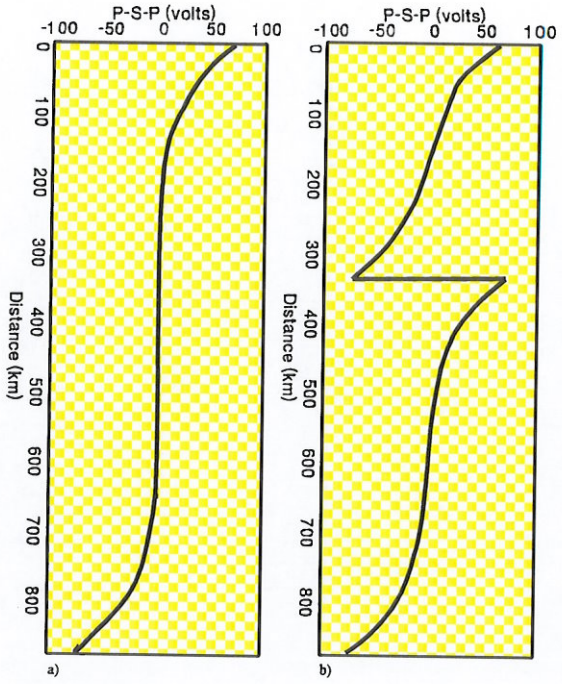

b)

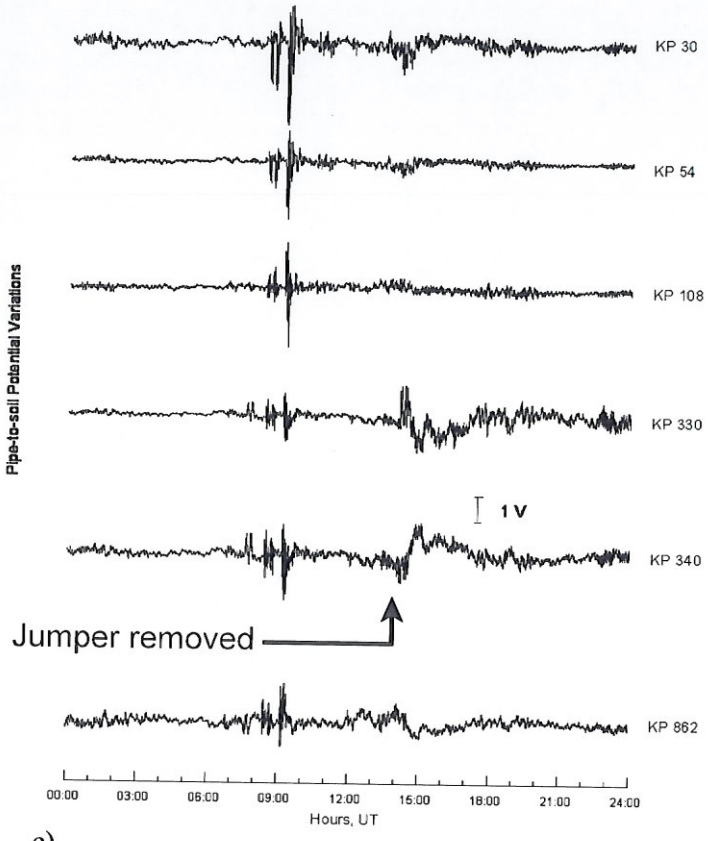

c)

Figure 1.7. Telluric currents on the Norman Wells - Zama Pipeline
a) Profile constructed from observations by Seager
b) Modeling results: with and without a flange
c) Recordings before and after jumper removed from flange.

References

Allison, N.J. and Huddleston, W.M.E. Extraneous Currents Noted on Large Transmission Pipe Line System, *Corrosion*, Vol. 8, No.1, pp.1, January 1952

Barlow, W.H., On the spontaneous electrical currents observed in wires of the electric telegraph, *Phil. Trans. Roy. Soc., London*, 139, 61-72, 1849.

Boteler, D.H., and Cookson, M.J., Telluric currents and their effects on pipelines in the Cook Strait region of New Zealand, *Mater. Perform.*, 25, 27-32, 1986.

Boteler, D.H., Distributed source transmission line theory for active terminations, *Proc. 1997 Zurich EMC Symposium*, Feb. 18-20, URSI supplement, 401-408, 1997.

Boteler, D.H. and Seager, W.H., Telluric currents: A meeting of theory and observation, *Corrosion*, 54, 751-755, 1998.

Boteler, D.H. and Trichtchenko, L., International Study of Telluric Current Effects on Pipelines, Final Report, *GSC Open File 3050*, 2000.

Boteler, D.H. and Trichtchenko, L., A Common Theoretical Framework for AC and Telluric Interference on Pipelines, *Paper No 05614, Proc. NACE CORROSION/2005*, April 2005.

Campbell, W.H., Induction of auroral zone electric currents within the Alaska pipeline, *Pure and Applied Geophysics*, 116, 1143-1173, 1978.

Degerstedt, R.M., K.J. Kennelley, P.F. Lara and O.C. Moghissi, Acquiring "telluric-nulled" pipe-to-soil potentials on the Trans Alaska pipeline, *CORROSION/95, paper no 345* NACE, 1995.

Gummow, R., Boteler, D.H., and Trichtchenko, L., Telluric and ocean current effects on buried pipelines and their cathodic protection systems, *Report for Pipeline Research Council International*, Catalog No. L51909, 2002

Peabody, A.W., Corrosion aspects of arctic pipelines, Materials Performance, 18, 5, 27-32, 1979.
Prescott, G.B., *History, Theory and Practice of the Electric Telegraph*, IV ed., Ticknor and Fields, Boston, 1866.

Proctor, T.G., Experience with telluric current interference in the cathodic protection of a buried pipeline in New Zealand, *Materials Performance*, 13, 24-30, 1974.

Rix, B.C. and Boteler, D.H. Telluric current considerations in the CP design for the Maritimes and Northeast Pipeline, *Paper 01317, Proceedings, CORROSION 2001*, NACE, Houston, March 11-16, 2001

Taflove, A. and Dabkowski, J., Prediction method for buried pipeline voltages due to 60 Hz AC inductive coupling, *IEEE Trans. Power Apparatus & Systems*, vol PAS-98, 780-794, 1979.

Trichtchenko, L. and Boteler, D.H., Specification of geomagnetically induced electric fields and currents in pipelines, *J. Geophys. Res.*, Vol. 106 , No. A10, 21039-21048, 2001.

Trichtchenko, L. and Boteler, D.H., Modelling of geomagnetic induction in pipelines, *Annales Geophysicae*, 20, 1063-1072, 2002.

Trichtchenko, L. Modelling electromagnetic induction in pipelines, *Paper 04212, Proceedings, CORROSION 2004*, NACE, New Orleans, April 2004.

Chapter 2

Geomagnetic Climatology

2.1. Introduction

The analysis of the geomagnetic activity in the Mackenzie Valley area was made using magnetic data from the nearest geomagnetic observatory located at Yellowknife with geographic coordinates: 62.82°° N, 245.518°° E.

Data sampling rate was 1 minute, which is the standard rate for digitally filtered samples of data for the INTERMAGNET geomagnetic observatory. Recordings consist of three components of the magnetic field, Bx-directed northward, By-directed eastward and Bz directed vertically down. For this study, Yellowknife observatory data cover the 30-year period from 1975 to 2004.

The data were processed to determine the maximum hourly range (i.e. the absolute difference between the lowest and highest 1-minute values within a particular hour) for both horizontal components for each hour of each day of each year. Therefore, for further study of the geomagnetic activity, we use hourly index, rather than minute-by-minute variation. The approach of utilizing indices is widely used in the geomagnetic field studies, see for example (Mayaud, 1980).

The hourly range indices HRX and HRY were then examined to identify and remove those hours when; (1) no data was available due to various causes at the observatory that resulted in no measurements being made, and, (2) there were less than 48 minutes of data available for a particular hour. The amount of "data loss" from year to year was variable as shown in Figure 2.1, ranging from 0.1 to 14.6 per cent with greatest loss during 1975 and 1976.

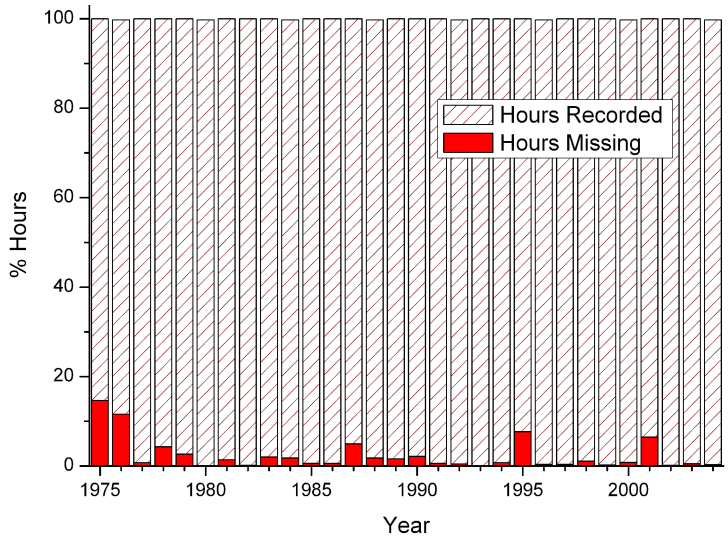

Fig.2.1. Data quality at Yellowknife magnetic observatory

To demonstrate the specifics of the geomagnetic activity in Mackenzie Valley, we compare hourly indices in Yellowknife (auroral zone) and in Ottawa (low latitude) magnetic observatory for the same representative year (2004). Statistical evaluation of the activity gives the possibility to define scale of geomagnetic activity in Mackenzie Valley area. Statistical description of 30 years of geomagnetic data for Yellowknife observatory results in the table, which evaluates the occurrence of the different activity levels and set the possible lowest and highest limits for the geomagnetic 'climate" in the area of pipeline route.

2.2. Geomagnetic Variations in Auroral Zone

For initial view of the geomagnetic activity in Mackenzie Valley, the typical year has been chosen. Year 2004 is in the declining phase of the solar cycle with two large geomagnetic storms, in July and November, and can represent the average annual geomagnetic situation. The evaluation of the geomagnetic activity was based on the hourly range of the geomagnetic field (all three components, HRX, HRY, HRZ). These are shown in Fig 2.2.

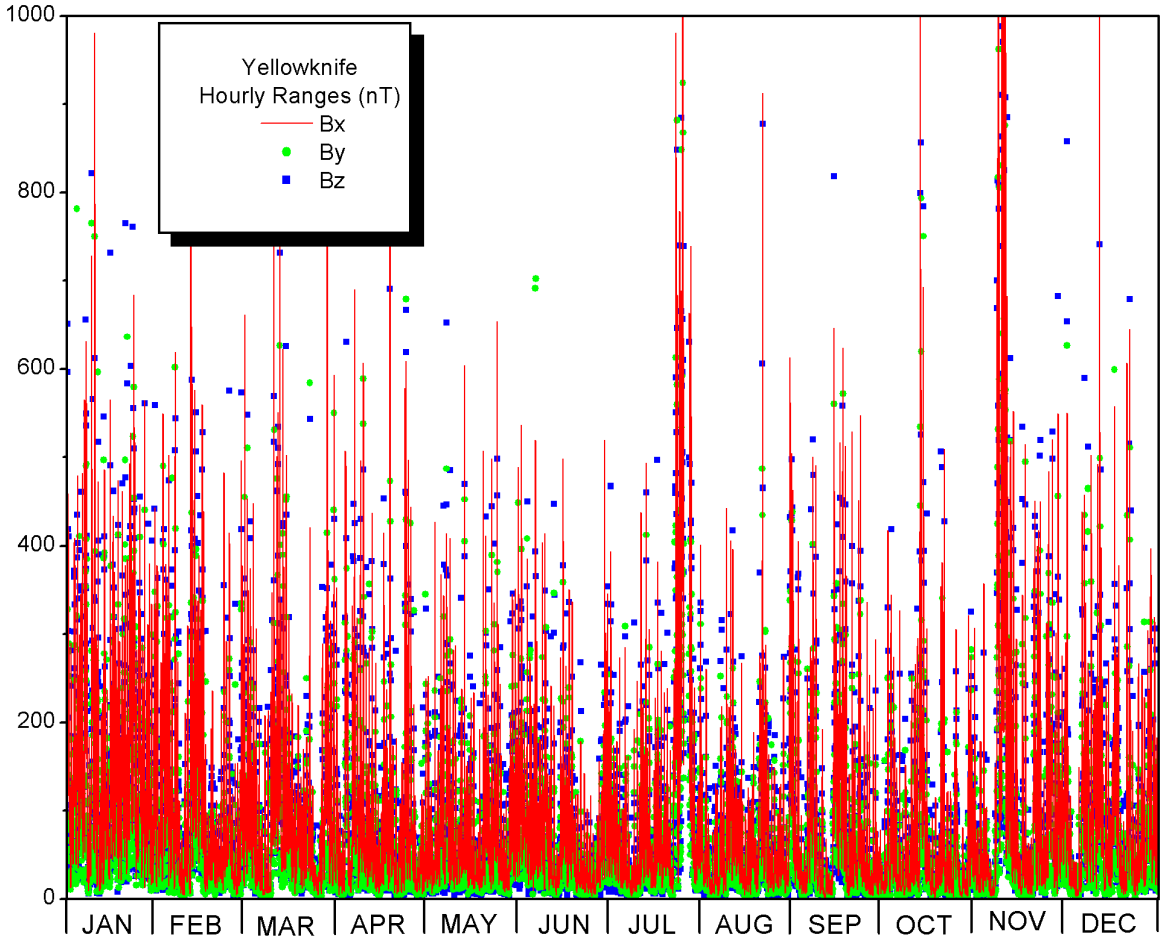

Fig. 2.2. Geomagnetic activity at Yellowknife during 2004

Visual examination of this plot gives an idea that most of the fluctuations are below 600 nT, but only comparison with data from other geomagnetic observatory can give the criteria of what is the geomagnetic activity situation at Yellowknife. Therefore, for comparison we choose Ottawa geomagnetic observatory, with its location at (OTT) located at : 45.403°° N, 284.448°° E. This observatory data represent mid-latitude location and have typical geomagnetic activity situation for the low-latitude areas. The hourly ranges at Ottawa, throughout 2004, are shown in Fig 2.3 on the same scale.

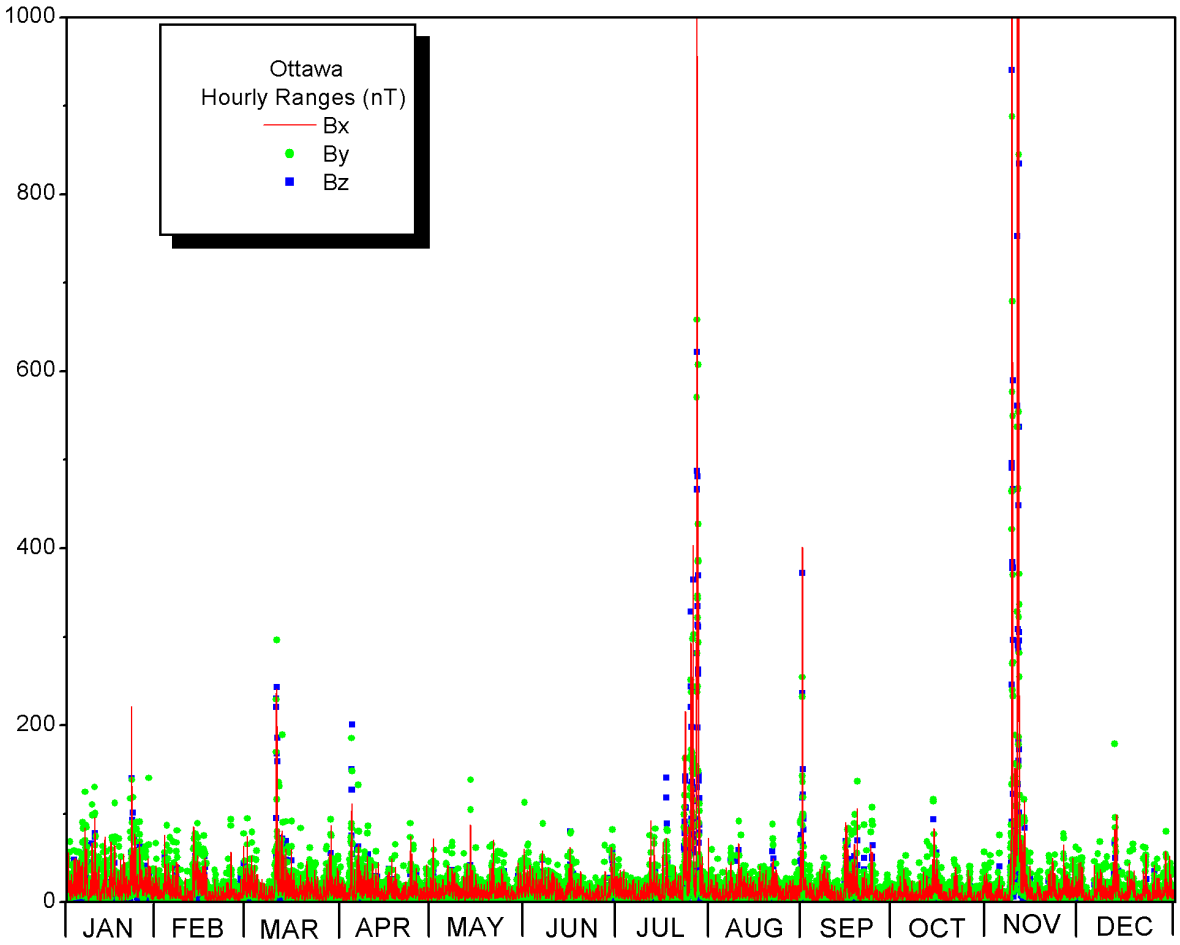

Fig. 2.3. Geomagnetic activity at Ottawa during 2004

Visual examination of Ottawa plot gives an approximate criteria of "normal" low-latitude geomagnetic activity of below 100 nT range. These two simple examples demonstrate the necessity of the detailed study of the geomagnetic activity in the auroral zone. This detailed study should include statistical analysis of the representative year as well as longer records for evaluation of the maximum and minimum geomagnetic variations of the local geomagnetic field.

2.3. Statistics of Geomagnetic Activity

The occurrence of different levels of geomagnetic activity was determined by counting the number of hourly ranges in bins 20 nT wide. Figs. 2.4 and 2.5 show the results for Yellowknife and Ottawa respectively. The lower part of the figure shows the total number of counts for the year in each bin. The upper part of the figure shows the cumulative counts as a percentage of the total number of hours in the year.

Comparison of Figs. 2.4 and 2.5 shows the markedly greater level of activity at Yellowknife compared to Ottawa. For 95% of the year geomagnetic field hourly ranges in Ottawa were lower than 40 nT. In contrast, this quiet level threshold was not being exceeded only near 40% of the year in Yellowknife.

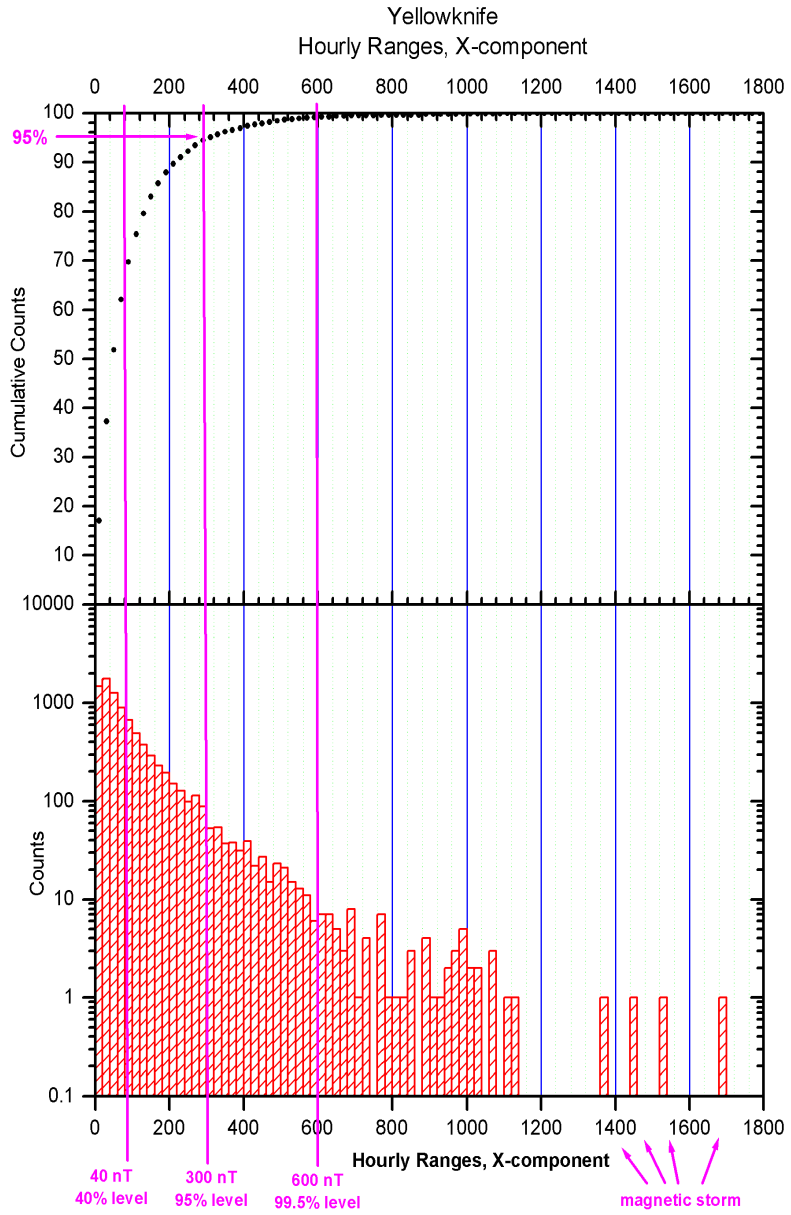

Fig. 2.4 Occurrence of geomagnetic activity at Yellowknife in 2004.

Looking at higher levels of activity: 95% of the year geomagnetic field was below 300 nT in Yellowknife, which has been defined as an unsettled level of the geomagnetic activity. While for 99.5 % of the year the geomagnetic field in YKC was below 600 nT, which has been defined as an active level of the geomagnetic field.

As representative extreme conditions, we use the geomagnetic storm on 7-8 November 2004. During these days the hourly ranges at Yellowknife reached values of 1400-1600 nT.

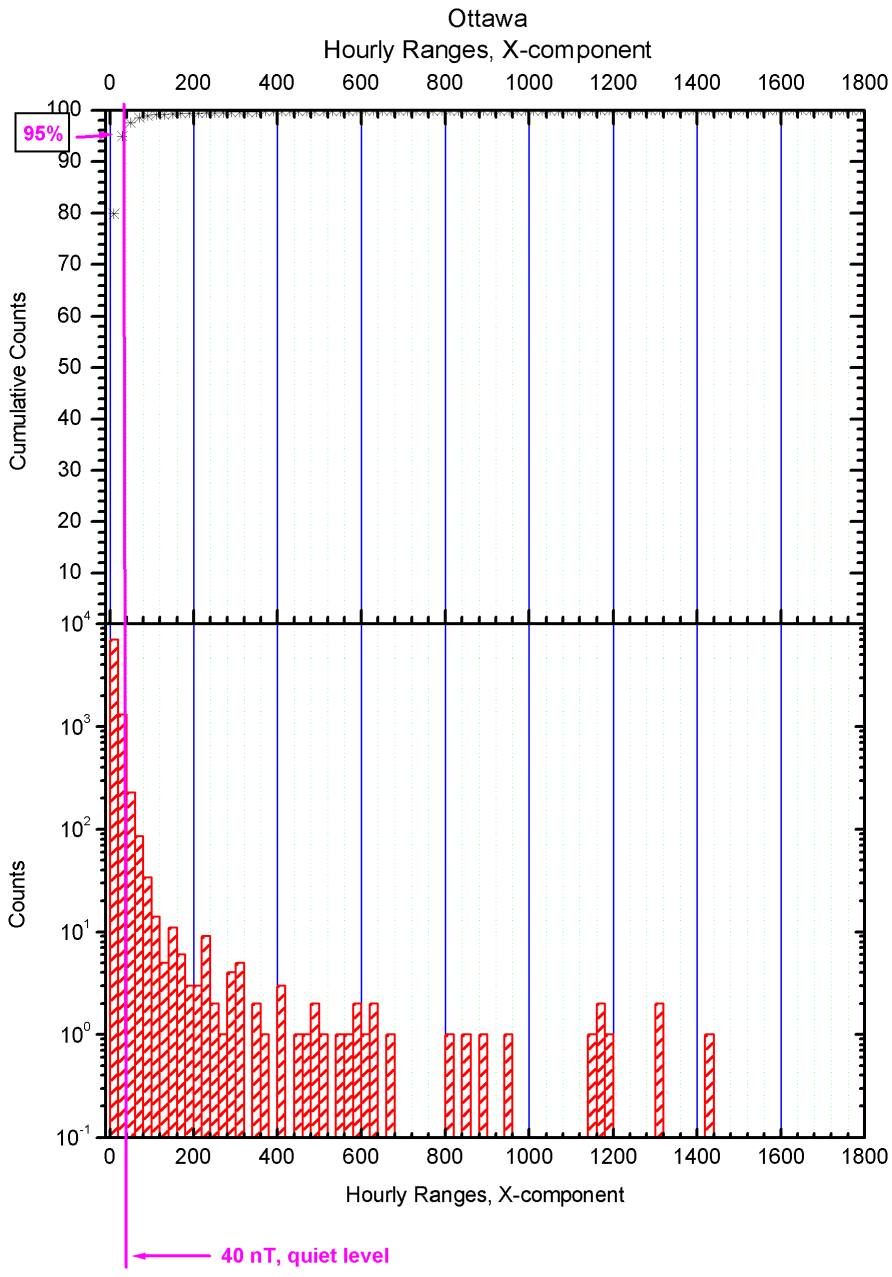

Fig. 2.5 Occurrence of geomagnetic activity at Ottawa in 2004.

2.4. Statistical Analysis of 30 years of Magnetic Recordings

For the extensive statistical analysis all available geomagnetic data for Yellowknife observatory have been utilised. These recordings cover period from 1975 to 2004, which encompasses almost three 11-years solar cycles.

Histograms for each year were constructed, with the hourly ranges sorted into 20 nT size histogram bins. Each bin associated with the number of occurrences of hourly range (within a year) falling within that bin's limits. The equivalent percentage of occurrence was also determined, and shown on the histogram. Next, the hours of exceedence for each of the histogram bins were calculated, and the equivalent percentage of exceedence was also determined. The exceedence values were plotted above the histogram columns. Histograms for the whole period 1975 - 2004 are presented in Figures 2.6. (HRX) and 2.7 (HRY).

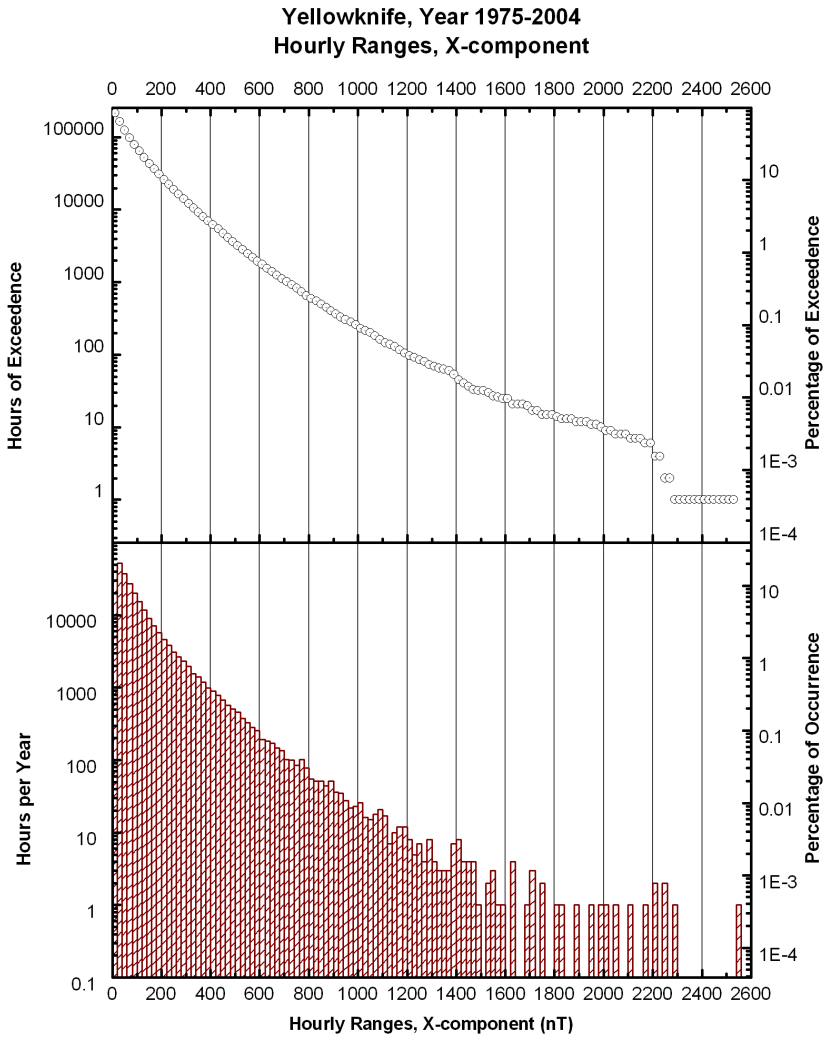

Fig.2.6. Histogram and hours of exceedence of HRX in Yellowknife in 1975-2004

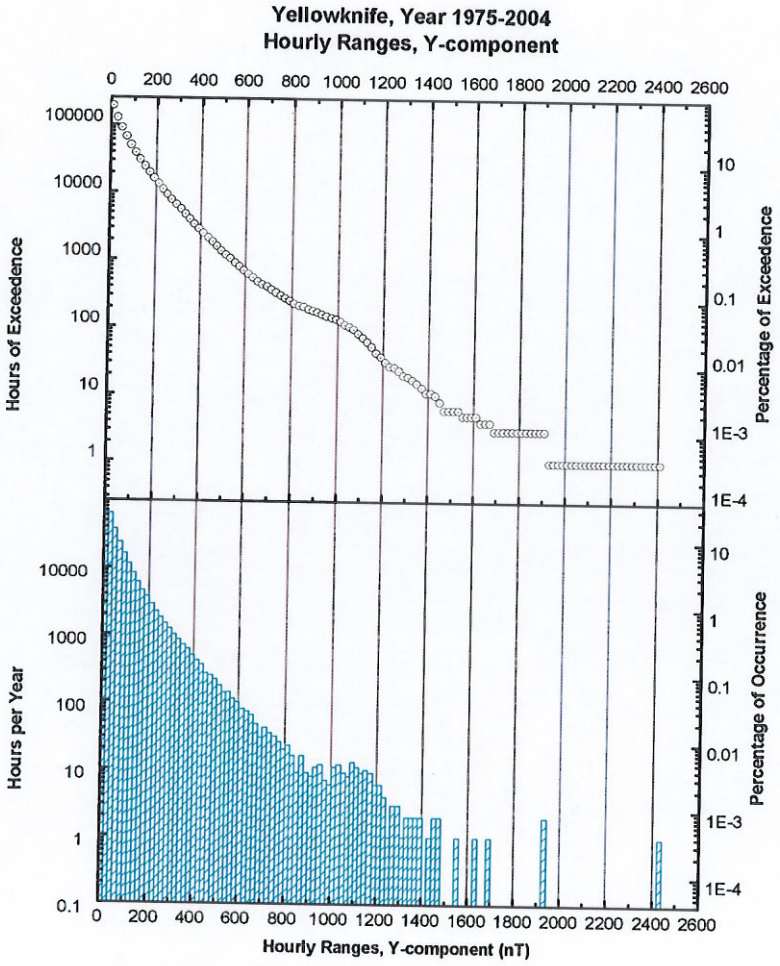

Fig.2.7. Histogram and hours of exceedence of HRY in Yellowknife in 1975-2004 years

It follows from the comparison of the histograms for two components, that geomagnetic field shows more variability in X-direction (North-South), which is reasonable for auroral electrojets, which are the source of the variability, flows in East-West direction. For the following statistical studies we will use only HRX data.

Using the exceedence plot lines on the histograms, the hours and percentage of Hx-component above the 20, 300 and 600 nT hourly ranges were determined for each year. The rationale for selection of these threshold hourly ranges is further described in the previous part.

Table 2.1 provides a list of the hours of exceedence for each threshold HRX. In total, the quiet level percentage was only 43 % of the time. Therefore, more than half of the time geomagnetic field fluctuations for the Yellowknife as a representative and for Mackenzie Valley as a whole, significantly higher, than normal (low latitude) level. At the same time, really exceptional variation, above 300 nT, are quite rare (only 5%).

Year	Hours Recorded	> 600 nT (hours)	> 600 nT (%)	> 300 nT (hours)	> 300 nT (%)	> 40 nT (hours)	> 40 nT (%)
1975	7478	54	0.7	446	6.0	4382	59
1976	7750	71	0.9	408	5.3	4389	57
1977	8696	43	0.5	333	3.8	4396	51
1978	8388	95	1.1	517	6.2	4751	57
1979	8531	31	0.4	285	3.3	4773	56
1980	8756	14	0.2	197	2.2	3700	42
1981	8639	45	0.5	392	4.5	4837	56
1982	8748	105	1.2	670	7.7	5943	68
1983	8585	79	0.9	560	6.5	5701	66
1984	8607	91	1.1	637	7.4	5651	66
1985	8712	78	0.9	442	5.1	4823	55
1986	8711	43	0.5	349	4.0	4353	50
1987	8328	29	0.3	294	3.5	3932	47
1988	8606	39	0.5	326	3.8	4301	50
1989	8622	72	0.8	502	5.8	5228	61
1990	8576	54	0.6	367	4.3	4857	57
1991	8711	95	1.1	609	7.0	5655	65
1992	8723	67	0.8	438	5.0	5054	58
1993	8758	65	0.7	488	5.6	5074	58
1994	8696	96	1.1	763	8.8	5645	65
1995	8755	62	0.7	411	4.7	4375	50
1996	8088	25	0.3	264	3.3	3907	48
1997	8730	23	0.3	214	2.5	3475	40
1998	8671	61	0.7	321	3.7	4236	49
1999	8745	55	0.6	425	4.9	4679	54
2000	8691	58	0.7	441	5.1	4866	56
2001	8198	46	0.6	307	3.7	3960	48
2002	8750	32	0.4	331	3.8	4427	51
2003	8719	145	1.7	897	10.3	6414	74
2004	8734	74	0.9	470	5.4	4835	55
Total	256702	1888	0.73	13198	5.1	146213	57

Table 2.1. Hours and percentage of HRX above 40, 300 and 600 nt ranges in years 1975 - 2004, Yellowknife Magnetic Observatory.

In order to find the years with lowest and highest geomagnetic activities for further applications in telluric impact assessment, we use a graphical representation of the percentage of exceedence for all three thresholds during the last 30 years, superimposed on the solar cycle.

These are presented in Fig. 2.8 for HRX above 40 nT and in Fig.2.9 for HRX above the 300 and 600 nT thresholds. It should be noted, that scales at both plots are different for more clear presentation small values in Fig. 2.9.

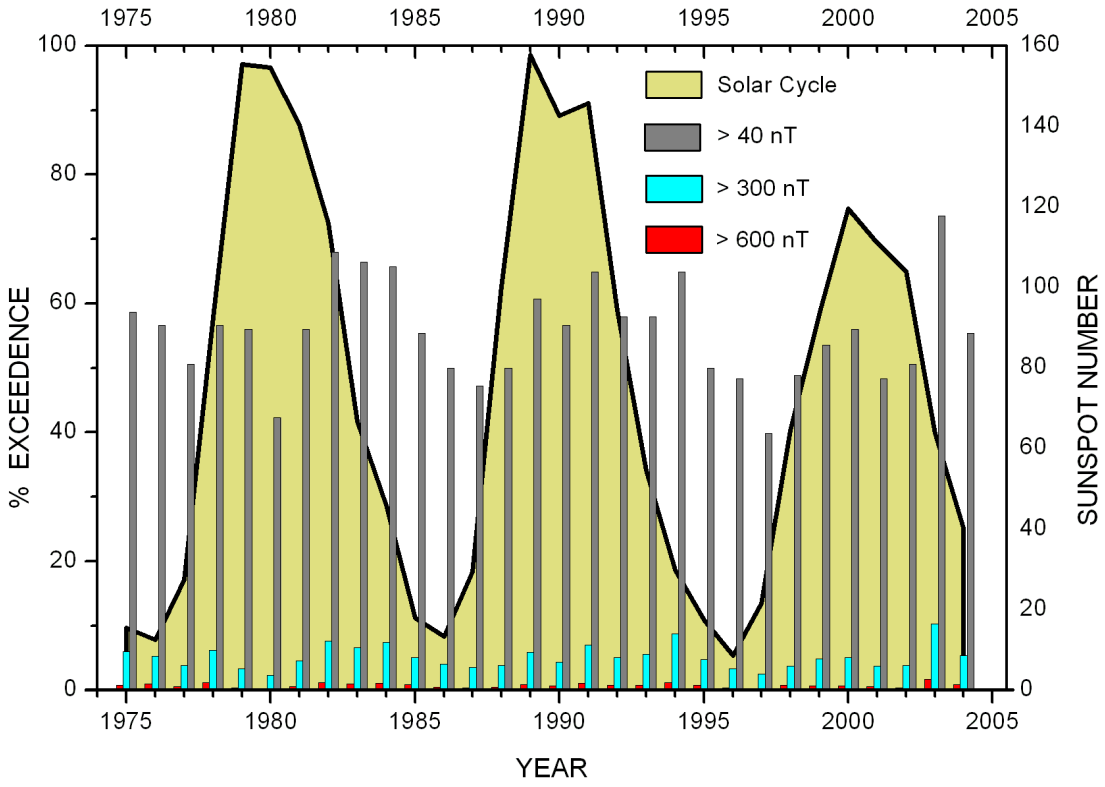

Fig.2.8. Percentage of exceedence of HRX in Yellowknife above three activity levels (left axis) with solar cycle variations of the sunspot number (right axis)

As follows from the table 2.1 and figures 2.8, 2.9, there is a long term variability in geomagnetic activity in Yellowknife area. The most active in 30 years is 2003, the most quiet is 1996 years.

Even the most quiet year in Yellowknife characterised by about 48 % of the year HRX above 40 nT, which represents quiet level (95% of the year) in low-latitude areas. There is never quiet in Yellowknife.

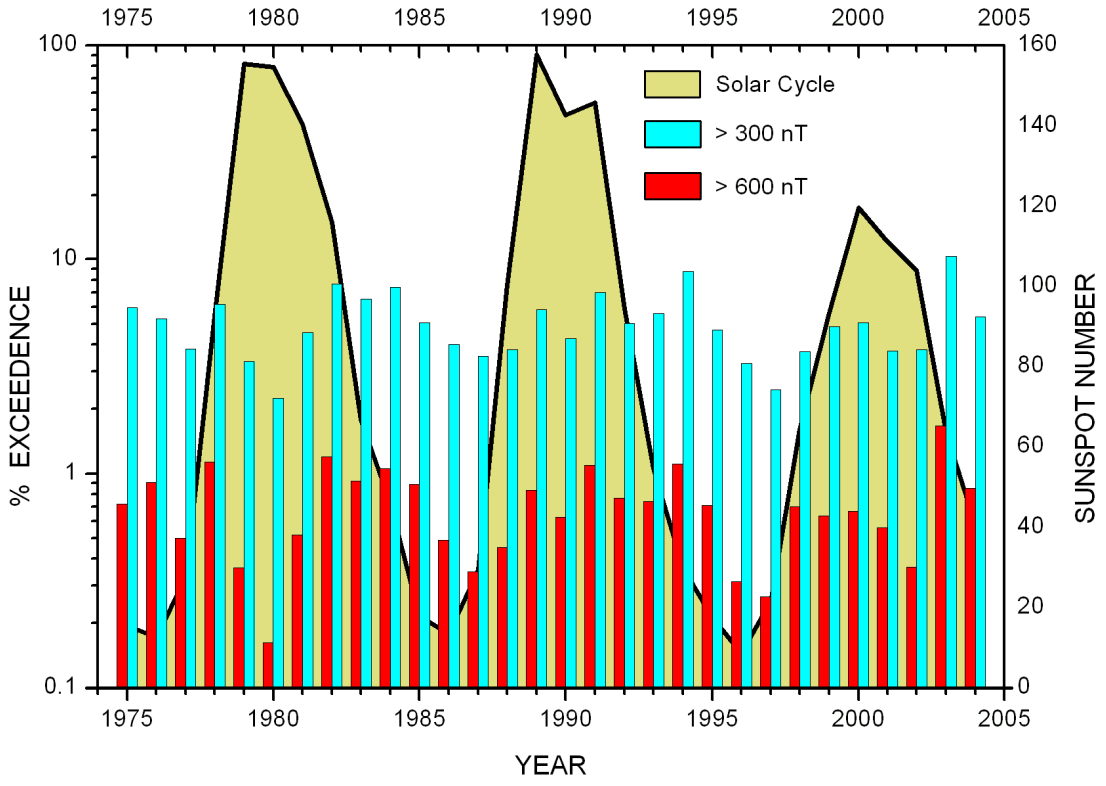

Fig. 2.9. Percent of exceedence of HRX in Yellowknife above 2 most active levels (left axis) with solar cycle variability of the sunspot number (right axis)

It can be mentioned, that we did not find well pronounced solar cycle variability in geomagnetic activity in Yellowknife area. This solar cycle variability in geomagnetic activity looks more well defined in the low-latitude locations (see Fig.1.5).

References:

Mayaud, P.N., 1980, *Derivation, Meaning, and Use of Geomagnetic Indices*, Geophysical Monograph 22, AGU, Washington, DC, pp. 40-52.

Chapter 3

Review of Geology and Conductivity Structure

3.1. Introduction

This chapter provides a compilation of the geological setting of the project area, and describes how one-dimensional (1D) models of the earth conductivity were developed, which in turn are utilized in the electric field and pipeline modeling.

3.1.1 Purpose

The purpose of this investigation was to:

(a) review both the deep and near surface (including permafrost) geological conditions, along the pipeline route because of its potential influence on the development of computer models used to investigate telluric current effects,

(b) review active layer and talik conditions along the pipeline route, for design considerations in placement of the cathodic protection system ground bed and anodes, and to;

(c) develop 1D models of the ground conductivity structure for different selected regions along the pipeline route, for use as input to electric field modeling.

3.1.2 Scope of Work

Publicly-available information was reviewed. The predominance of information was obtained from recent geological reports, scientific journals, compilation studies of the Mackenzie Valley, and assorted on-line documents available through internet searches.

Selected figures from the reviewed material are reproduced in this report. On some figures, the general trend of the pipeline route has been drawn for reference.

3.1.3 Methodology

Compilation of the geology, and other physical attributes, was generally limited proximal to the pipeline route. Simple overlays of the pipeline route were placed onto generalized surficial geology and permafrost maps to determine the approximate extent of a particular geological material or permafrost condition.

Data on electrical resistivity, both for unfrozen and frozen ground, were obtained from tables, diagrams or cross-sections presented in the various source information. For diagrams that presented a compilation of electrical resistivity ranges for various soils, the values were hand measured. Where mentioned in the source material, a note was made as to whether the electrical resistivity value was an in-situ measurement (generally a laboratory test) or an ex-situ measurement (from a surface geophysics survey). In the latter case, it is an apparent resistivity[1] that has been measured.

[1] *Apparent resistivity* is the average resistivity over the penetration depth of the signals.

3.1.4 Kilometer Points

The kilometer distance used in this report to describe points along the pipeline route is the same utilized by the Mackenzie Gas Producers Group (MGP). Starting at kilometer point KP 0 at Inuvik, the pipeline right-of-way (ROW) continues southeasterly to KP 473, near Norman Wells, where it joins the existing Enbridge oil pipeline, and then both continue to KP 1221 at the Alberta – Northwest Territories (NWT) provincial boundary. Figure 3.1 illustrates the pipeline route.

North of KP 0 at Inuvik, the pipeline ROW – as a gathering lateral line to the gas fields – continues 133 km to Taglu on the coast of the Beaufort Sea. Two additional short lateral lines branch off the Taglu to Inuvik lateral line. The first runs 15 km west of Taglu. The second runs 27.5 km east of Storm Hills.

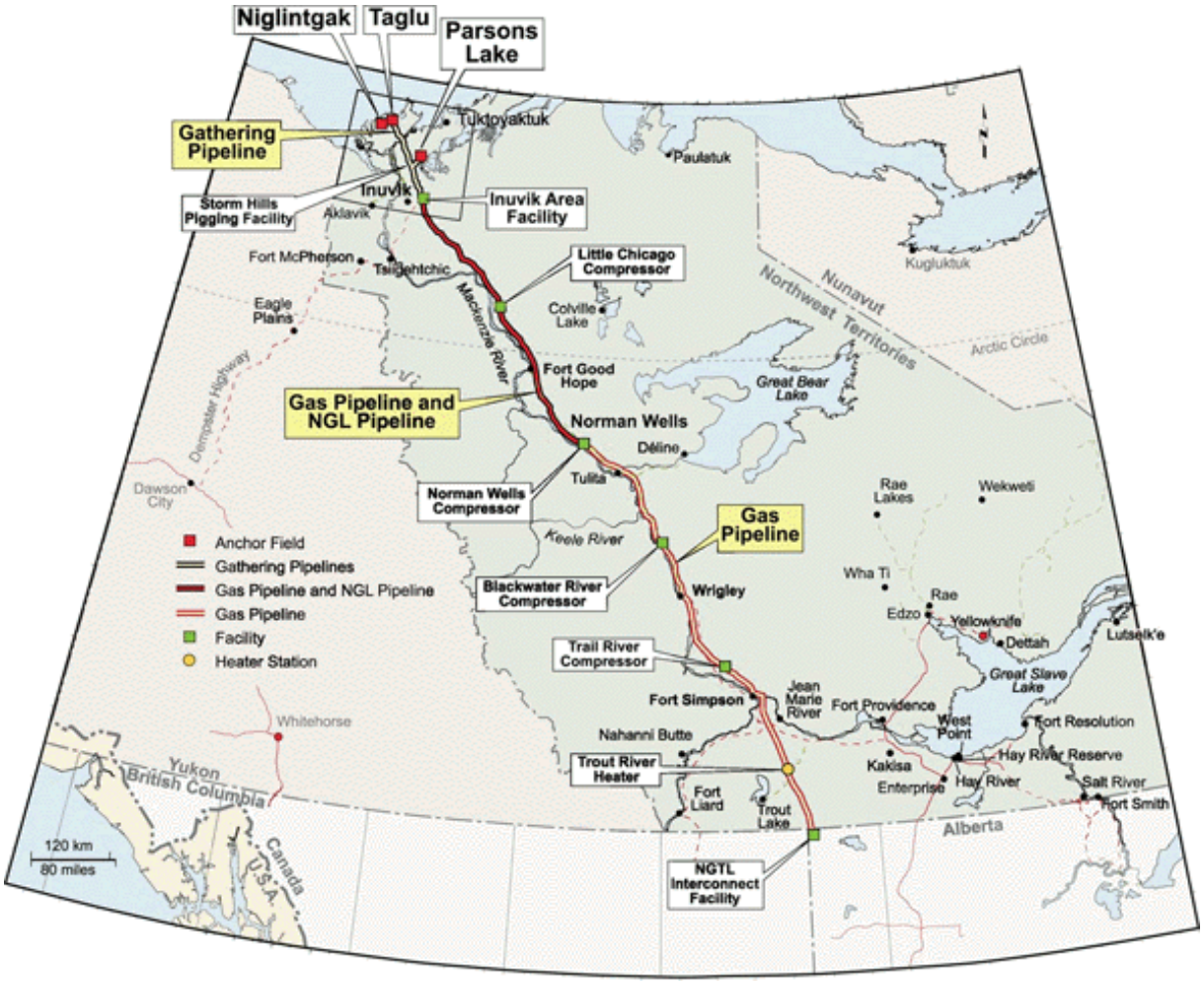

Figure 3.1. Route plan for the proposed Mackenzie Valley gas pipeline (from Mackenzie Gas Project, www.mackenziegas project.com/theProject/overview/index/html Accessed April 2005)

3.2. Geological and Physiographic Setting

3.2.1. Introduction

A brief overview of the geological features, as well as the overall physiography is presented.

The geological structure of the Mackenzie Valley pipeline corridor consists of a thin cover of unconsolidated, glacially derived, sediments on top of the nearly horizontal sedimentary bedrock (1000 m – several km thick) of the Interior Platform, and in turn overlying the ancient sedimentary and crystalline rocks of the Canadian Shield. Figure 3.2 shows a simplified map of the geological provinces in north western Canada.

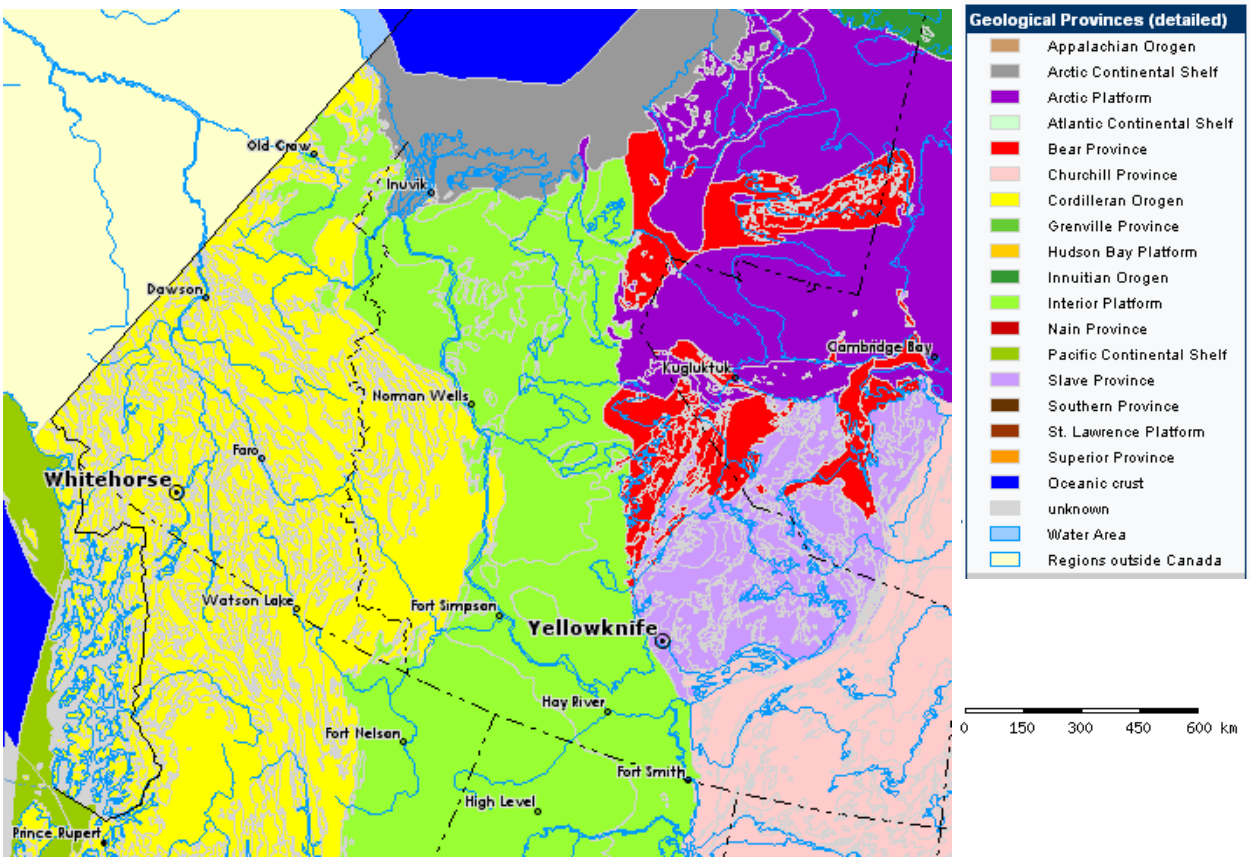

Figure 3.2. Geological Provinces, north western Canada (from Atlas of Canada, http://atlas.gc.ca/site/english/maps/environment/geology/geological provinces. Accessed April 2005)

Permafrost is an important characteristic of the Mackenzie Valley, resulting in frozen surficial sediments; patchy and thin, only a few meters thick, in the south, and almost continuous and deep in the north (Dyke and Brooks, 2000).

The pipeline route crosses the following four geological sub regions (as defined by reports prepared by the Mackenzie Gas Producer Group, April 2003).

- Mackenzie Valley Delta
- Mackenzie Valley North
- Mackenzie Valley South
- Great Slave Plain – Alberta Plateau

Appendix 3.1 contains a chart showing the age and duration of the various geological time designators used throughout this report. Broadly, geological time[1] is divided into three eons; the very early Archean (> 2.5 Ga), the Proterozoic (2.5 – 0.5 Ga), and later Phanerozoic (540 Ma – present day) Eons. The Precambrian refers to all time prior to 540 Ma, which includes about 90 % of all geologic time.

3.2.2. Physiographic Regions

Mackenzie Valley Delta

The Mackenzie Delta physiographic region (Fig. 3.3) is a flat lying, near sea-level composite delta. It comprises a modern active delta of alluvial silts deposited on top of an older Pleistocene (to 1.8 ma) delta complex consisting of fluvial and glacial deposits of Richards Island and Tuktoyaktuk Peninsula . Over 25,000 lakes and interlaced channels form the delta plain. The ancient deltaic plain of Tuktoyaktuk Peninsula is pockmarked with numerous small lakes

Sedimentary bedrock underlying the Mackenzie Delta is composed mainly of Tertiary shale and deltaic sandstone (MGP, 2003) on top of earlier faulted Paleozoic carbonates. The Tertiary sediments thicken to more than 12 km a short distance seaward of the present shoreline (Collette and Dallimore, 2002). On shore, the same Tertiary sediments are about 1 km and overly about a 1 km thickness of Paleozoic carbonate rock. Depth to bedrock varies, from 70 m near Inuvik, 60 m on Richards Island, and increases to over 150 m near the seaward limit of the modern delta (MGP, 2003). Large scale faults are present in the Tertiary sedimentary rocks near the Beaufort Sea continental margin.

The Beaufort – Mackenzie region hosts 53 significant oil and natural gas discoveries (Lane, 2002) several of which underlie the pipeline route.

Mackenzie Valley North

Mackenzie Valley North is within the broad Anderson Plain physiographic region (Fig. 3.3) and is underlain by flat-lying Upper and Middle Devonian shale (MGP, 2003). Surficial deposits consist of hummocky moraine (2 to 20 m thick) and glaciolacustrine silt and clay (2 to 15m thick, occasionally 25 m thick). Northern portions of the pipeline corridor are covered by areas of bog and fen and thermokarst[2] depressions filled with organic-rich silts and clays (MGP, 2003).

[1] Billion years are abbreviated as *ga*, and million years as *ma*.
[2] *Thermokarst* refers to collapse landforms (troughs and depressions) resulting from thawing of ice-rich permafrost.

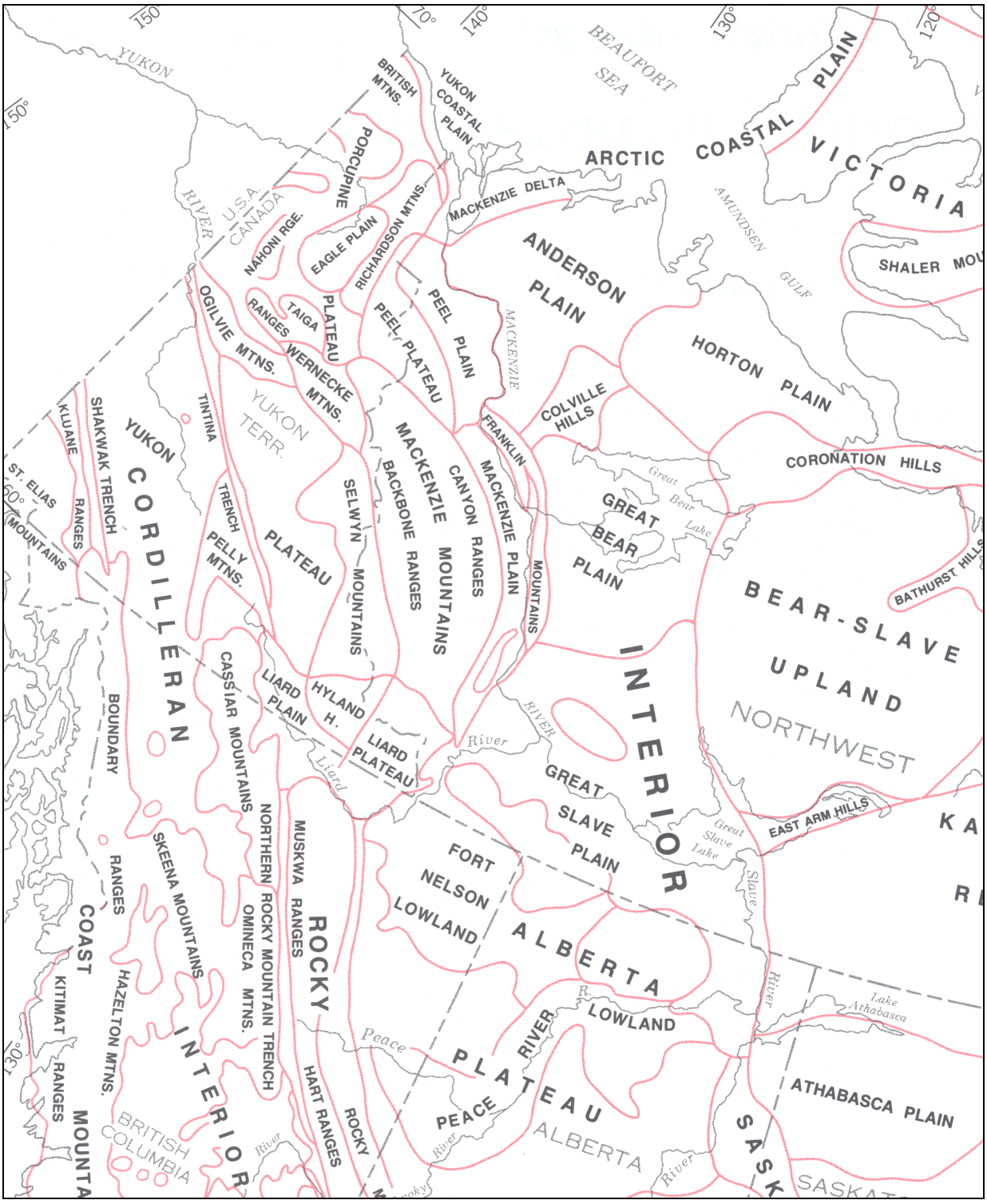

Figure 3.3. Physiographic elements of the Interior Platform, north western Canada. (from Stott and Klassen, 1993).

Terrain is relatively flat and featureless. A few areas have hummocky topography with drumlins (MGP, 2003). Elevation ranges from 90 to 300m, with highest point north of Fort Good Hope and lowest in the narrow lowland adjacent to the Mackenzie River.

Mackenzie Valley South

Mackenzie Valley South is situated in the Mackenzie Plain physiographic region, with the Mackenzie river separating the Franklin Mountains to the east and the Mackenzie Mountains to the west. Much of the area is underlain by weakly resistant Lower Cretaceous bentonitic clay shale and sandstone (Stott and Klassen, 1993; MGP, 2003). Upper Devonian and Lower Cretaceous shales underlie the southern part.

Surficial geology is complex, and includes glacial moraine till (2 to 20m thick), galciolustrine sediments (1.5 to 15m thick) and bedrock exposures.

Terrain varies from level to undulating topography. Elevation is about 50 m in the north, to rolling topography with elevations between 200 and 300 m in the south end (MGP, 2003). Elevations on adjacent mountain ranges exceed 1,500m.

Great Slave Plain – Alberta Plateau

This geological subregion lies within the Great Slave Plain – Alberta Plateau physiographic region. The pipeline crosses the Great Slave Plain portion of the Great Slave Plain – Alberta Plateau physiographic region, which has generally little relief and is underlain by Upper Devonian mudstone, siltstone and shale, and Lower Cretaceous shale.

Former Glacial Lake McConnell, which extended from modern Great Bear Lake to Lake Athabasca, deposited a thick mantle of glaciolucustrine silts, eolian sand and alluvial sand and gravel deposits within the present Mackenzie River valley. Glacial till moraine was also deposited. Surficial sediments can be up to 20 m thick (Aylsworth et al., 2000). Poor drainage has resulted in large areas of peatland (Stott and Klassen, 1993).

Terrain is level to gently undulating. Elevation ranges from 150 m near the Mackenzie River rising to a maximum of 750 m at the Redknife Hill located between the Great Slave plain and the Alberta Plateau.

3.2.3 Surficial Deposits

Figure 3.4 shows the distribution of the dominant surficial deposits along the pipeline route. North and south ends of the pipeline are underlain by morainal deposits, with lacustrine deposits underlying the remainder of the route.

Most of the Mackenzie Valley is covered by a thin and discontinuous to thick and continuous ground moraine (till[1]) deposits. In places, the moraine blankets or veneers the underlying bedrock and in other locations the moraine deposits produce a hummocky, rolling topography (Aylsworth et al., 2000). Till is often present beneath other kinds of surficial deposits.

[1] *Till* is poorly sorted, nonstratified sediment (composed of clay-size to boulder-size material) carried or deposited by a glacier; where the matrix is fine grained, ground ice is often present (Aylsworth et al., 2000)

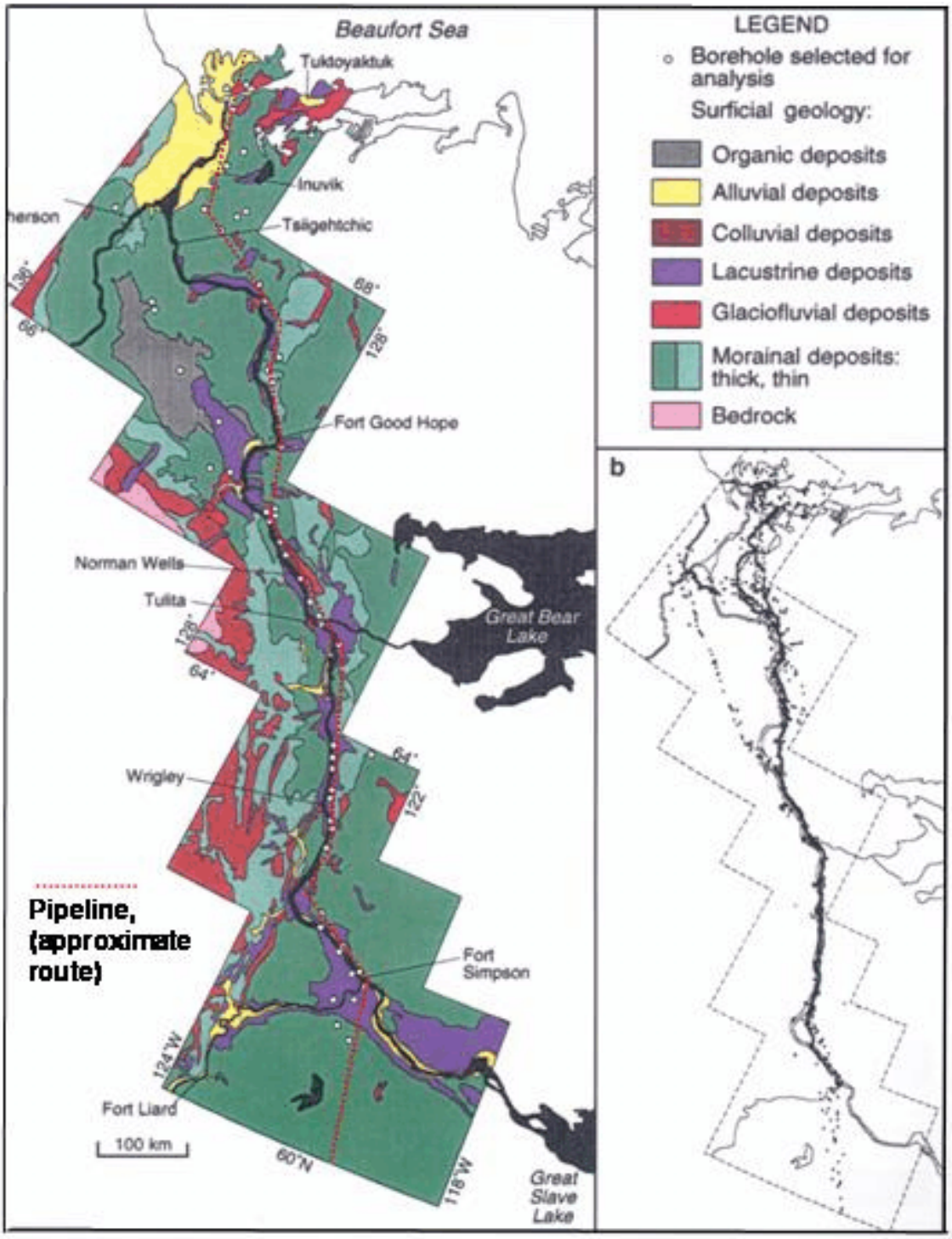

Figure 3.4. Major surficial deposits along pipeline route in the Mackenzie Valley. (modified after Aylsworth et al., 2002).

Much of the central axis of the Mackenzie Valley (bounding the river) is characterized by thick deposits of glaciolacustrine and lacustrine[1] silt and clay, as a result of temporary, large lake basins formed during deglaciation (Aylsworth et al., 2000). Formation of ground ice is common in these fine-grained sediments, and has resulted in development of thermokarst features. Raised sand deltas cover the sand and clay deposits in the Norman Wells and Fort Good Hope areas.

Glaciofluvial[2] deposits of sand and gravel underlie parts of the northern most portion of the pipeline, particularly along the lateral line from KP 0 at Taglu to KP 0 at Storm Hills. These coarser-grained sediments are less susceptible to ground-ice formation because they are usually well-drained (Aylsworth et al., 2000).

Alluvial sediments, ranging from silt to sand to gravel, cap alluvial terraces formed as the Mackenzie River and its tributaries eroded down through the lacustrine deposits, but are usually situated adjacent to the river and off the pipeline route.

The Mackenzie Delta, where the Mackenzie River empties into the Beaufort Sea, is characterized by modern alluvial deposition onto a broad floodplain, and point bars and channel bars of the numerous meandering river channels. Except in the vicinity of the KP 0 Taglu lateral line, the pipeline does not cross the delta sediments.

Organic deposits–both fen and bog dominant peatlands – occur along the pipeline route in the vicinity of, and to the south of Fort Simpson. Bogs are commonly frozen (0.3-0.5 m below ground surface to a depth of 6 to 8 m or more) and ground ice is common (Aylsworth and Kettles, 2000). Fens are generally unfrozen, and found on the route immediately south of Fort Simpson between KP 1000 and KP 1045.

3.2.4. Sedimentary Bedrock

The sedimentary cover rocks within the Mackenzie Valley are the northern continuation of the Interior Platform (Fig 3.2), and were deposited during the Phanerozoic Eon some 540 to 70 million years ago. Here, lower and middle Paleozoic clastic (siltstone, sandstones), carbonate (limestone, dolomite) and evaporate (halite, gypsum) beds lie on the older Precambrian sedimentary and crystalline rocks of the Canadian Shield as an eastward tapering wedge onto the shield (Stott and Aitken, 1993). A veneer of Cretaceous-age clastic rocks forms the upper part of the Interior Platform.

The thickest sedimentary cover occurs west of Mackenzie River in the folded Cordilleran mountain ranges and in Mackenzie Delta and its offshore Beaufort Sea. Maximum thickness exceeds 7 km (Stott and Aitken, 1993). North of 60 degree latitude, the Interior Platform has a number of sub-basins.

In the Fort Simpson area, the Interior Platform is shallower. Here, the Precambrian basement rocks are covered by up to 1000 m of Devonian sedimentary rocks, consisting of gently westward-dipping shale, siltstone and limestone. (Wu et al, 2005).

[1] *Glaciolacustrine* and *lacustrine* pertain to deposits produced by, or belonging to glacial formed lakes and non-glacial lakes (Easterbrook, 1999)

[2] *Glaciofluvial* pertains to deposits formed by meltwater streams flowing from glaciers (Easterbrook, 1999)

In the Norman Wells area, the 200-1000m thick Upper Cambrian Saline River salt and evaporate layer is situated 1.5 – 2 km below at the base of the 2 km thick Interior Platform sedimentary rock. Regional compressional tectonics has resulted in low angle thrust faults at depth in the underlying sedimentary rock.

Based on the scale of geological maps reviewed, it does not appear that the pipeline route crosses surface exposures of bedrock. In the vicinity of Wrigley, between about KP 720 and KP 840, bedrock is present some 5 to 15 km east of the route.

3.2.5 Tectonic Framework

Figure 3.5 shows the tectonic elements - major structural features - in the Mackenzie Valley region.

Interior Platform

The northern portion of the Phanerozoic Interior Platform is situated between two orogens (mountain building episodes), represented by the Franklin Mountains to the east and the Mackenzie Mountains to the west. It represents shale and sandstone deposits derived from sediments shed off the ancient western margins of the paleo North American continent, and limestone accumulated during quiescent times.

Gently deformed Cambrian to Devonian (540- 355 ma) strata of the western Canada sedimentary basin form a "thin" 7 km veneer over the older Proterozoic rocks of the underlying Canadian Shield. Sub-basins and arches developed on the regional paleo Precambrian topography cause a down and upwarping of the Interior Platform sedimentary rock.

The Beaufort Sea continental margin is structural complex, involving rifting and compressional episodes that lead to formation of the Beaufort-Mackenzie Basin (O'Leary et al., 1995), a subsiding trough formed by opening of the western Arctic ocean. The distant floor of the basin is oceanic crust. Proximal to the coastline the basin floor is sedimentary rocks of the Interior Platform resting on top of crystalline rocks of the Canadian Shield. Crustal-scale listric faults of the Eskimo Lake Fault Zone define the onshore southeast margin of the basin (Dixon et al., 2001).

Basement

Lying beneath the sedimentary rocks of the Interior Platform are the Proterozoic and Archean age basement rocks of the Canadian Shield. The northwestern Canadian Shield (the Slave craton) was assembled 4.0 – 3.5 to ~ 2.5 ga (Veijo and Clowes, 2003) by tectonic accretion as oceanic lithosphere was consumed by multiple subduction and rifting into the Slave craton (Cook et al., 1999). Later, about 1.9 to 1.8 ga during the Wopmay orogenic episode, micro continents and volcanic islands collided with and welded to the western margin of the ancient Slave craton by subduction of the lithosphere (analogous to the Pacific plate diving beneath the North American continent). Remnants of the subduction zone are visible today as seismic reflections dipping from

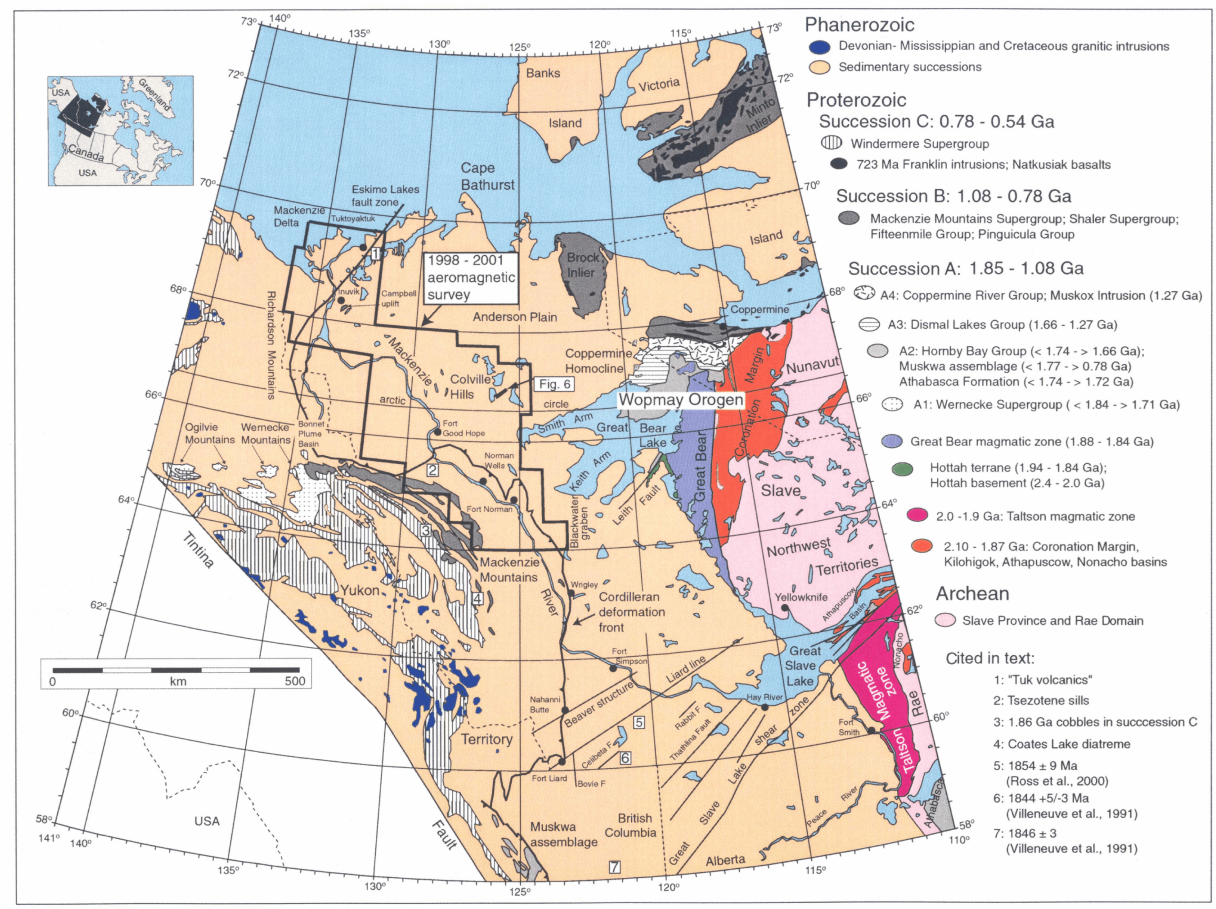

Figure 3.5. Major tectonic elements, north western Canada (from Aspler et al., 2003).

the crust to 80-100 km deep into the upper mantle (Cook et al., 1999). The various terranes[1] comprising the Wopmay orogen occur beneath and flank the Mackenzie Valley, but are covered by the Interior Platform sedimentary rocks. Figure 3.6 shows the interpreted distribution of the tectonic domains beneath the Interior Platform sedimentary cover and along the Mackenzie Valley

Following collision of the westernmost terranes, regional tectonic extension, around 1.75 Ga, in western Canada produced a 1500 km long north-south trending margin or series of basins into which huge (>20 km) deposits of sedimentary rocks were deposited (Cook et al., 1999), including the Fort Simpson Basin.

[1] *Terranes* are distinctive assemblages of rock deposited into specific tectonic environments during particular periods of time (OFR 2948).

Faults and Other Structures Crossing Pipeline Route

Major faults and other structures crossing the pipeline route occur at the following locations, as shown on Figure 3.6:

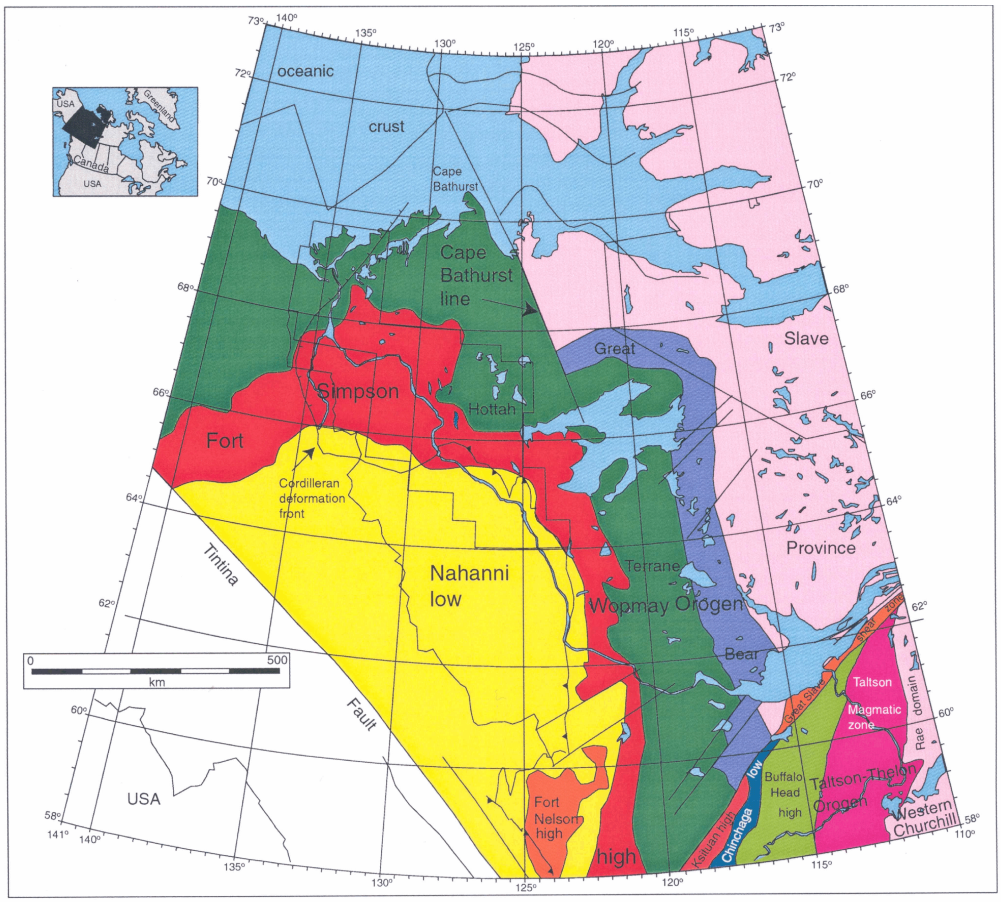

Figure 3.6. Interpreted basement tectonic domains and structural elements in northwestern Canada (from Aspler et al., 2003).

- Laird Line - at about KP1100 - marks a change in the character of the Fort Simpson Magnetic Anomaly. North of the line are the 1.2 Ga Tweed Lake basalts lying within Proterozoic sedimentary strata. South of the line are granites of the Fort Simpson Terrane that underlie the Proterozoic sediments (Asper et al, 2003)
- Beaver River Structure – at about KP 1010 – is ancient, possibly Precambrian, significant cross-strike structural discontinuity.
- Cordilleran Deformation Front – swings across the pipeline at about KP 545 – 875
- East Eskimo Lakes Fault Zone – about 30 km north of Inuvik - is an array of northeast striking echelon[1] faults, which define the southeast margin of the Beaufort-Mackenzie Basin.

The 1.2 Ga old Mackenzie dyke swarm was a widespread igneous event that resulted in intrusion of narrow bands of basaltic rock into the pre-existing Proterozoic sedimentary rock.

[1] *En echelon* denotes overlapping or offset geological structures.

3.3. Permafrost Conditions along Pipeline Route

3.3.1 Distribution of Permafrost

Permafrost[1] underlies most of the Mackenzie Valley. As a result, surficial deposits are usually frozen and often contain ground ice (Aylsworth et al., 2000). Figure 3.7 shows the distribution of permafrost zones and ground ice conditions in Canada. Figure 3.8 provides a more detailed view along the Mackenzie Valley and pipeline route and description of the various permafrost zones. Table 3.1 provides a list of pipeline kilometer points for eacy permafrost zone. The route crosses thick and cold continuous permafrost in the north to warm thin permafrost in the south (Terrain Science Division, 2005a).

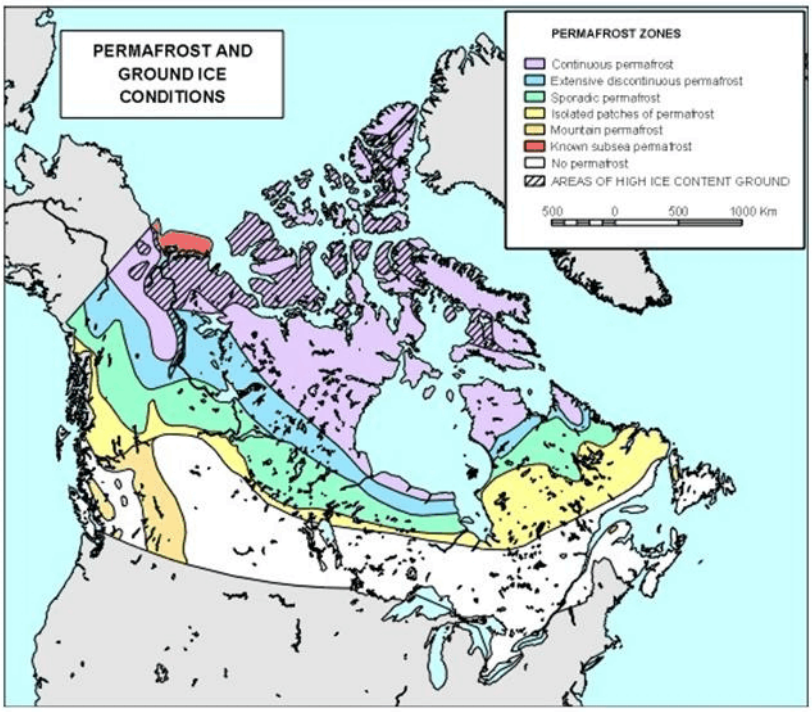

Figure 3.7. Permafrost zones in Canada (from Geological Survey of Canada, http://sts.gsc.nrcan.ca/permafrost/pfmapheg2.jpg Accessed April 2005).

The northern most 20% of the route lies within the Continuous Permafrost Zone, except for a small portion in the Mackenzie Delta which is in the Intermediate Discontinuous Zone.

The central part, about 45% of the route, lies within the Discontinuous Permafrost Zones where there is a decreasing coverage of permafrost from extensive to intermediate discontinuous.

The southern 35% of the route is within the Sporadic Discontinuous Permafrost Zone. However, south of KP 1150 permafrost occurrence increases in a southerly direction as terrain increases in elevation onto the Alberta Plateau (Burgess and Smith 2000).

[1] *Permafrost* is ground (soil, rock) that remains at or below 0°C for at least two consecutive years.

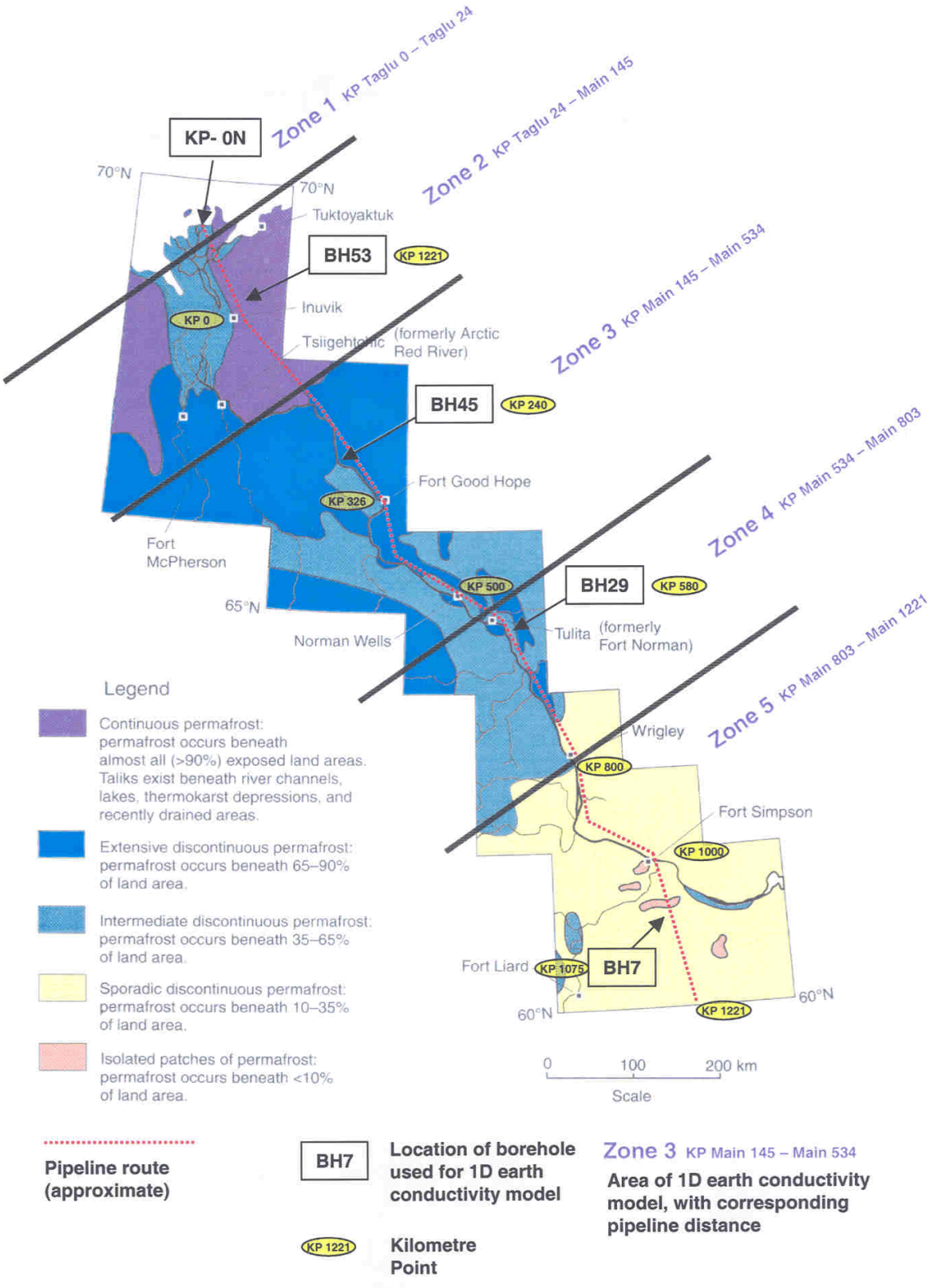

Figure 3.8. Extent of permafrost along pipeline route in the Mackenzie Valley (modified after Heginbottom, 2002). Zones 1 to 5 refer to regions where the different 1D earth conductivity models apply.

Table 3.1: Permafrost zones underlying the proposed MGP pipeline.

Kilometer Point	Permafrost Zone	Permafrost Extent
KP 0 at Taglu – KP 25 lateral	Intermediate Discontinuous	35 – 65 %
KP 25 lateral – KP 0 at Inuvik – KP 125	Continuous	> 90 %
KP 125 – KP 200	Extensive Discontinuous	65 – 90 %
KP 200 – KP 750	Intermediate Discontinuous	35 – 65 %
KP 750 – KP 1221	Sporadic Discontinuous	10 – 35 %

Figure 3.9 illustrates the distribution of ground ice along the pipeline route. About two-thirds of the route is underlain by *Moderate Ice Content* permafrost. This is the most extensive category in the Mackenzie Valley (from KP 0 at Taglu to KP 680 mainline, and KP 1060 to KP 1221), containing

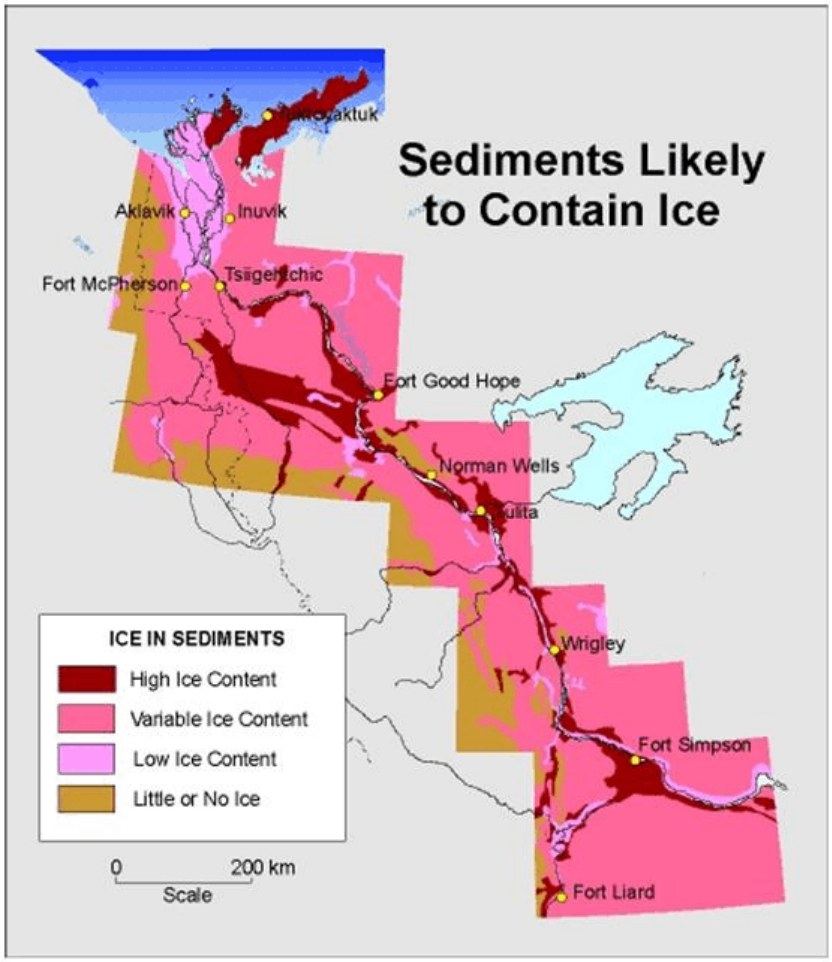

Figure 3.9. Distribution of ground ice in the Mackenzie Valley.
(http://sts.gsc.nrcan.ca/permafrost/climate.html Accessed April 2005).

5 % to 15 % ice. It is most common in areas of till plains, including those with extensive peat cover, and the Mackenzie Delta Plain. About 25 % of the route (from KP 680 to KP 1000) passes through several different types of ice content permafrost, ranging from *Variable* (0- > 15 %), *Nil* (0 %), *Low* (0 – 5 %) to *Moderate* (5 – 15 %) depending on proximity of the route to the Mackenzie River.

The majority of the route is within the *Variable* class where the ice content varies greatly in space, on scales of meters to kilometers and from high to negligible ice content (Heginbottom, 2000). Along the Norman Wells (KP 473 to KP 1221) portion of the pipeline route, within the permafrost encountered the average visible ice content was about 20 % by volume but was commonly up to 40 % (Burgess and Lawrence, 2000).

Ground ice occurs in two main forms (Heginbottom, 2000), as follows:

(a) structure forming ice, where the ice bonds the sediments, and consists of segregated ice, intrusive ice, reticulate vein ice, ice crystals, and icy coatings on particles, and;

(b) pure ice, consisting of large bodies of more or less pure ice, and found in pingo cores, as massive icy beds and icy wedges.

In the Fort Simpson area (KP 1000 to KP 1060), at the confluence of the Laird and Mackenzie Rivers, the route passes through an area mostly free of permafrost and therefore lacks perennial ground ice (Heginbottom, 2000). In the Parsons Lake area, the ice content is variable (0 - >15 %).

3.3.2 Permafrost Thickness

Figures 3.10 and 3.11 show the permafrost thickness varies along the north and south parts pipeline route. Figure 3.12 shows the latitude variation of permafrost thickness, and describes how earlier climatic conditions controlled permafrost development. Permafrost thickness is a function of surface (air) temperature for the past hundreds to thousand years, and the ground thermal properties (Taylor et al., 2000). Permafrost may be twice as thick in sands or sandstone as in clays or shale, because the thermal conductivity of sands and sandstone are typically twice that of clays or shale (Taylor et al., 2000).

A review of *The Physical Environment of the Mackenzie Valley Northwest Territories: A Base Line for the Assessment of Environmental Change* report revealed the following permafrost thickness depths:

- Mackenzie Delta, less than 100m, and in the adjoining Tuktoyaktuk coastlands up to 663 m (Taylor et al 2000). Warming of the local landscape by the Mackenzie River and shifting channels has resulted in a discontinuous and thinner permafrost in the Mackenzie Delta (Kokelj, 2003) than surrounding ground.
- Inuvik area, thicknesses greater than 100 m are common.
- Parson's Lake area, variable thickness from 350 m to 588 m (Taylor et al., 2000)
- On pipeline ROW, west of Parson's Lake, thickness is 347 m (Taylor et al., 2000)
- In the mid-valley (Norman Wells area), thickness varies from 35 m to 143 m (Taylor et al., 2000)
- In the upper valley (Fort Simpson), permafrost is thin or absent (Taylor et al 2000)

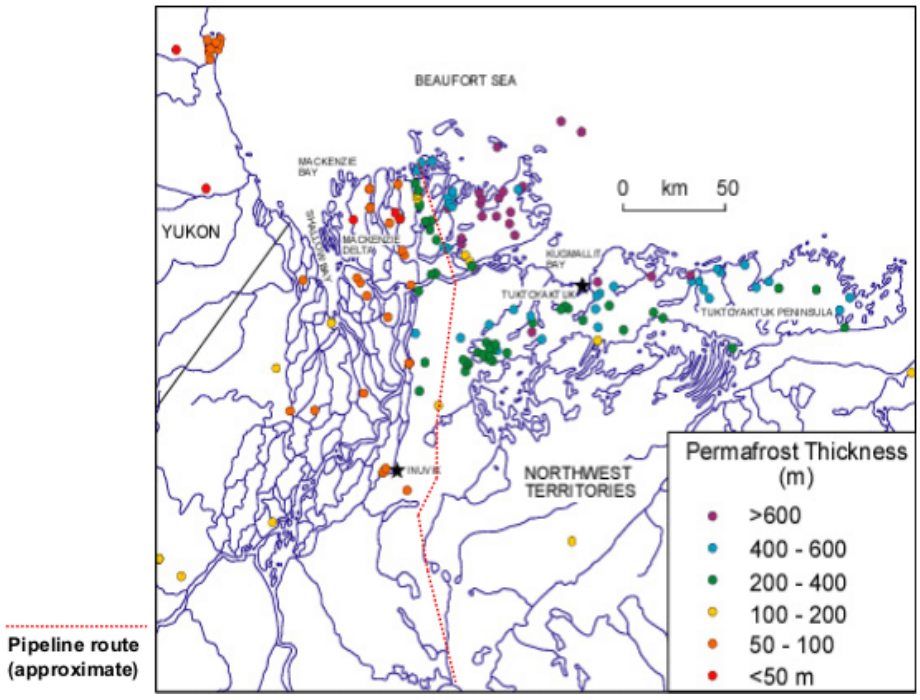

Figure 3.10. Permafrost thickness along pipeline route, Mackenzie Delta portion (http://sts.gsc.nrcan.ca/permafrost/permafrostdatabases/pfthickedelta.jpg Accessed April 2005).

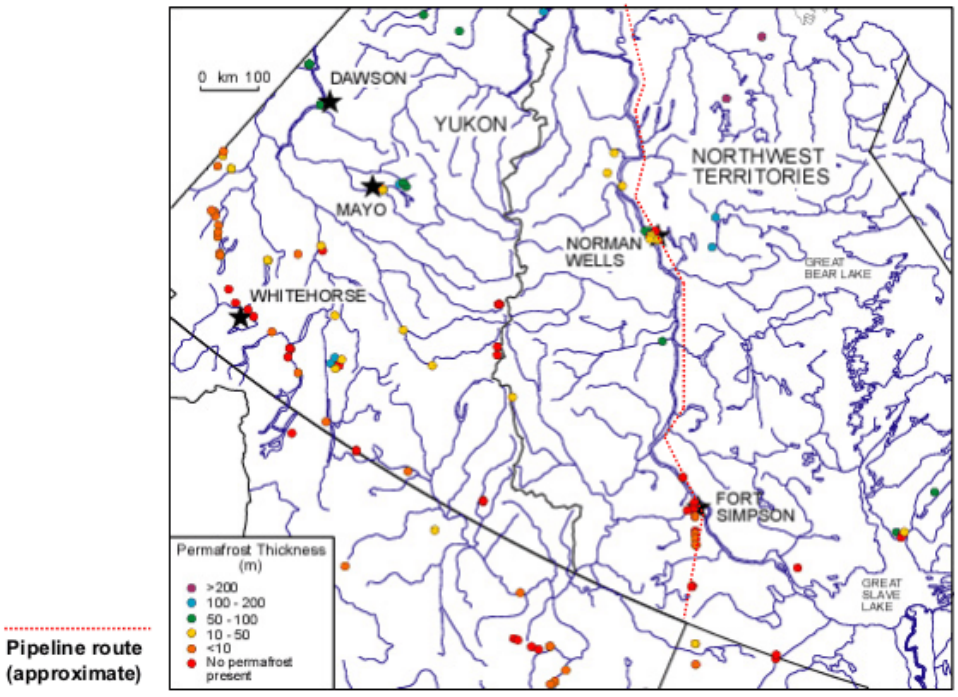

Figure 3.11. Permafrost thickness along pipeline route, central and southern Mackenzie Valley portion (http://sts.gsc.nrcan.ca/permafrost/permafrostdatabases/pfthickvalley.jpg Accessed April 2005).

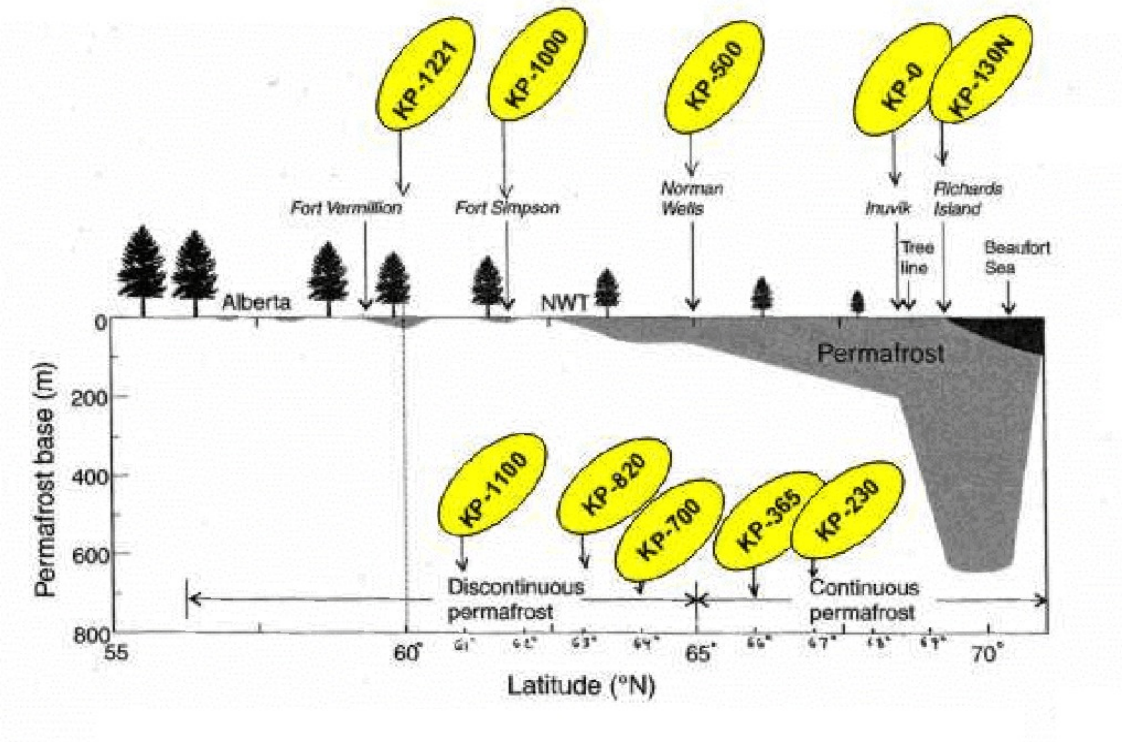

Figure 3.12. Latitudinal variation in permafrost thickness from the offshore region of the Beaufort Sea through the Mackenzie Valley to northern Alberta. During last glaciation, the Richards Island area and adjacent Beaufort shelf were exposed to cold temperature due to absence of glacial ice or recession of seawater, allowing development of very thick permafrost. Ice sheets insulating the ground from subzero temperatures retarded development of thick permafrost in areas to the south. (from Smith et al., 2001).

3.3.3. Active Layer Thickness along Pipeline Route

Background

The upper part of the ground that thaws each summer and freezes each winter is the active[1] layer, and is not considered to be part of the permafrost (Smith et al., 2000). Climate and local factors such as soil properties, vegetation, presence or absence of organic layer, thermal properties of soil and/or rock, angle of ground slope and orientation to sun, and snow cover all influence the thickness of the active layer, as well as latitude and altitude. However, active layer thickness varies more with local soil properties (texture, moisture content), vegetation and microclimate than with regional atmospheric climate (Nixon et al, 2003).

Extent of surface organic cover is the most effective local factor on the development of an active layer, with snow depth, density and duration also having a strong influence (Nixon, 2000), because they insulate the active layer and retard the amount of thaw the following summer. Bedrock areas may have an active layer several meters deep, whereas in vegetated, organic terrain, under similar climatic conditions, the active layer may be less than 0.5 m thick (Smith et al., 2000).

[1] *Active layer* is the top layer of the ground that is subjected to annual thawing and freezing in areas underlain by permafrost.

Variations of Active Layer Thickness along the Mackenzie Valley

Since 1987, a long-term active layer monitoring program has been maintained throughout the 1400 km length of the Mackenzie Valley (Nixon et al, 2003). Figure 3.13 shows the locations of 17 monitoring sites representative of undisturbed landform and vegetation found in the Arctic, Subarctic and Boreal ecoregions, including both continuous and discontinuous permafrost zones. Figure 3.14 is a plot of active layer thickness versus distance southward along the Mackenzie Valley corridor.

The findings of the study by Nixon et al (2003) are as follows:

- Depth of thaw penetration has increased at most sites (numbers 1-6, 8-13, 15 and 16) over the past 10 - 15 years, but active layer thickness has not always proportionally increased because of variable thaw settlement.
- Active layer thickness is sensitive to yearly fluctuations of atmospheric temperature. Late summer 1996 was one of coolest periods for the region, and there was a noticeable decrease in active layer thickness at many sites. Warmest year on record was in 1998, and there was a marked increase in both active layer thickness and subsidence.
- Active layer thicknesses at Arctic, Subarctic and Boreal sites can be similar in spite of the environmental gradient, demonstrating that factors such as tree cover, organic cover and snow allow development of near-surface permafrost somewhat irrespective of latitude.

  In the Subarctic, tree cover and thicker vegetation insulate the soils allowing an active layer thickness similar to that found in the Arctic ecoregion where there is little or no surface organic cover.
- Within an ecoclimatic province the active layer thickness is controlled by soil properties (texture, moisture and thickness of surface organic layer), vegetation and snow cover.

  In coarse textured Arctic soils (sites 3 and 4) the active layer is thicker than in fine textured soils (sites 1 and 2). In Subarctic soils the texture is not as important a control on active layer thickness because a thick organic surface layer covers most sites.

  In perennially frozen peat deposits (sites 7, 14 and 17), the active layer thickness is always less than the surrounding mineral soils because the peat is a good insulator during summer even though peatlands are sparsely vegetated.
- Ice content of soils has an effect on thaw penetration and subsidence, and ultimately the active layer thickness.
- For high ice content soils (sites 5 and 11) the accumulative thaw depth (active layer + subsidence) is a better indicator of changes in the thawing of soil as a result of (a) climate change, or (b) natural and human disturbance than by examination of the active layer thickness alone.

  For coarse-textured mineral soils with low ice content and peat soils (sites 4, 7, 14, 16 and 17) active layer thickness is a good indicator of the effect of climate changes since little or no subsidence occurs.

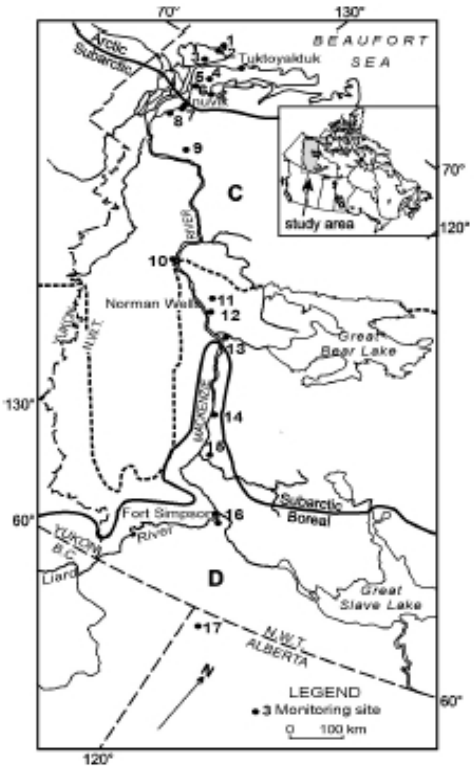

Site	Landform	Vegetation
	ARCTIC	
1	thermokarst coastal plain	low shrub tundra
2	thermokarst slope	low shrub tundra
3	glaciofluvial ridge	low shrub tundra
4	hummocky glaciofluvial	medium shrub tundra
5	till plain	medium shrub tundra
6	valley bottom	high shrub tundra
	SUBARCTIC	
7	polygonal peat plateau	low shrub
8	till plain	open black spruce forest
9	undulating till plain	open black spruce forest
10	fluvial terrace	open black spruce forest
11	lacustrine plain	open black spruce forest
12	fluvial terrace on till	mixed spruce–feather moss
13	alluvial terrace	open black spruce forest
	BOREAL	
14	fluvial terrace in glacio lacustrine plain	mixed black spruce forest
15	abandoned fluvial bar	white spruce–feather moss
16	river bank	birch, aspen, willow forest
17	peat plateau	black spruce forest

Figure 3.13. Locations of active layer monitoring sites along Mackenzie Corridor. Solid lines separate ecoclimatic provinces; dashed line separates **D**iscontinous from **C**ontinous permafrost (from Nixon et al, 2003).

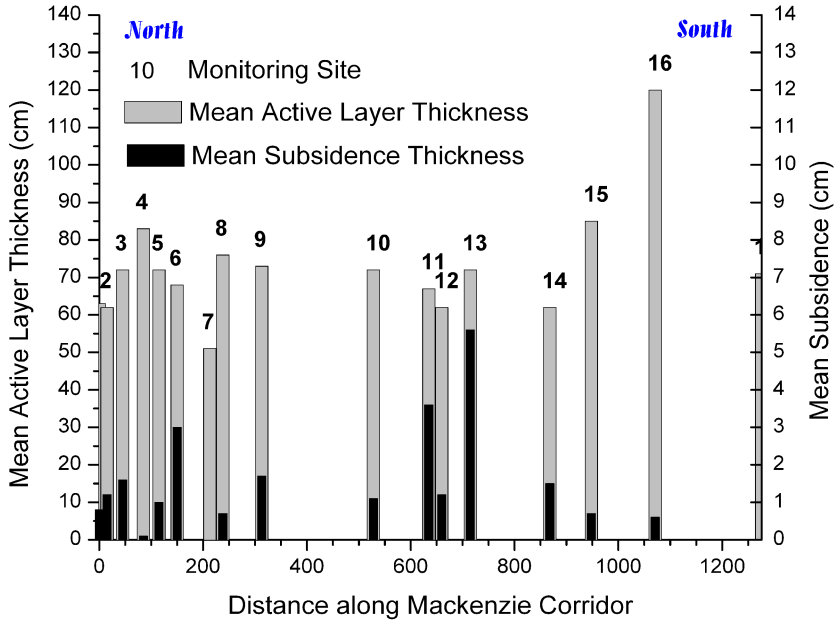

Figure 3.14. Mean active layer thickness and mean subsidence at 17 monitoring sites along the Mackenzie Corridor transect, recorded 1987/93 to 2000. Site locations shown in Figure 3.13. Data from Table 3 in Nixon et al, 2003.

An earlier investigation (Smith et al, 2001) of active layer thickness was undertaken in the Mackenzie Delta – Tuktoyaktuk peninsula region. Figure 3.15 shows the location of the nine monitoring sites, and Figure 3.16 shows the variation of active layer thickness and summer thaw penetration during the eight year period from 1991 to 1998.

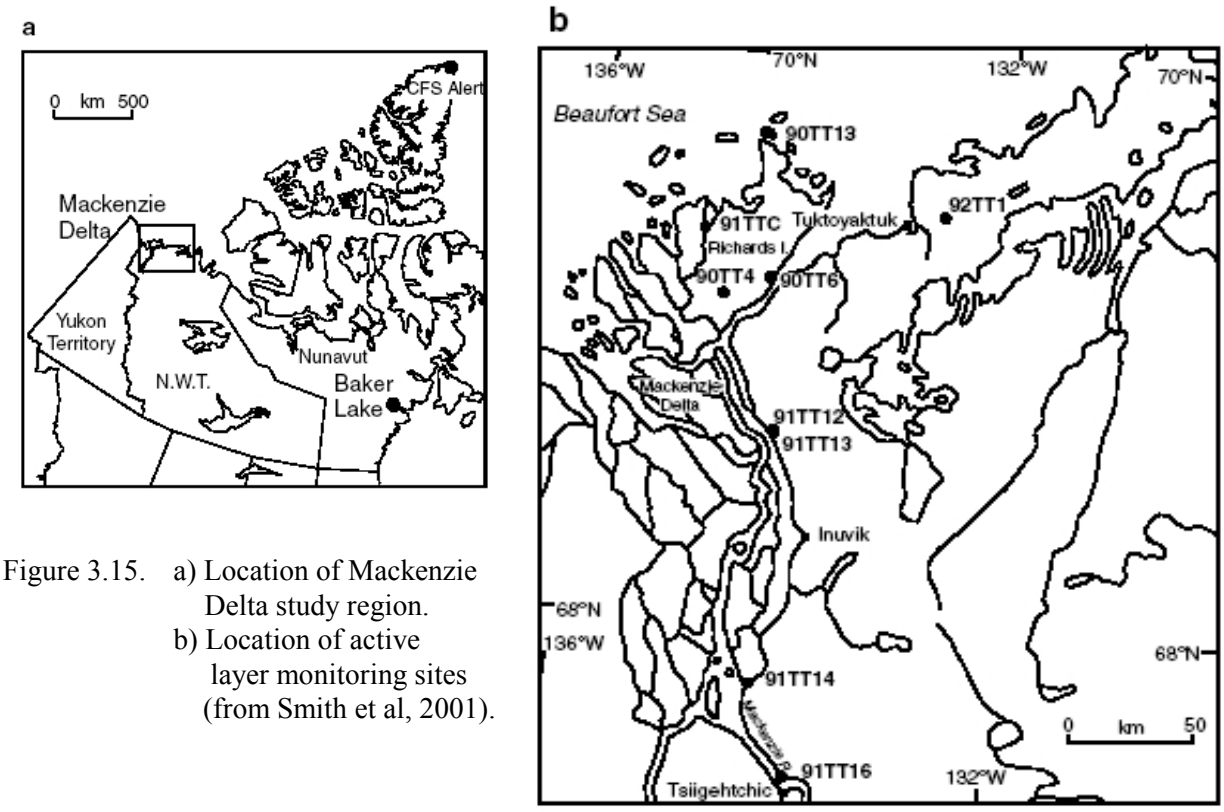

Figure 3.15. a) Location of Mackenzie Delta study region.
b) Location of active layer monitoring sites (from Smith et al, 2001).

The study revealed that:

- Active layer thickness range was;
  - 50 cm – 100 cm in the tundra of the Tuktoyaktuk coastlands,
  - 135 cm – 165 cm in the Mackenzie Delta, and,
  - 107 cm – 140 cm in the lower Mackenzie Valley (south of Inuvik)
- Significant interannual variation of active layer thickness occurred at some sites, with the thickness active layers being observed in 1998 the warmest year on record. The same trend was observed for thaw penetration.
- Ice-rich soils may experience significant settlement of the ground surface as the seasonal thaw depth increases. At Involuted Hill (site 92TT1), representative of fine-grained ice-rich soil, a large increase in thaw penetration was accompanied by significant ground subsidence and hence very little change in active layer thickness.

In 1994 a monitoring program of the active layer within the Mackenzie Valley revealed the thickness to vary from 38 cm to 182 cm as a result of a complex interplay of site specific and regional factors (Nixon, 2000).

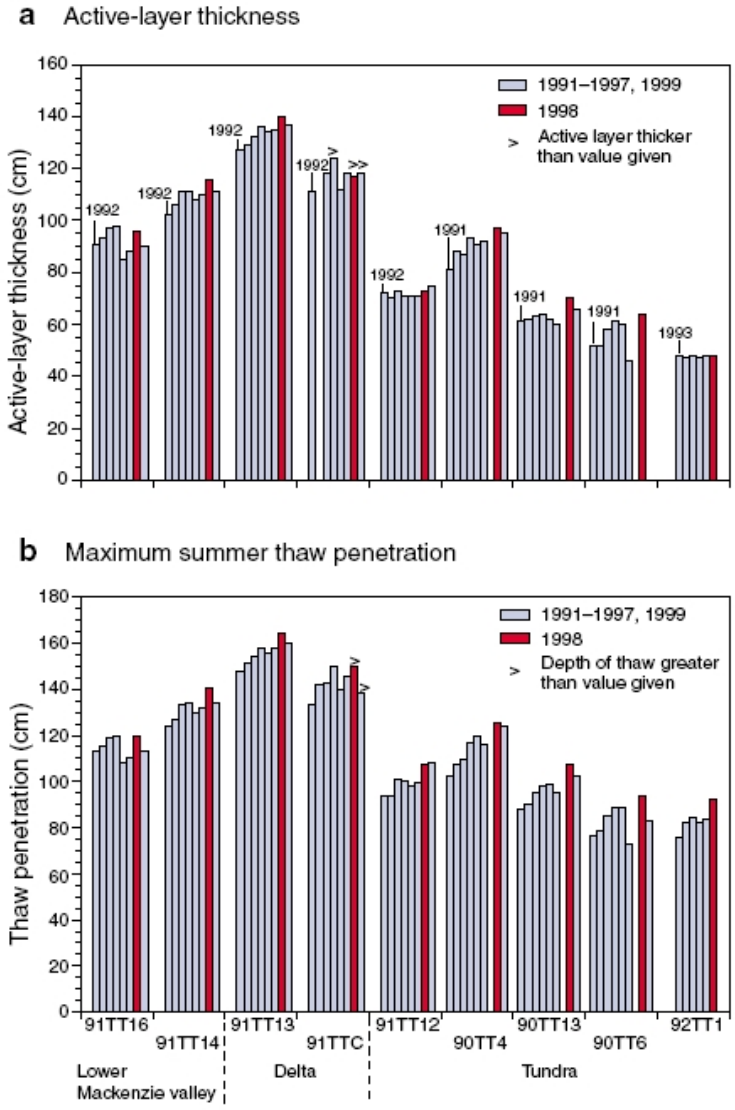

Figure 3.16. a) Active layer thickness and b) maximum summer thaw penetration determined fornine sites in the Mackenzie – Tuktoyaktuk Peninsula region between 1991 and 1999. Thaw penetration is measured relative to a fixed point above the ground surface. A ">" symbol indicates that thaw depth was greater than the maximum value that could be measured (from Smith el al, 2001).

Regional Variations of Active Layer Thickness due to Climate

NWCIMP (2004) reports that from approximately 1990 to 1998, there was a general increase in active layer depth throughout the Mackenzie Valley of about 15 cm. In 1998, the temperature in the Mackenzie region was 3.9 degrees warmer than normal, the warmest year since 1948 when temperature recording began. However, since 1999 the active layer thickness in the Mackenzie Valley has decreased on average more than 10 cm in response to a cooling trend. In 2003, the mean active layer depth was only 1 cm thicker that the active layer a decade earlier.

Variations of Active Layer Thickness along Norman Wells Pipeline

Burgess and Smith (2003) have compiled 17 years of thaw penetration and surface settlement observations along the Norman Wells pipeline extending across 869 km of permafrost terrain. Over the northern half of the pipeline route, lacustrine soils and tills are dominant; in the south half, tills and organic terrain are prevalent.

Active Layer Thickness Observations

Thaw has continued to progress beneath the pipeline ROW after 17 years of pipeline operation (Burgess and Smith, 2003). Clearing of vegetation cover along the pipeline ROW has resulted in alteration of ground surface temperature and accompanying increase in the depth of the active layer (Burgess and Smith, 2000). Prior to construction of the Norman Wells oil pipeline, the active layer depth was generally about 1m or less, and then after construction with removal of organic cover and subsequently a warm pipe-operating temperature, the active layer increased, varying in depth from 1m to 4m. (Burgess and Smith 2000).

Thaw depths on-ROW increased most rapidly within the first 7 years after site establishment, but then continued slowly thereafter. During clearing of the ROW, removal of vegetation (and its insulating effect on thaw prevention) and grading for travel during construction has resulted in the exposure and/or thinning of the surface organic layer, thereby promoting penetration of thaw. A climatic warming period coincided with construction and first years of pipeline operation, and may have contributed to an accelerated rate of ROW thaw (Burgess and Smith, 2003). Subsequent operation of the ambient temperature pipeline, as well as response to thermal effects of ROW clearing and trenching for the pipe have caused thaw to continue downwards.

In 2001, thaw depths on and off-ROW with respect to soil type are listed in Table 3.2 below.

Table 3.2: Thaw depths along Norman Wells pipeline right-of-way.

Proposed Mackenzie Route KP[1]	Existing Norman Wells Pipeline KP[2]	Soil Type	2001 On-ROW Thaw Depth (m)	2001 Off-ROW[3] Thaw Depth (m)	Permafrost Depth (m)
473	0	lacustrine (colder)	3 m - 4 m	< 2 m	50
492	19	coarse mineral soils	5 m to > 7 m	about 2 m	50
744	271	lacustrine (warm)	5 m	< 2m	40
1031	558	coarse mineral soils	5 m to > 7 m	about 3 m	12
1256	783	organic (warm)	3 m - 4 m	2 – 2.5 m	13.5

1. KP - kilometer distance along route, south from Inuvik
2. KP - kilometer distance along pipeline, south from Norman Wells
3. location ranges 20 to 24 m from ROW centre

(Source: Burgess and Smith, 2003, pp. 108)

The rate of an increase of active layer thickness depends on the initial ice content of the soil (Smith, pers. comm.), and in turn the ice content varies with soil type.

3.3.4 Taliks along Pipeline Route

Background

Taliks (also called thaw-bulbs) are unique features in permafrost terrain and are potential sites for placement of components of a pipeline's cathodic protection system. Specifically, the lower electrical resistivity of a talik (in contrast to the more resistive frozen ground) makes it a suitable location for a ground bed or anode. Of particular engineering interest, is the vertical depth and lateral extent of a talik beneath or near surface water courses and lakes along the Mackenzie Valley corridor because it may allow for placement of ribbon anodes where the pipeline crosses a stream or river.

The majority of investigations pertaining to taliks have been focused in the northern part of the Mackenzie corridor, specifically the Mackenzie River, its delta, and adjacent Tuktoyaktuk coastlands. No studies were found specific to tributary creeks and streams that cross the remainder of the pipeline route. Recent environmental assessments completed for the Mackenzie Gas Project (MGP) have noted that "field data on extent and depth of taliks beneath rivers at [pipeline] crossing sites are not provided and are required" (Imperial Oil, 2005). However, some studies have been completed on thawed ground distribution beneath small creeks in the vicinity of the Trans-Alaskan pipeline, and these results are also presented below.

Talik Description and Type

Taliks are locally unfrozen areas of variable shape within or below the continuous and discontinuous zones of permafrost, and exist continuously for more than one year. In comparison the active layer is a laterally continuous zone of thawed ground, seasonally affected. Taliks can be formed both by nature and by man.

Imperial Oil (2005) describes talik type and extent as follows:

> "Taliks are unfrozen zones that are located on top, underneath, or within masses of permafrost. Often, they occur beneath lakes or perennial streams and rivers as a result of water's ability to store and transfer heat from the surface. The vertical extent of taliks is related to the depth and volume of overlying water. Large and deep waterbodies can store and transfer large amounts of heat energy downward into the permafrost. The lateral extent of a talik generally coincides with the edges of the waterbody or are slightly larger. In the case of large rivers that change and move periodically (meander), remnant taliks can exist for a period of time in the location once occupied by the river channel.
>
> *Open* taliks exist between the bottom of small to medium-sized waterbodies and the top of the permafrost surface. *Through* taliks penetrate fully below the base of the permafrost. *Closed* taliks are completely encased in the permafrost and can develop when lakes fill in and become bogs. In these cases, the ground surface freezes over as a result of the removal of surface water, which results in poor heat transfer because of exposure of a ground surface with a low specific heat. Taliks exist at locations coincident with the right-of-way, such as perennial stream crossings. Ephemeral streams are less likely to contain through-taliks but might contain open taliks beneath the substrate surface."

Figure 3.17 illustrates the three common types of taliks; open, through and closed. A glossary of talik terminology and summary of the types and mechanisms of talik formation is provided in Appendix 3.2. Open taliks are characteristically unfrozen ground beneath a surface water body, but can also be in contact with the seasonally thawed active layer. Within discontinuous permafrost, unfrozen ground above and below the permafrost can be connected by chimney-like taliks (sometimes known as through taliks) that perforate the frozen ground (Trenhaile, 1998).

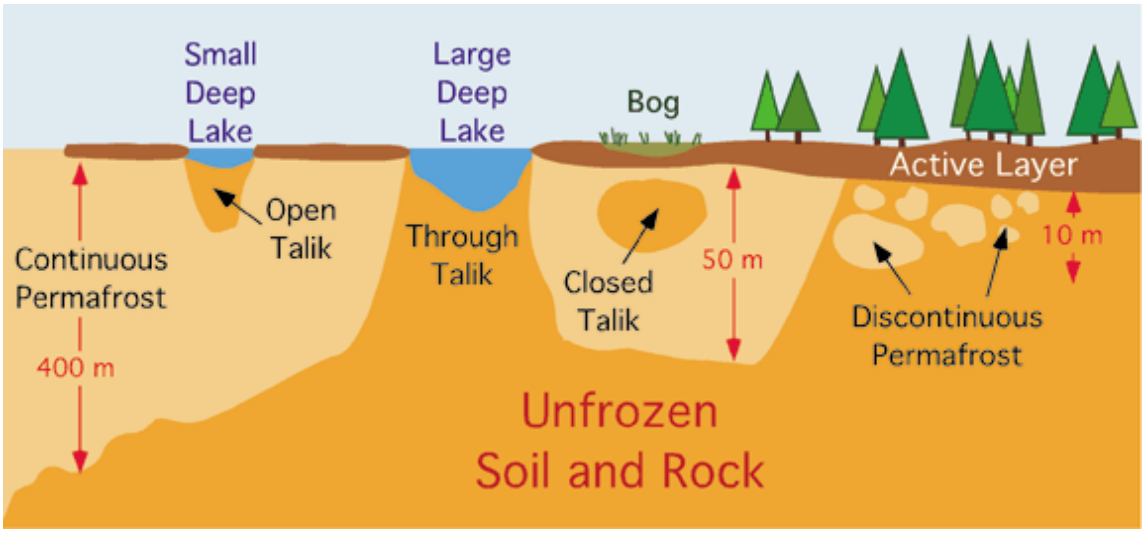

Figure 3.17. Cartoon illustrating the three main types of talik development. (from Pidwirny, 2005).

Factors Affecting Talik Formation

Depth of water appears to be a significant factor in the development of a talik because it prevents or retards the effect of cold air from penetrating and freezing the ground. Many open taliks are the result of heat accumulated in larger and deeper lakes and rivers. If the lake or stream-bottom temperatures falls below 0°C the water body freezes through and the underlying ground remains frozen, as happens with smaller water courses. As water depth of a stream decreases, the duration of ice contact increases, producing lower ground temperature and thicker permafrost, and hence it is less likely that a talik will develop (Dyke 2000). As a general rule, if the water depth is greater than the annual thickness of ice formation, a talik can exist (Imperial Oil, 2005).

Taliks beneath a river bed are not solely formed by the warming effect of flowing surface water, groundwater flow can also have a significant effect (Yershov, 1998), resulting in a greater lateral extent of the talik than may otherwise be anticipated. Presence and type of vegetation is another important factor in the preservation of permafrost along water course shorelines (Dyke 2000). Snow, trapped by vegetation, acts as an insulator thereby raising the ground surface temperature and depressing the depth of the permafrost table. Willows trap more snow and sedge meadows limit snow entrapment (Dyke, 2000). Topography of a stream channel also has an effect. Narrow secondary channel may offer greater protection for snow accumulation, and even if unvegetated, the greater snow drift accumulation has a greater insulation value.

Talik Distribution and Extent – Mackenzie Corridor

Previous investigations, focused on the northern end of the Mackenzie Corridor, have determined talik distribution and dimensions in the following areas:

- Mackenzie Delta: Over 15 % of the terrain in the Mackenzie Delta and adjacent Tuktoyaktuk Coastlands is covered by lakes and drained-lake basins, many of which are underlain by taliks, some of which may penetrate permafrost (Burn, 2002). Many of the 10,000 lakes situated in these areas have shallow (< 1m water depth) terraces up to 100m from the shore, surrounding a deeper central pool. During winter the shallow water over the terrace freezes allowing development of permafrost beneath the terrace but not under the deeper and warmer water of the central pool. Permafrost below the terrace is likely to terminate in a near-vertical surface at the edge of the deeper water (Burn, 2002).

  In absence of a terrace, deep, circular lakes of radius 180 m and oval lakes of half-width 130 m are likely to have through taliks beneath them. However, where lake terraces are 100 m wide, a talik may be present if the radius of a circular lake is greater than 250 m, and if the half-width of an oval lake is 160m or greater (Burn, 2002). Lakes with minimum widths of twice the permafrost thickness are underlain by through-going taliks (work undertaken by Mackay in1979), and all lakes greater than 2 m deep will posses some sort of talik (French, 1996). Former shallow channel or lake deposits situated in the depressions of the hummocky ground surface can have taliks extending down to a depth of 100 m (Pole and Lawton 1991).

- Mackenzie River Channels: Beneath the channels of the Mackenzie River taliks are said to be 200 – 300 m deep (J. Hunter, pers. comm., 2005). During winter there is a substantial amount of water flow in the main channels of the Mackenzie River, beneath the ice cover, which helps to maintain the presence of a talik below the main river channels. Some of these taliks are suspected to extend through to the base of the permafrost (Shell Canada, 2004). Dyke (2000) has commented that a through talik will exist for any channel wider than 70 m. However if it is a migrating channel then the channel width required increases for a through talik to be produced. Figure 3.18 shows the predicted vertical depth and horizontal extent of a talik beneath a 200m wide meandering secondary channel.
- Richards Island: It is estimated that on Richards Island, a lake dominated area between the Harry and East channels of the Mackenzie River, 23 % of the lakes and 10 to 15 % of the island's surface area is underlain by through taliks (Burn, 2002).
- Tuktoyaktuk Coastlands: Taliks underlie all lakes with water depths greater than about 2/3 of the maximum thickness of lake ice, commonly 1.5 to 2 m (Mackay and Burn 2002).
- Niglintak and Taglu gas producing areas: Extensive or through taliks are likely to occur beneath the deep larger lakes and river channels (Shell Canada, 2004), which insulate the underlying soils (Pool and Lawton 1991). Investigations by Shell Canada reveal that across part of the Taglu area, there is a laterally continuous, relatively shallow closed talik, 20 to 60 m thick, situated between an overlying 35 - to 90 m thick permafrost cap and the underlying main permafrost body. It is not known if there are interconnections between the surface water bodies and underlying taliks.

- Parsons Lake: Test drilling results suggest that taliks exist beneath the central parts of Husky Lake and Parsons Lake (Shell Canada, 2004).
- Mackenzie Valley streams: Most small streams in the Mackenzie Valley are shallow and frozen at the bottom during winter, and thus very unlikely to have talik development beneath [S. Smith, pers. comm., 2005]. Depending on water depth, some of the large streams may be underlain by taliks but it is unlikely to be a through talik [S. Smith, pers. comm., 2005].
- Norman Wells Pipeline: Geophysical surveying of the Norman Wells Pipeline in 1977, has shown that near kilometer point KP1100, a talik beneath a 24 m diameter pond extended some 1.5 to 2 m beyond the actively degrading shore embankment (Northern Engineering, 1977). Figure 3.19 shows a typical situation of a talik beneath a small creek crossing a peatland. Here the talik is about 3 m deep and extends some 2.5 m laterally on both sides of the creek.

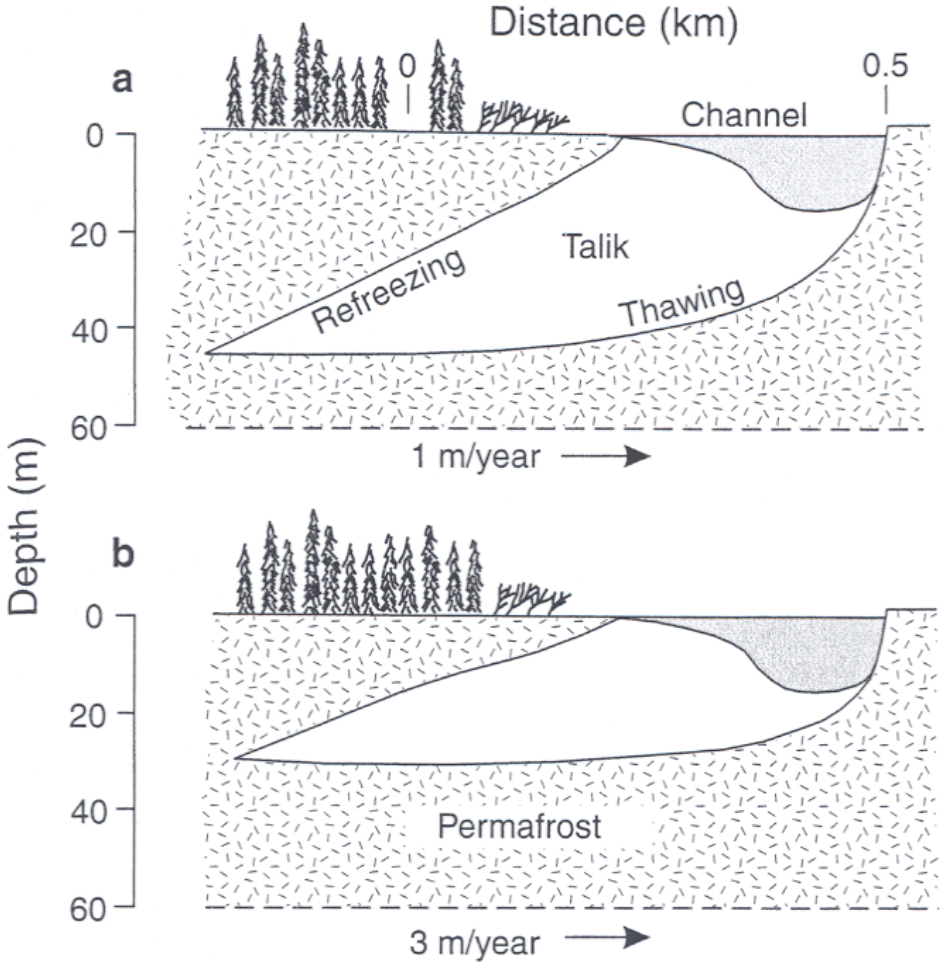

Figure 3.18. Predicted vertical depth and horizontal extent of talik development in the Mackenzie Delta below a secondary river channel migrating at a rate of a) 1 m / year, and b) 3 m / year. (from Dyke, 2000).

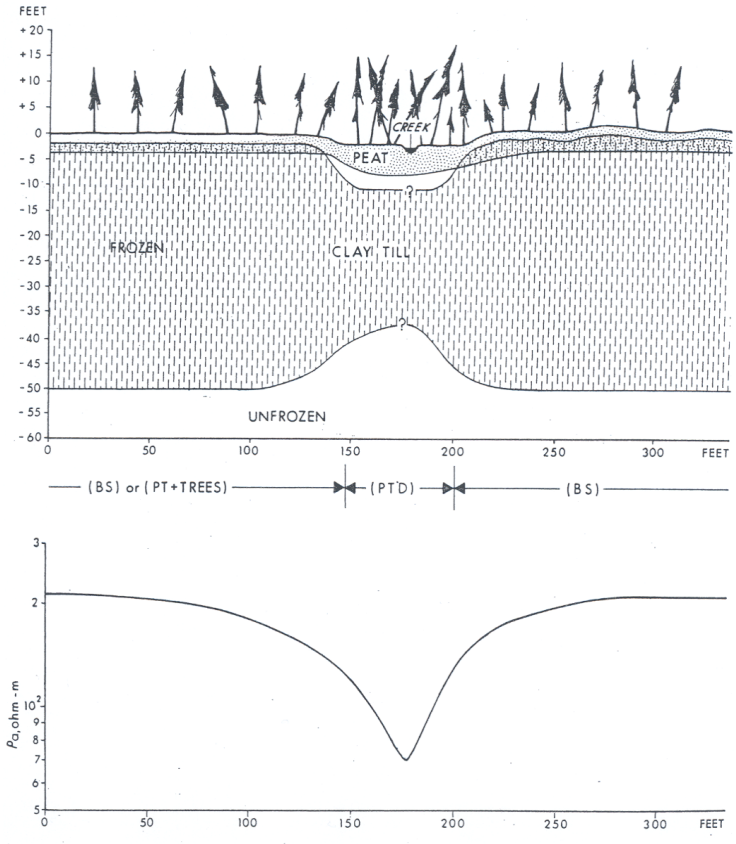

Figure 3.19. Top - An interpreted talik development below a small creek on the Mackenzie pipeline corridor south of Willowlake River (south of KP900). Bottom – the electrical resistivity profile as measured by an EM31 geophysical instrument. (from Northern Engineering Company Limited, 1977).

Talik Distribution and Extent – Other Locations

Past investigations for the Alaska pipeline have shown talik dimensions at these locations, as well as recent work at the Snap Lake diamond mine:

- Sagvanirktok River, Alaska: Geophysical investigations in 1977 were done to map the presence of the talik beneath the west channel of the Sagvanirktok River behind Prudhoe Bay (Northern Engineering, 1976). Results of the survey are shown in Figure 3.20. Thawed gravels beneath the river valley extend about 25 m laterally and some 4 to 20 m deep. Taliks along braided channels of the river were found to occur locally and were of limited width (< 50 m) and length (< 800 m), and depth greater than 12 m (Northern Engineering, 1976).

  A 1998 study of talik depths on the Sagavanirktok river flood plain (25 km south of Prudhoe Bay) in Alaska revealed talik thicknesses to be seasonally variable with talik depth also varying with channel bathymetry (Arcone et al, 1998). Size of the taliks shrinks as it propagates downward during the winter months. In January the talik was thickest beneath the deepest part of the river channel, but almost completely frozen by mid-April. By mid-winter the taliks appeared to be a thin layer extending nearly the width of the river channel, as shown in Figure 3.21.

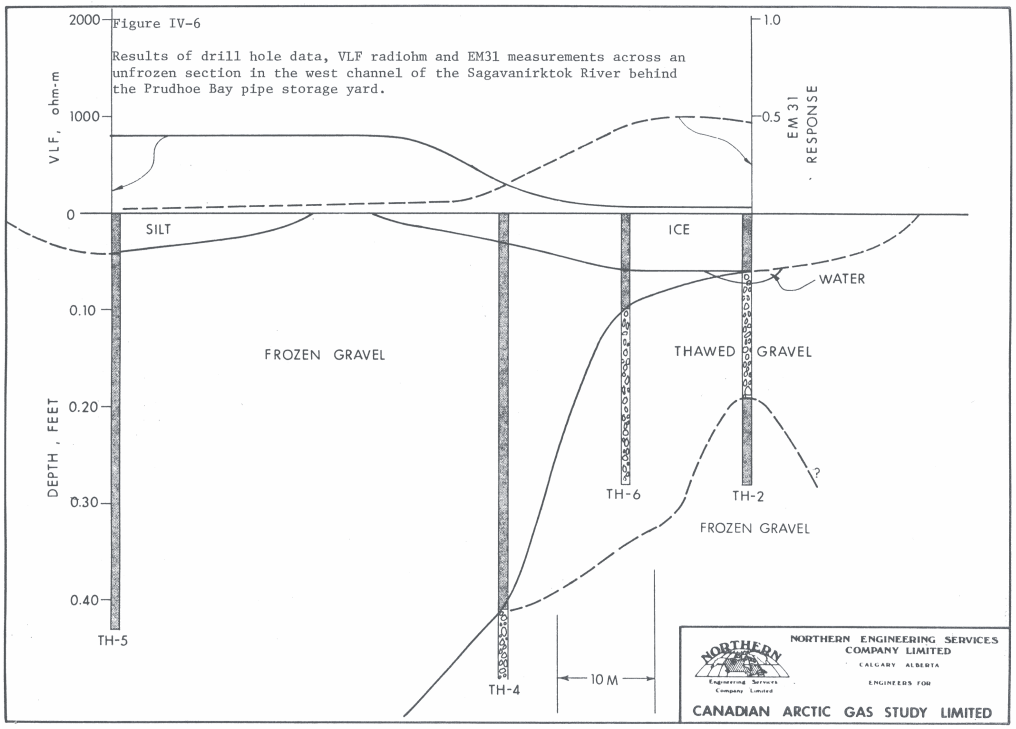

Figure 3.20. Results of boreholes and geophysical surveys (VLF and EM31 instruments) across an unfrozen section in the west channel of the Sagavanirktok River behind the Prudhoe Bay pipe storage yard. Note the thawed gravel talik below the river channel (from Northern Engineering Services Company Limited, 1976).

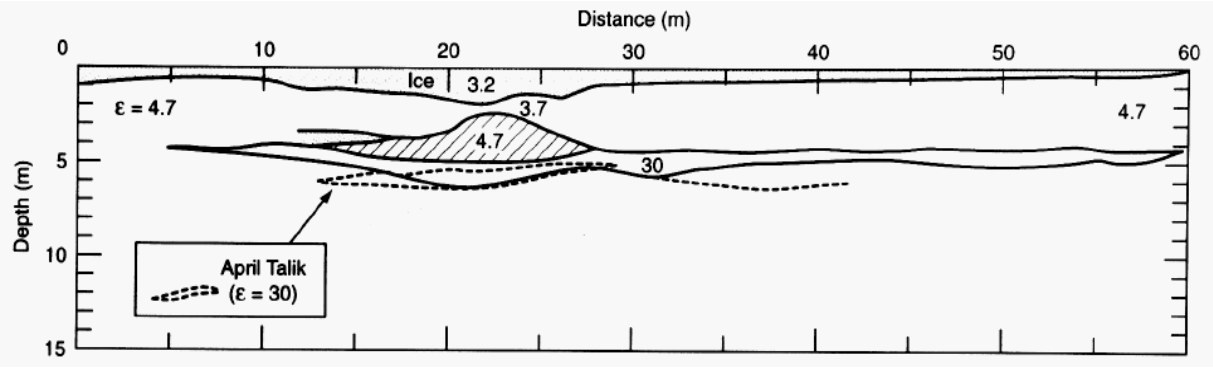

Figure 3.21. Interpretation of a ground-penetrating radar profile across a closed talik located below a shallow river channel 65 m wide situated on the Sagavanirktok River, Alaska, floodplain. The cross hatched area is a partially frozen section of the talik in January. The dashed lenticular outline is interpreted to be the diminished talik that migrated deeper by April. The numbers are the dielectric permittivity (ε) values (from Arcone et al, 1998).

Beneath a typical 1.8 m deep frozen channel (about 40m wide), depth to the talik was 3.7 m deep and the talik had almost the same width as the channel, and edges of the talik were about 5 m inbound of the channel edge. Below deeper channels the talik depth was greater than 3.7m (Arcone et al, 1998).

- Colville River, Alaska: On the Colville River in Alaska, which lies within a continuous permafrost zone, taliks only occur beneath water bodies with depths greater than 2m. If the water depth is irregular, then the up- and down-stream continuity of the talik may be broken. (Walker, 1983).
- Northern Alaska: An investigation undertaken in 2003 streams in northern Alaska showed an increasing talik thickness with increasing stream depth (Bradford et al, 2005). Three sites within 5 km of the Trans-Alaska Pipeline were examined; two were located on a small tributary of a larger river, and the third was a meandering stream. All sites appear to be situated on peatland. Table 3.3 provides a summary of site characteristics, channel width and depth, and talik dimensions. Figure 3.22 reproduces the ground-penetrating radar image and interpreted cross-section of each three sites.

  Factors likely to influence depth of the thaw include permeability of the hyproheic zone (boundary between surface and groundwater regimes), flow rate in the channel, water depth, and solar heat input (both locally and upstream) (Branford et al, 2005). However, the greatest talik depth was observed beneath the deepest channel investigated, but this was also a ponded area, thus having the lowest surface water flow rate of the three sites investigated.

- Coastal Plain, Alaska: Investigations on the Alaskan coastal plain in areas of thermokarst terrain have shown that if water in a pond is greater than 1 m to 2 m deep, it will not completely freeze during winter, thereby allowing a talik to develop below the pond (Univ. of Alaska, 2005).

Table 3.3: Stream and Talik Dimensions, northern Alaska test area

		Channel		Talik	
Site	Description	Width	Depth	Thickness	Lateral
1	Narrow stream channel	0.91 m	0.27 m	0.53 m	coincide with channel wall[A]
2	Ponded interval along tributary	12.8 m	2.1 m	1.8 m	0.5 – 1 m [A]
3	Meandering stream	2 m	1.3 m	0.61	0.5 – 0.75 m [A]

Note: A = dimension obtained from inspection of figures in Bradford et al (2003).

- Snap Lake, Northwest Territories: At Snap Lake (4 km by 6 km), situated just within the continuous permafrost zone, a talik exists beneath the lake and extends 20 to 40 m out beyond the shoreline (Cumberland Resources, 2004).
- Banks Island, Northwest Territories: Numerical simulation (performed in 1982) of geothermal disturbances resulting from water bodies in the Sachs River lowlands, southwest Banks Island in the western Arctic revealed the following talik sizes with respect to lake size (French,1996):

Approximate Lake Size	Talik Depth
50 m diameter	Shallow open talik
250 m diameter	40 m open talik
> 1 km diameter	through-going

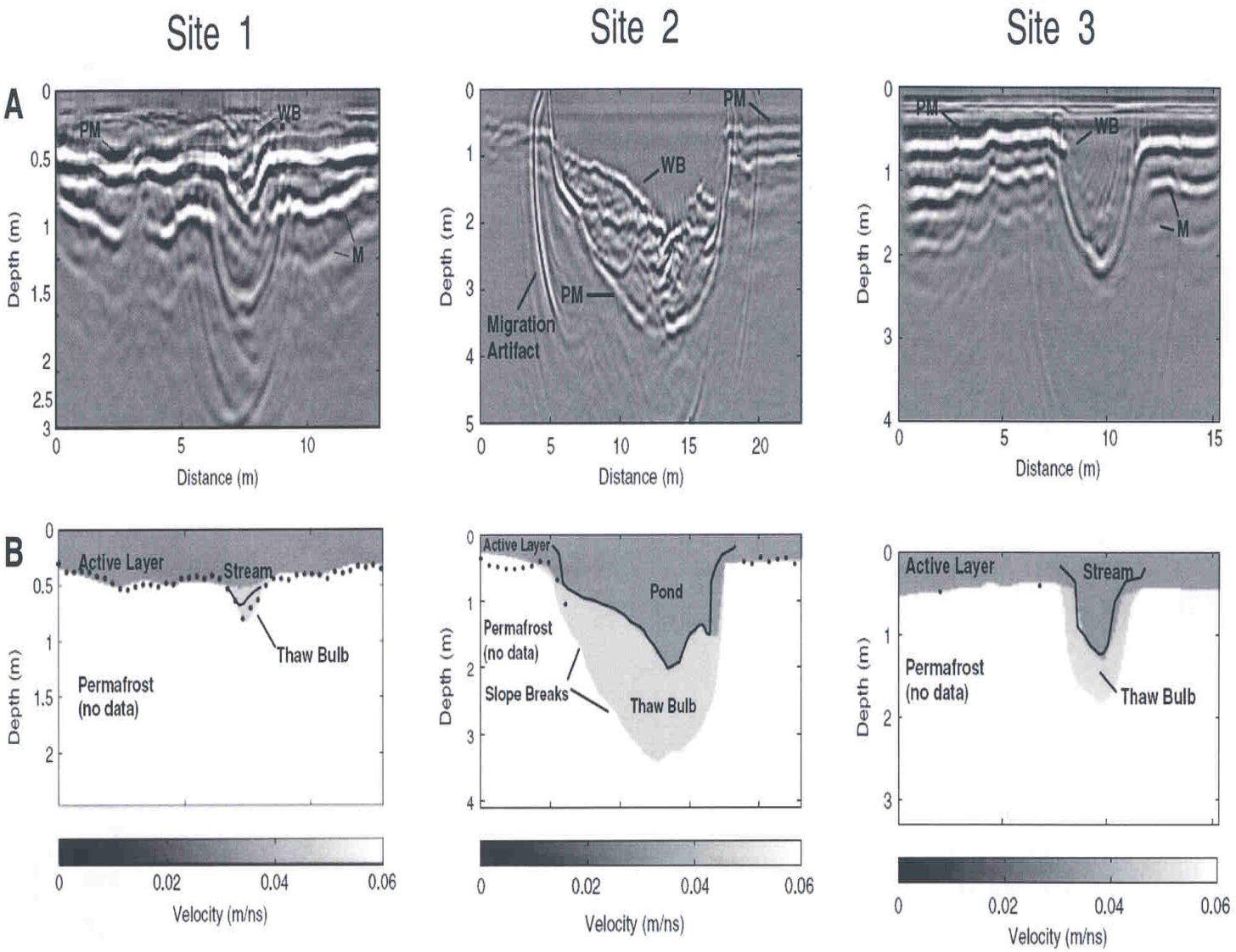

Figure 3.22. (a) Image from ground-penetrating radar, and (b) interpreted cross-section of test sites three small streams located proximal to the Trans-Alaskan pipeline, showing the vertical depth and lateral extent of the thaw-bulb (talik). (modified figure from Branford et al, 2005).

3.4. Earth Structure and Electrical Conductivity / Resistivity

3.4.1 Introduction

The Earth's electrical conductivity (resistivity being its reciprocal) increases rapidly with depth as a function of major changes in the Earth's internal structure. Changes to the abundance and distribution of conductive minerals, the volume and shape of pores, and pore fluid composition affect the electrical conductivity of soils and rock (Ferguson, 2005). For the purpose of electric modeling, Earth can be divided into small scale and large scale structures in which electrical conductivity is affected by different factors, and in turn, this influences the electric field to differing degrees.

Small scale Earth structure is considered to be soil (unfrozen and frozen) and near surface bedrock. Within 500m of the ground surface, properties such as the soil/rock lithology, groundwater content and salinity, fracture distribution and clay content influence the near-surface electrical conductivity (Ferguson, 2005). The effect on induced electric fields (from geomagnetic disturbances) may likely be less, but may more importantly influence the placement of ground beds used for pipeline corrosion protection systems and / or modify the effective resistance of the pipe-to-soil grounding.

Large scale Earth structure includes the crust and mantle. Conductivity of the crust is controlled by the rock type, concentration of metallic minerals and graphite, fracture zones, aqueous phases and temperature (Ferguson, 2005). In the upper mantle, the degree of chemical depletion, metasomatism, partial melting, and possibly hydrogen diffusion are important controls (Ferguson, 2005). Deep seated geological features that are electrically conductive are likely to have the greatest influence on the induced electric field and flow of telluric current through pipelines.

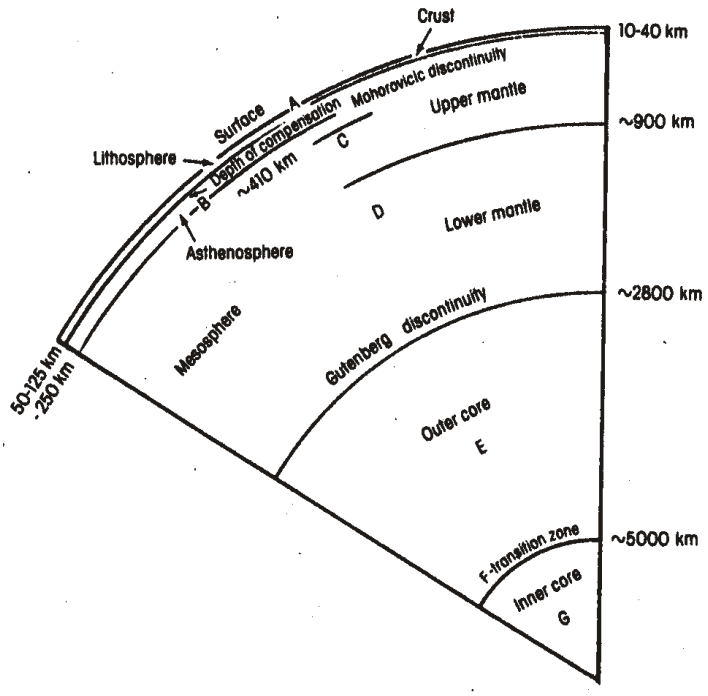

Figure 3.23. Earth's internal layering (from Sherriff, 2002).

3.4.2 Earth's Interior Structure (Crust to Mantle)

Earth's interior structure is divisible into three main layers: *crust, mantle,* and *core* as shown in Figure 3.23, and each layer can be further sub-divided based on unique physical differences. The outermost, thin, rigid crust is underlain by the dense, hot layer of semi-solid rock of the mantle. The crust to mantle boundary is defined by the Mohorovicic discontinuity ("Moho" for short), a seismic velocity discontinuity that varies in depth depending whether it is under continental or oceanic crust.

Boundaries within the crust (upper, middle and lower) and mantle (upper and lower) have been seismically defined as being transitional zones where seismic velocity changes. At about 100 km down is a transitional zone. The 400-km discontinuity represents a phase change where the dominant minerals (olivine and pyroxene) comprising the mantle at this depth transform to a more compact form (Mussett and Khan, 2000). At 660-km is the boundary between the upper and lower mantle. Between 400 and 660 km there is a transition zone that is thought to due to a mineral phase change in addition to increasing density.

The thickness of the continental crust in Canada ranges from about 25 km to 50 km (Ferguson and Odwar, 1997). At the southern end of the Mackenzie Valley, depth to the Moho beneath Fort Simpson is about 30 km and increases eastward to either 36 – 38 km (Cook et al., 1999) or 32 -35 km (Viejo and Clowes, 2003). The decrease of Moho depth is thought to be related to Proterozoic extensional processes (Viejo and Clowes, 2003).

In the Beaufort-Mackenzie Basin, at the northern terminus of the pipeline route, depth to Moho varies little, lying between 35 and 38 km (O'Leary, 1995). Interpreted depths and thicknesses of the sedimentary cover rock and underlying crust are shown in Figure 3.24 (O'Leary, 1995).

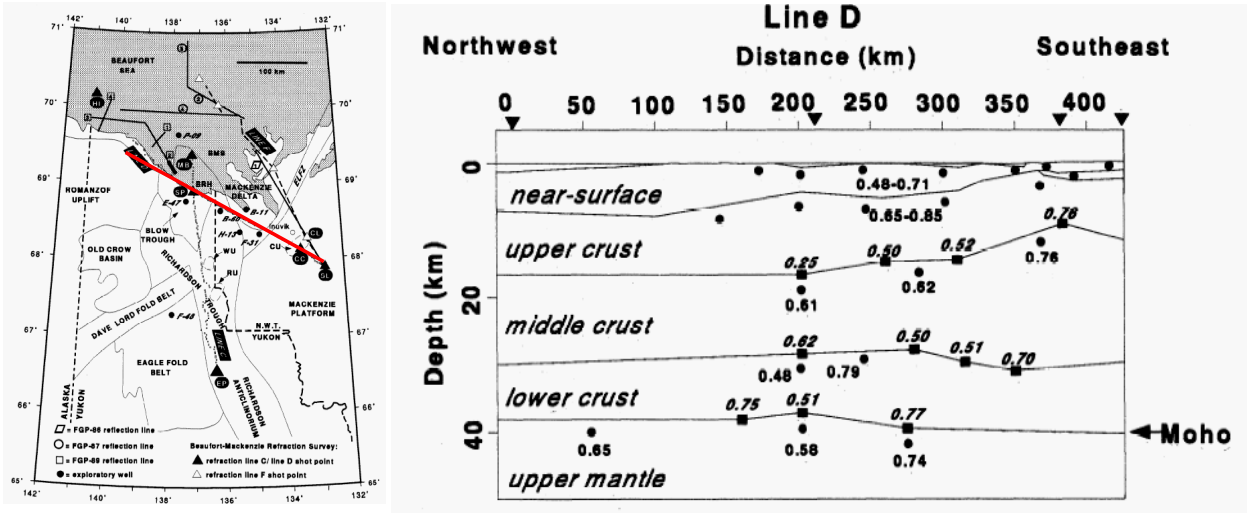

Figure 3.24. Left - Tectonic map of the Mackenzie Delta. Right - Interpreted cross-section showing thickness of near-surface rocks, crust and mantle layers from seismic Line D shown as red line on tectonic map (from O'Leary et al., 1995).

3.4.3. Electrical Resistivity

Resistivity is one of the most widely varying – ranging from 10 to 10,000 ohm-m - of the physical properties (Assoc. Mining, 2004) and exhibits a considerable overlap in the resistivity ranges of earth materials, as shown in Figure 3.25. Figure 3.26 is another summary of electrical properties of rocks and common earth materials, and includes the world-wide range of resistivity in crust, and continental and oceanic mantle as determined from ex-situ measurement by geophysical survey.

Soil, Near-Surface Bedrock, Ice

In surficial soils and near-surface bedrock, the porosity and type and quantity of pore fluids are determining factors in the resistivity of an earth material (Assoc. Mining, 2004). Pore fluids effect the electrolytic (ionic) conduction - which depends on current being passed by ions of pore fluids - of electric current flow through various earth materials. Therefore the measured resistivity value of frozen ground is dependent on the following variables; composition, temperature, water/ice (moisture) content, and salinity; all or any of which can determine the amount and pattern of unfrozen water distribution within the soil or rock material (Yershov, 1998 p.281).

Soil resistivity can have a general correlation with topographic variations, and also can vary with season. The topographic effect is partially a function of moisture content, but more likely due to concentration of soil salts because long term leaching tends to concentrate soluble soil minerals into low lying areas and to deplete elevated regions (Wawruck, 1971). For the same soil, the lowest soil resistivity is likely to be found in low lying areas such as marches, and river flood plains; intermediate resistivity in plains between foothills and river plains; and, highest soil resistivity on slopes, foothill areas, and river escarpments (Wawruck, 1971). Furthermore, presence of salts in soils lowers the freezing point (Mackay, 1969).

Ground temperature variations in conjunction with development of the active layer greatly influence the soil resistivity when measured at different times of the year (MacKay, 1970). Mackay (1970) showed that in Inuvik, at the end of May, soil resistivity had dropped to half of its March maximum. Conversely, for every drop of 1.5C to 2C in the top three meters of frozen gravels, the resistivity doubled.

Presence of oil, natural gas or brine water in the pore structure of rock may increase the resistivity significantly compared to a complete water saturated rock (Parkhomenko, 1967). Equally, resistivity decreases if an increasing sediment / rock pore volume is filled with a fluid of higher conductivity like water. The effect of pore water salinity is dependent on grain size. Fine-grained rocks, such as shale, with a high salinity brine is greater than the resistivity of medium- or fine-grained rocks saturated with the same brine. With low salinities, the opposite is true (Parkhomenko, 1967)

Ice has a higher resistivity than water and if present in sufficient quantity it will increase the resistivity of an unfrozen substance (Assoc. Mining, 2004). Thus, resistivity of ice-bearing soils and rock is a function of the unfrozen water content. Frozen rock exhibits a varying resistivity depending on its water content, porosity, salinity of the pore water, and grain size of the rock (Parkhomenko, 1967). At -12C, the resistivity of a rock is about 10 to 100 times larger than when measured at 18C (Mackay, 1970). However, if the rock is relatively impermeable to water, then the resistivity when frozen may not be too different from the unfrozen condition.

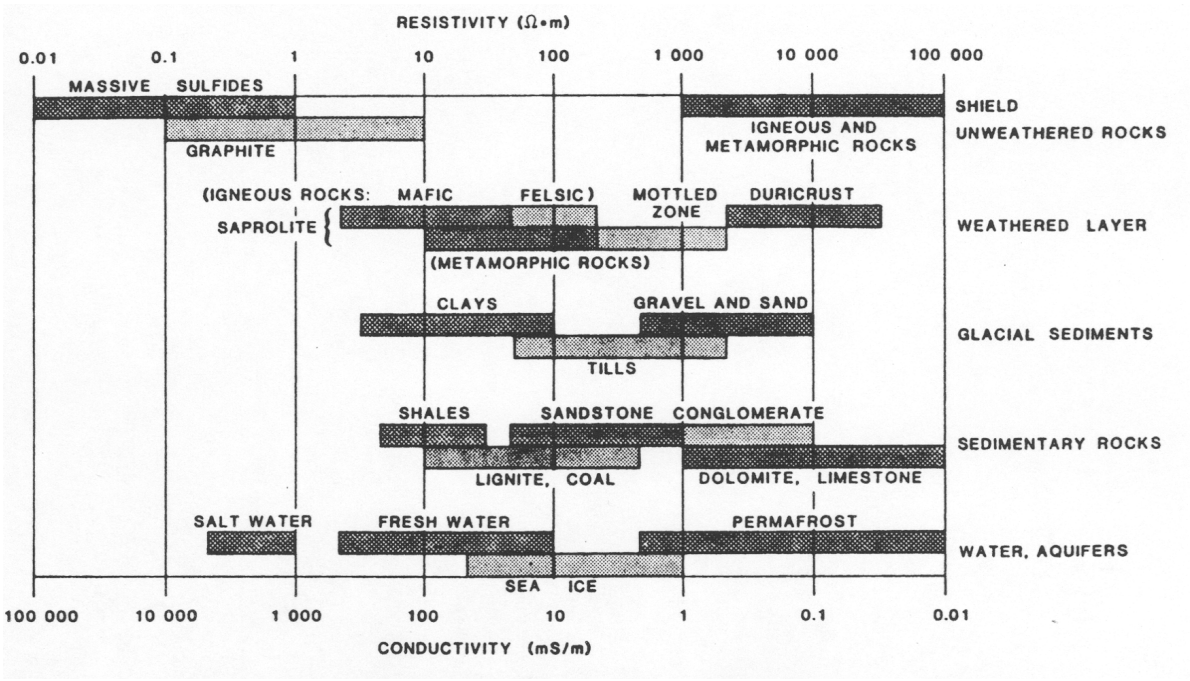

Figure 3.25. Typical ranges of resistivities of earth materials. (from Sheriff, 2002).

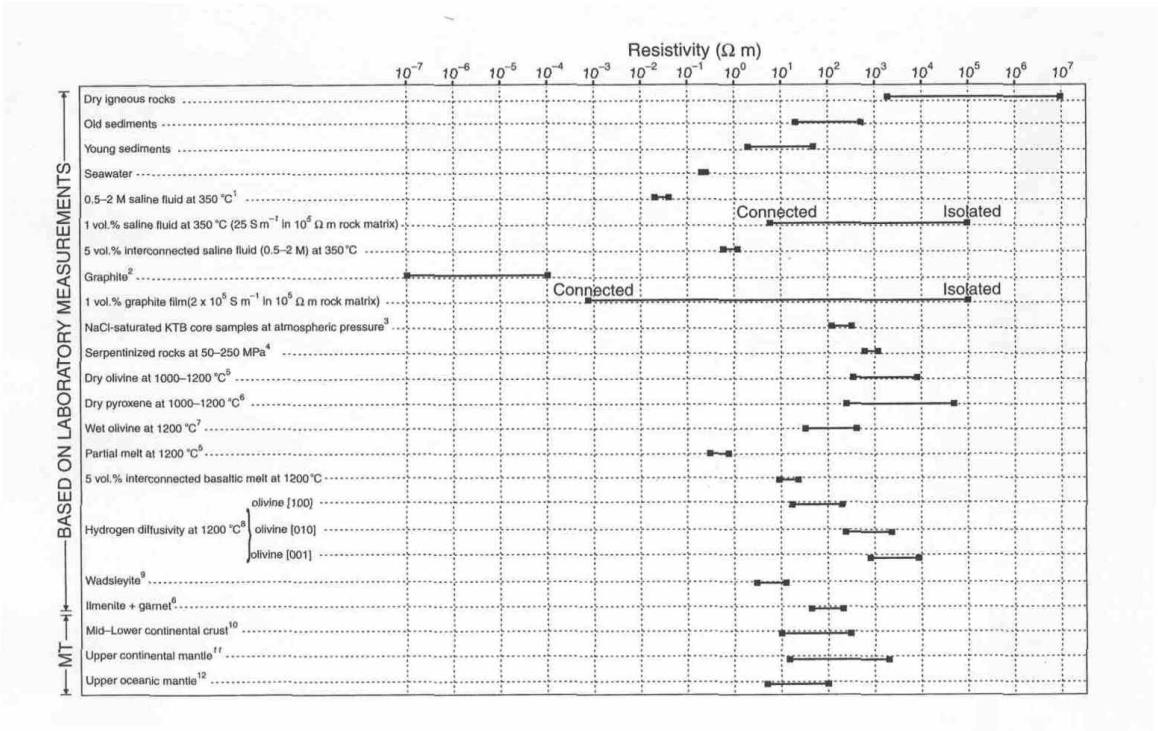

Figure 3.26. Electrical resistivities of rocks and other common Earth materials. MT denotes resistivity determined by magnetotelluric geophysical method (from Simpson and Bahr, 2005).

Electrical properties of overburden change when frozen, as illustrated in Figure 3.27. Below 0° there is a notable increase of resistivity as the amount of unfrozen water decreases. Formation of ice within the soil causes a marked increase of electrical resistivity because the conductivity of ice is exceptionally low. With increasing ice content in a frozen soil, the resistivity will exponentially increase as shown in Figure 3.28 but is independent of soil type and temperature. The lowest resistivity (i.e. highest conductivity) in frozen ground is associated with wet clays, with resistivity becoming progressively higher in peat, silt and sands, with highest values in frozen sand and pure ice (Wawruck, 1971). However, there can be a significant overlap of electrical properties for different types of soil, and between frozen and unfrozen states of the same soil type, as shown in Figure 3.29.

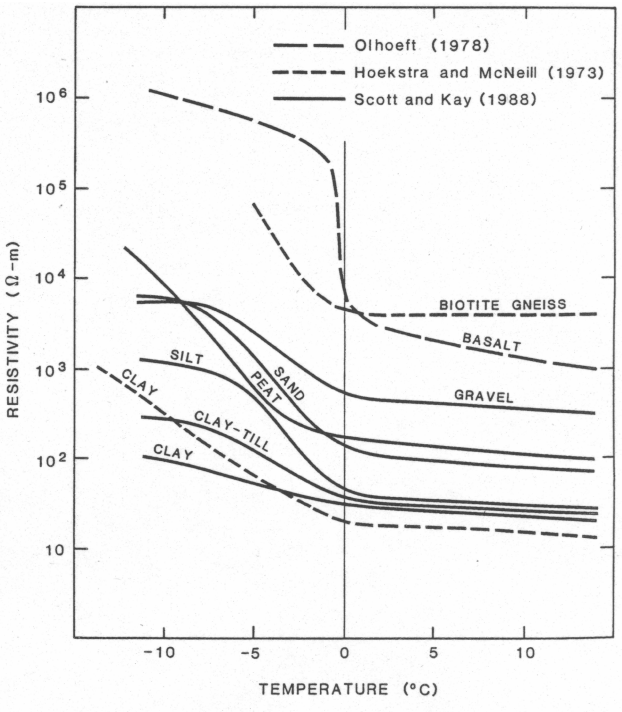

Figure 3.27. Variations in resistivity with temperature for some earth materials (from Scott et al., 1990).

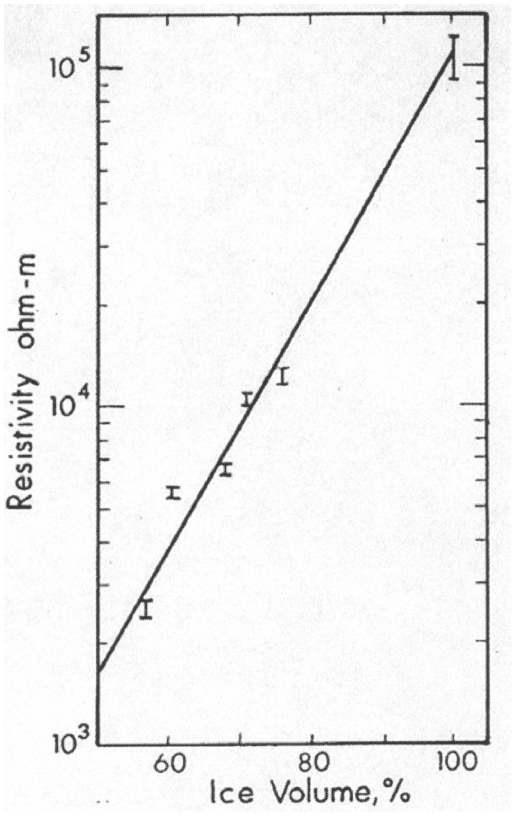

A major control on resistivity is the clay content of the soil or rock type (Assoc. Mining, 2004). The amount of fine-grained material (clay, silt) in a soil will strongly control the unfrozen water content (Delaney et al, 1998), and thus resistivity when frozen. At temperatures below 0C, resistivity of clay does not rise as quickly as in silt or sand with high water content because moist clays retained some measure of ion mobility. Previous geophysical investigation on the Norman Wells pipeline route found that for a clay till, the frozen ground apparent resistivity is typically two to three times greater than the unfrozen equivalence (Northern Engineering, 1977). In addition, the presence of clay in silts tends to reduce resistivity to a value below that of silt alone (Wawruck, 1971).

Figure 3.28. Relationship between resistivity and ice content (from Associated Mining, 2004).

Further examples of resistivity values in permafrost terrain are provided in Table 3.4 which lists the apparent resistivity of thawed and frozen materials in the Mackenzie Delta. It should also be noted that the deeper the permafrost, the higher the apparent electrical resistivity is for the same material, as shown in Figure 3.30.

In summary, the electrical resistivity increases in northern overburden due to changes in soil type, temperature and ice content.

Table 3.4: Apparent resistivity of thawed and frozen materials, Mackenzie Delta

Soil Materials	**Apparent Resistivity** (ohm-m)
Thawed	
Fine lake bottom sediments	2 – 20
Saturated peat	4 – 10
Sandy or gravely, silt	4 – 60
Sand and gravel beach	15 – 80
Moist gravel	80 – 200
Ice muddy silt	120 – 300
Moist peat	800 – 1000
Frozen	
Silt	1000 – 1200
Old high level beach gravel	900 – 1500
Icy Peat	3300 – 6100
Fine cross-bedded sands with thin beds of peat	3600 – 4000
Muddy gravel	4500 – 6000
Segregated ice	6000 +
Sand, silt and gravel mix with ice lenses, pipes and dikes	9500 +
Silty peat	13000 +
Sand with gravel lenses	15000 – 20000
Gravel and sand ridge	20000 – 22000
Note: Apparent resistivities were estimated by logarithmic curve matching.	
Source: Mackay, 1970	

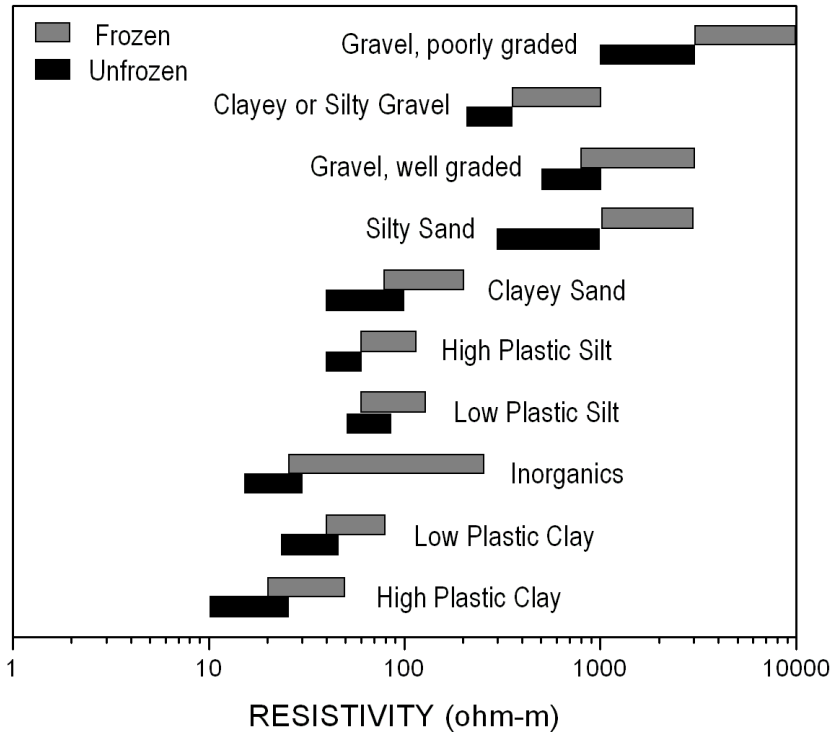

Figure 3.29. Range of resistivity values for frozen and unfrozen soil types in the Fort Simpson region, Northwest Territories (from Associated Mining, 2004).

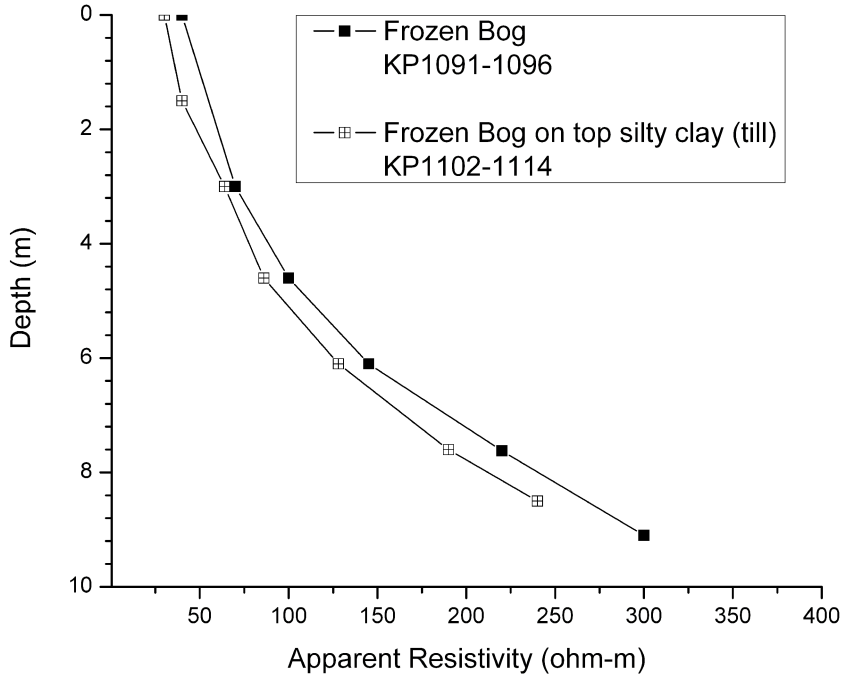

Figure 3.30. Variation with depth of apparent resistivity within same material. Sites located at Kilometre Points KP1091-1096 and 1102-1114, south of Fort Simpson. (Plotted from data contained in Northern Engineering Services Company Limited, 1977)

Active Layer, Talik

The electrical resistivity of near-surface soils can show a seasonal variation since the active layer is frozen during winter months. Seasonal electrical resistivity values for specific locations where active layer occurs where not found during preparation of this report. However, measurements obtained at the Arctic Test Facility at San Sault, NWT, showed that a shallow (0.15 to 1.5 m) active layer had a relatively low resistivity (20 to 300 ohm-m) over a thick permafrost layer of very high resistivity (1500 to 7500 ohm-m) (Northern Engineering, 1972) . Soil stratigraphy consisted of an uppermost peat, and then interlayered silty sand to sand with lenses of clay, all overlying clay till.

Because of the transition between unfrozen and frozen ground, the electrical resistivity of a talik will differ from surrounding permafrost. The lower resistivity of the talik will be sandwiched between higher resistive frozen ground. Such transitions can be abrupt and can be reflected as a "geographic" break in a resistivity profile performed across a river.

Crust, Mantle

Although most rock-forming minerals and rocks are resistive, variations of the electrical conductivity (inverse of reactivity) in the Earth's crust and upper mantle are produced by both lateral and vertical changes in rock temperature, porosity and fluid content, and/or in the concentration and continuity of conducting minerals (Sweeney, et al., 1991). Several mechanisms that can enhance conductivity in the crust, include; enhanced ionic conduction in aqueous fluids and partial melted rock; and enhanced electronic conduction at grain-boundary films of carbon, or interconnected grains of graphite, sulphide or metal oxides. (Wu, 2005). In the mantle, conductivity is enhanced by partial melt fluids, graphite films, and preferential mineral crustal orientation.

In the mid-to-lower continental crust there is a zone of conductivity, possibly representing a mix of resistive rock matrix and a more conductive second component, such as partial melt. Also the there is a change at the crust to mantle boundary (the Moho) from high resistivity to low resistivity (more conductive). The mantle is a semi-conductor, where the conductivity increases as depth and temperature increase. Olivine and pyroxene minerals (which make up the upper mantle) undergo a phase change to a more dense form that greatly increases (by 2 orders of magnitude) the electrical conductivity. The phase changes occur at transition zones in the crust at depths of about 410 km, 520 km and 660 km. Partial melted lower crust and mantle rock is 1 to 2 orders of magnitude more conductive than solid rock (Simpson and Bahr, 2005).

Deep crust and mantle can exhibit electrical anisotropy due to deep seated structure and alignment of olivine crystals.

Magnetotelluric (MT) surveys are the only geophysical technique with the ability to provide an image and resolution of the Earth electrical structure over a depth range extending from uppermost crust (several tens to hundreds of meters) to the deep lithospheric mantle (>100s km) (Wu et al, 2005). MT is particularly sensitive to changes in certain minor constituents of rock, such as graphite, interconnecting grains of sulphides, mineralogical changes, and presence of fluids, which help define zones of differing resistivity that reflect the earth layered structure.

3.5. 1-D Earth Conductivity Model

3.5.1 Introduction

As a first approximation to determine the Earth conductivity (or its reciprocal, resistivity) structure across the length of the Mackenzie Valley pipeline route, a 1D one-dimension representation (i.e. layered structures) was chosen as it contains the least amount of structural complication and is the simplest for which to broadly assign resistivity values to any particular layer. Resistivity values are used in the 1D model because geophysical survey methods used to determine the earth conductivity actually measure the apparent resistivity of the subsurface.

The 1D model is divided into a series of layers that represent (from surface downward) the regional near-surface geology and deeper Earth's internal divisions. From the surface downward, these layers are soils / overburden, unconsolidated sediments, sedimentary cover rock, crust and mantle. The presence of permafrost (frozen ground) within the Mackenzie Valley is an additional layer which needs to be accounted for, but can readily be considered as a very thin layer. The gently dipping sedimentary cover rocks of the Interior Platform have an approximate 1D structure. Although the upper crust can be geologically complicated, in that it is more two-dimensional (changes in rock type vertically and laterally) it is considered as a single homogenous layer. The lowermost model layers represent divisions (i.e. transitional zones) within the lower crust and mantle reflect significant physical and mineral differences which affect the electrical resistivity. It should be noted that while a 1D model is unlikely to represent the true conductivity / resistivity structure, it can be used to determine the extent to which telluric currents can be modified by gross changes within the Earth.

Electrical resistivity values were obtained from published reports. The resistivity for the various layers extend over several orders of magnitude. Of particular interest were resistivity measurements obtained from geophysical surveys undertaken in the Mackenzie Valley, and wherever possible these resistivity values were used in the 1D model. Geophysical surveys measure an apparent resistivity which would better represent the "bulk" resistivity of the earth materials over a larger area than a laboratory sample that is specific and sometimes unique to a particular location. While there have been a considerable number of surveys focused on the permafrost zone in various areas of the Mackenzie Valley, there has only been one geophysical survey investigating the deep electric structure across the valley, specifically at the south end.

3.5.2 Surficial Sediments & Permafrost

Surficial sediments, for the purpose of the 1D model, are considered to be unconsolidated. In general, these surficial sediments will have variable resistivity ranging from about 10 Ohm-m to around 1000 Ohm-m dependent on the porosity, groundwater conductivity, and clay content (Ferguson and Odwar, 1997). Palacky (1988) shows that glacial sediments have a resistivity range of <10 – 10,000 Ohm-m with the lowest values in clays, mid values for till, and highest in gravel and sand. Where permafrost is present, the resistivity generally doubles in fine sized sediments such as clay and silt, and increases for a half-order magnitude for the coarser sands and gravels.

For the 1D model, resistivity values were obtained from; (1) the 1996 SNORCLE transect, (2) a compilation of electrical resistivity for frozen and unfrozen soils in the Fort Simpson region, and (3) a geophysical survey in the Mackenzie Delta transitional to the Tuktoyaktuk highlands.

Surficial sediments located in the southern end of the pipeline corridor were assigned an average resistivity (60 Ohm-m) the same as obtained from the 1996 geophysics survey. On the assumption that the 1996 survey crossed surficial sediments representative of the region, the same 60 Ohm-m average resistivity was applied to many of the 1D model locations. A possible range of resistivity was also considered, using the values from Fort Simpson as shown in Figure 3.29, and selected to represent the dominant surficial sediment (e.g. clay, silt, sand) at the location of the 1D model.

North of Inuvik, where deep permafrost occurs, the average resistivity (>100 Ohm-m) is much greater as based on geophysical survey results as shown in Figure 3.31. Presence of ice lenses, which can be common, will increase the resistivity several magnitudes (> 5000 Ohm-m), and would form the upper end of the resistivity range in a 1D model.

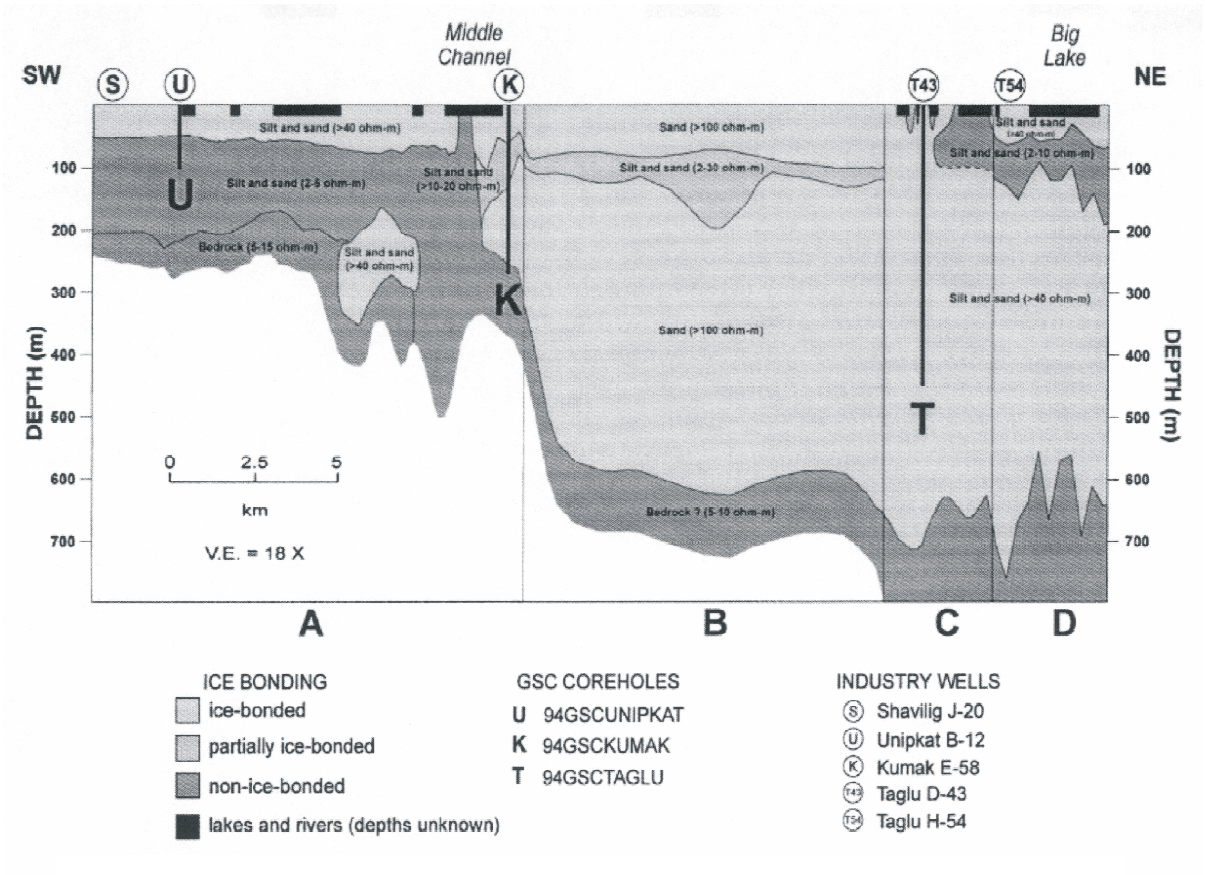

Figure 3.31. Resistivity cross-section based on a TDEM electromagnetic ground survey in the Mackenzie Delta – Tuktoyaktuk area (Adapted from Redman and Bauman, 2004).

3.5.3 Sedimentary Bedrock

World-wide conductivity surveys have shown that near surface sedimentary rock has a much higher conductivity than underlying crystalline metamorphic and igneous rocks (Ferguson and Odwar, 1999). Local variations are always a possibility that can modify the conductivity contrast.

According to Ferguson and Odwar (1997) the average resistivity of unmetamorphosed to slightly-metamorphosed sedimentary rocks in the Western Canadian Basin is 10 – 30 Ohm-m. Resistance will vary among the different types of sedimentary rock, being higher where there is proportionally more limestone than shale and sandstone, and least for shale dominant rock.

Results from the 1996 SNORCLE Lithoprobe survey across the south end of the Mackenzie Valley show that the Phanerozoic sedimentary rocks (of the Interior Platform) form a relatively thick, conductive, near surface layer (~10 Ohm-m) (Wu, 2001). This sedimentary cover rock thins to the east and west of Fort Simpson, but its northerly depth is not known. Hydrocarbon exploration drilling in the area reveals a range of 8 – > 500 Ohm-m in the underlying limestone and dolostone dominant sedimentary rock (Wu, 2001). The ~10 Ohm-m value obtained from the MT survey was adopted for 1D models situated along the south half of the pipeline route as being the most broadly representative of overall sedimentary bedrock.

For the central portion of the route, the average resistivity value for sedimentary bedrock (20 Ohm-m) based on Ferguson and Odwar's (1997) prairie model was used. For some 1D model locations, on the basis of the on the underlying bedrock geology, a range of resistivity values was chosen to reflect the dominant underlying bedrock geology as shown on geological maps or exploration well logs. As an alternative, global resistivity ranges (Simpson and Bahr, 2005) for old sediments (~20 - 800 Ohm-m) can be used.

At the north end of the pipeline route, the resistivity values were obtained from a geophysical survey and are in agreement with values used for other 1D model locations.

3.5.4 Crustal Rocks, Mantle

The crust is divisible into three zones based on geological and geophysical differences, and where electrical resistivity varies as follows (Ferguson and Odwar, 1997);

- Upper crust; surface to depth of 10 to 15 km, generally electrically resistive
- Middle crust; base of upper crust to about 25 km, less resistive than upper crust
- Lower crust; between mid crust and top of mantle, commonly more resistive than mid crust

Thickness of the continental crust varies across Canada from about 25 km to around 50 km (Ferguson and Odwar, 1997). Along the pipeline route, the depth to the crust – mantle boundary was found to range from about 34 km to 40 km, but this value is dependent on the quality of available information. At the south and north ends of the route, crustal thicknesses have been determined fairly accurately by deep sensing geophysical surveys using seismic / magnetotelluric in the south and seismic in the north. For the central portions of the route, a general depth of 40 km

has been applied, the same as the average 1D resistivity model for the provinces adopted by Ferguson and Odwar (1997).

Average resistivity values, based on Ferguson and Odwar's (1997) prairie provinces model were used for the upper (3000 Ohm-m), middle (300 Ohm-m) and lower portions (10 Ohm-m) of the mantle. The exception was at the south end of the route where a 1996 MT survey indicated that the 30 – 100 km upper mantle (100 Ohm-m) has an anomalous zone of lower resistivity attributed to deep seated structures (Wu et al., 2005).

Electrical conductivity surveys have shown that the conductivity structure of Precambrian Shield regions, comprised of crystalline metamorphic and igneous rocks, usually differs from that of Phanerozoic regions (Ferguson and Odwar, 1997). MT studies in adjacent Slave craton show step-like change in conductivity at Moho depth due to enhanced electrical conductivity (Jones and Ferguson, 2001)

3.5.5. Conductive Anomalies along Pipeline Route

MT soundings made across the south end of the Mackenzie Valley, as part of the 1996 SNORCLE Lithoprobe transect identified several electrical features which are related to the tectonic evolution of the region, including ancient subduction of oceanic crust akin to modern-day plate tectonics. Wu et al. (2005) identified the following electrical anomalies as shown in cross-section on Figure 3.32. Figure 3.32 is a schematic cross-section representation of the Earth's mantle beneath the south end of the pipeline route.

- A northeast-southwest trending geoelectric fabric within the crust and mantle, which reflects past and present structural deformation of the region.

  At crustal depths, the average geoelectric strike of N34^{o}E has been interpreted by Wu et al (2005) to be associated with pervasive transcurrent faulting as a result of collision of the various tectonic terranes during the Proterozoic. At mantle depths of 100 to 120 km, the geoelectric strike has rotated clockwise to N62^{o}E possibly due to on-going shearing at the base of the sub continental lithosphere.

  In the Fort Simpson area, the geoelectric strike at mantle depth is more north-south trending and is though to reflect structures associated with early rifting that resulted in the formation of the Fort Simpson Basin. The Fort Simpson Basin contains Proterozoic sedimentary rocks.

- A relatively resistive body (> 400 to > 1000 Ohm-m) in the upper crust located some 50 km south of Fort Simpson, and possibly beneath the pipeline route. This west-dipping body (Item B on Fig. 3.32) has a maximum depth of 20 – 25 km, and in conjunction with seismic surveys, it has been interpreted to represent an old buried sedimentary basin, specifically the Proterozoic Fort Simpson Basin. Of significance, is that it represents a layer of more resistive rock sandwiched between two less resistive layers; the upper near-surface Interior Platform sedimentary rocks, and the lower underlying crust.

- The crust (item C on Fig. 3.32) below the Fort Simpson Basin rocks are more conductive (~130-250 Ohm-m) than surrounding areas. The reason for this 100 to 150 km wide anomalous zone is not fully understood. Wu et al. (2005) suggests that the decreased resistivity may be due to

modification of the crust during rifting or basin formation associated with development of the Fort Simpson Basin.

- A prominent conductive zone (<100 Ohm-m) occurs some 50 km east of Fort Simpson, with the top of the zone between 5 to 10 km deep and extending to significant depth in the crust. The anomaly (item D on Fig. 3.32) is interpreted by Wu et al. (2005) to be caused by enhanced electronic conduction as a result of fluids released from subducting oceanic crust during collision of the terranes. Seismic studies (Cook et al., 1999) suggest an accretionary wedge of sedimentary rock caused by ancient eastward subduction of oceanic crust.
- An anomalous low resistivity zone (item I on Fig. 3.32) has been interpreted by Wu et al. (2005) to be the result of introduction of carbonaceous or sulphidic rocks into the crust during past subduction.

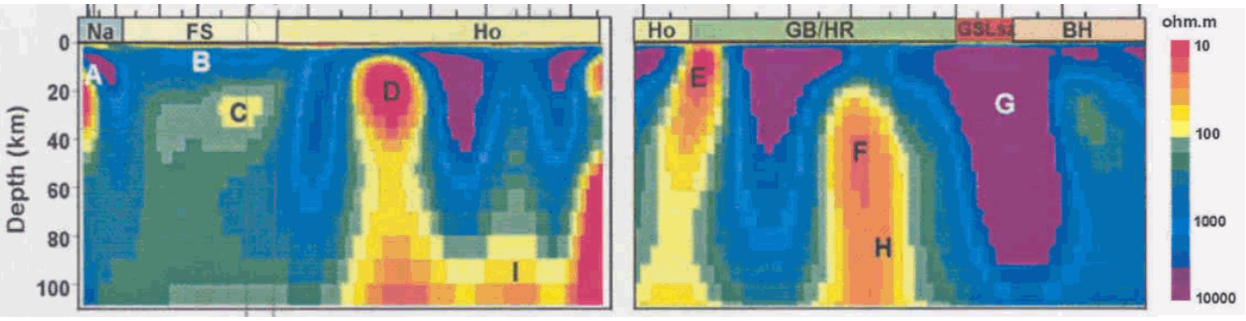

Figure 3.32. Two-dimensional resistivity model for the western portion of the 1996 SNORCLE Lithoprobe magnetotelluric survey component (from Wu et al., 2005). Labelled structures are discussed in text

3.5.6 Conductivity Models

Figures 3.33 to 3.37 show the 1D models of the Earth conductivity for the five zones along the pipeline route. Additional details are given in Tables 3.5 to 3.9 which summarize the layer thicknesses and estimated electrical resistivity for each 1D model section. These tables also provide background information on justification and source of the assigned thickness and resistivity. Explanatory notes for these tables are given in Table 3.10.

Resistivity values and depths used to develop the Zone 5 model (from overburden down to the upper mantle) are considered to a best representation of actual conditions since they are ex-situ measurements obtained from a combined MT / seismic survey through this region. Values for the bottom most portion of the model are the more general measurements used to describe the middle and lower mantle in western Canada. For the other zones the resistivity values are derived from typical values for the structures and depths are based on published seismic survey results as describd in the previous sections. In Zone 1 the sedimentary basin is assigned a low resistivity value (compared to the other zones) on the basis of ex-situ values obtained from a TDEM geophysical survey in this area.

Zone 1

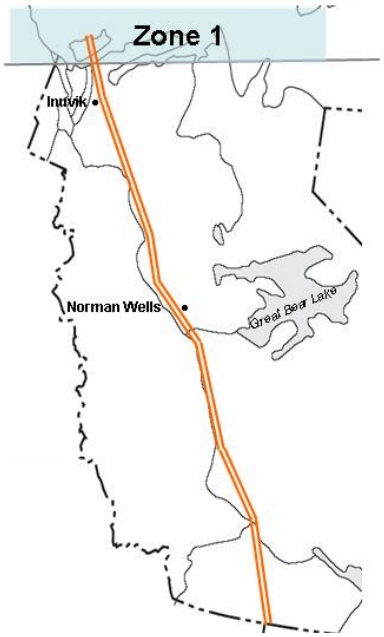

Zone 1, covering the Beaufort Sea and Mackenzie Delta contains the deepest permafrost, extending some 400 to 600 m deep.in a thick layer of surficial sediments with a resistivity of 100 ohm-m. Below this is an exceptionally thick (12.5 km) sedimentary basin with low resistivity (10 ohm-m). This dominates the electromagnetic response in theis area.

The deeper structure comprises a thin upper crust and below this we assume a typical model of a resistive upper mantle above a lower mantle become more conducting with increasing depth due to the increasing temperature and pressure within the Earth.

Zone 1 will be the site of KP 0 to KP 24 of the Taglu lateral.

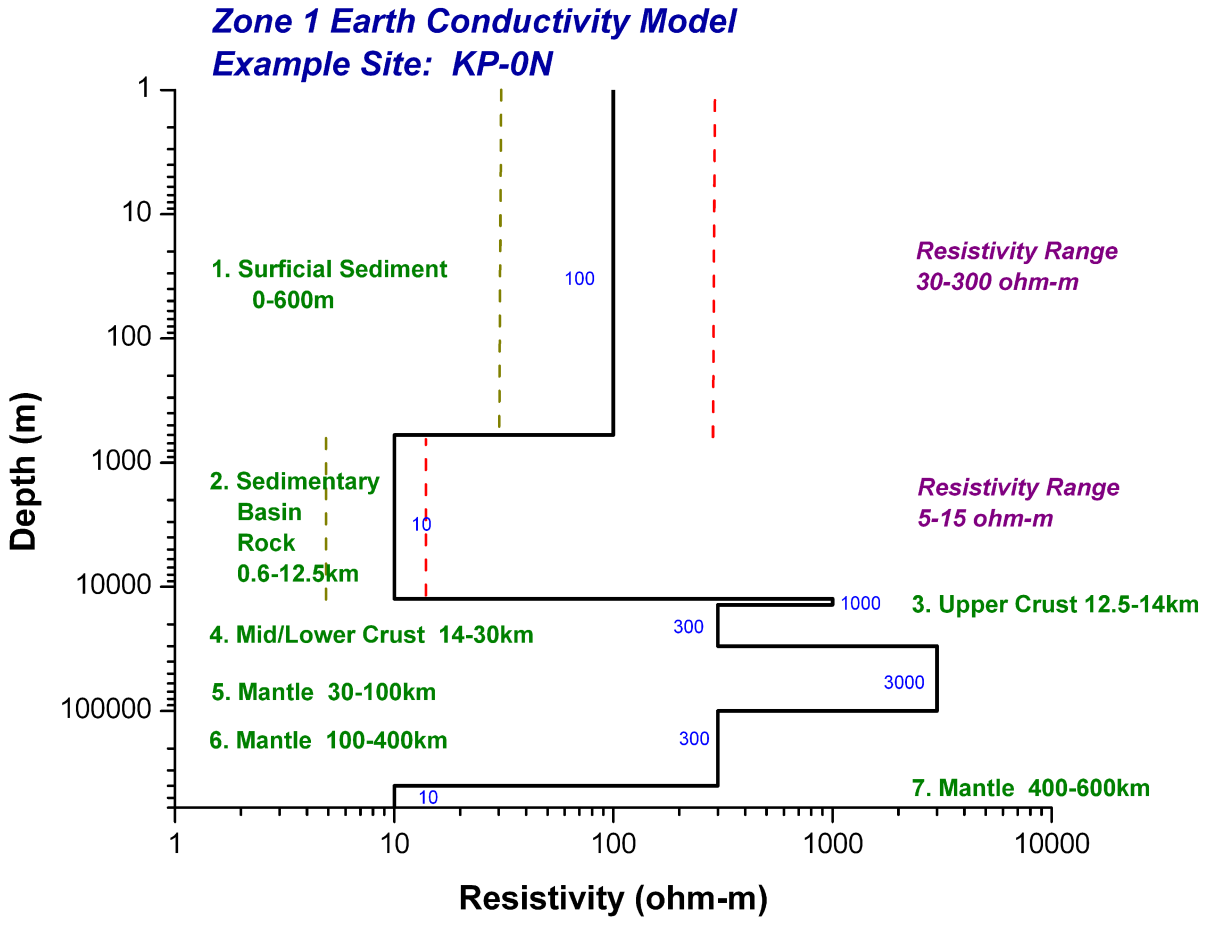

Figure 3.33. Earth conductivity model for Zone 1.
Refer to Table 3.5 for additional details.

TABLE 3.5: ZONE 1 EARTH CONDUCTIVITY MODEL

EXAMPLE BOREHOLE: none, site at **Kilometer Point KP-0N** (Beaufort Coastline, 120 km north of Inuvik)
LAT / LONG: approx. 69°, 25' / 135°, 00'

Geological Unit	Resistivity (Ωm) Avg	Range	Determination, Confidence (A,B,C)	Resistivity Reference	Comments
1. Surficial Sediments (silt, fine sand, clayey silt), *frozen* (0 – ~ 600 m)	>100 > 5,000 ice lens	30-300	In-situ (laboratory), A for avg > 100 Ex-situ (TDEM survey), A, for range 30-300 Ex-situ (DC restv'y) B for >5000 for high-ice content silts	Todd & Dallimore 1998, Fig. 8 Todd & Dallimore 1998, Fig. 8 Assoc. Mining 2004, p.64	• Geol. unit source: Bull.547. Fig.1a, map shows alluvial plain • area of abundant massive ice • 600m depth to bedrock measured from Todd & Dallimore 1988 Fig.8, uncertain if incorporates older sedimentary rock (depth to bedrock is reported as 60m on Richards Island)
2. Sedimentary Basin Rock (~0.6 km ~12.5 km)	10	5 - 15	Ex-situ (TDEM survey), A, for average & range	Todd & Dallimore 1998, Fig. 8	• 12.5 km depth hand-scaled from crustal seismic lines in Aspler et al 2003 , O'Leary 1995.
3. Upper Crust (~0 – 12.5 km)	> 1000 avg rge 1000-10,000		Ex-situ (MT survey), C	Wu et al 2005, p.25, p.31 p.71, for value Ferguson & Odwar for range	• 14 km depth hand-scaled from crustal x-section in Aspler et al 2004, O'Leary et al 1995 • Used Wu's average value from site 07 located 1100 km south of site 53 • Used Ferguson's range value from resistivity model for Prairie Provinces
4. Middle – Lower Crust (12.5 – 30 km)	300	10 - 200	Ex-situ (MT survey), C	Ferguson & Odwar for average Simpson & Bahr 2005, p.11 for range	• Depth from Ferguson & Odwar's Prairie Provinces model • Avg resistivity value from Ferguson & Odwar's Prairie Provinces model • Range resistivity for mid-lower continental crust
5. Mantle (30 - 100 km)	3000	15 - 2000	Ex-situ (MT survey), C	Ferguson & Odwar for average Simpson & Bahr 2005, p.11 for range	• 30 km upper depth from gravity model by Stephenson et al 1994, p.385 • 100 km lower depth from Ferguson's resistivity model for Prairie Provinces • Used avg value from Ferguson's resistivity model for Prairie Provinces • Used Simpson's range value for mid-lower continental crust
6. Mantle (100 - 400 km)	300	---	Ex-situ (MT survey), C	Ferguson & Odwar for average	• depth & resistivity from Ferguson & Odwar's Prairie Provinces model
7. Mantle (400 - 600 km)	10	---	Ex-situ (MT survey), C	Ferguson & Odwar for average	• depth & resistivity from Ferguson & Odwar's Prairie Provinces model

Zone 2

In Zone 2, the area around Inuvik, the permafrost depth was assumed to be the same as depth of surficial sediments, being about 60 m, although permafrost can be anywhere from 50 to 400 m deep. The sedimentary basin is shallower (depth = 3600 m) and more resistive than in Zone 1. Below the sedimentary basin the upper crust is thicker than in Zone 1. The higher resistivity of the crust, compared to the sedimentary basin, gives a more resistive response for this Earth model.

Zone 2 will be the site of KP 24 of the Taglu lateral to KP 145 of the main pipeline.

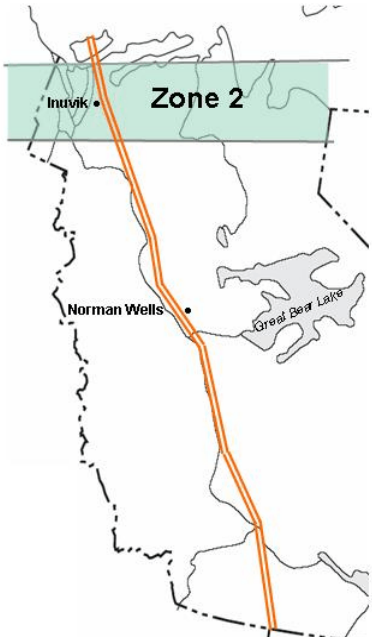

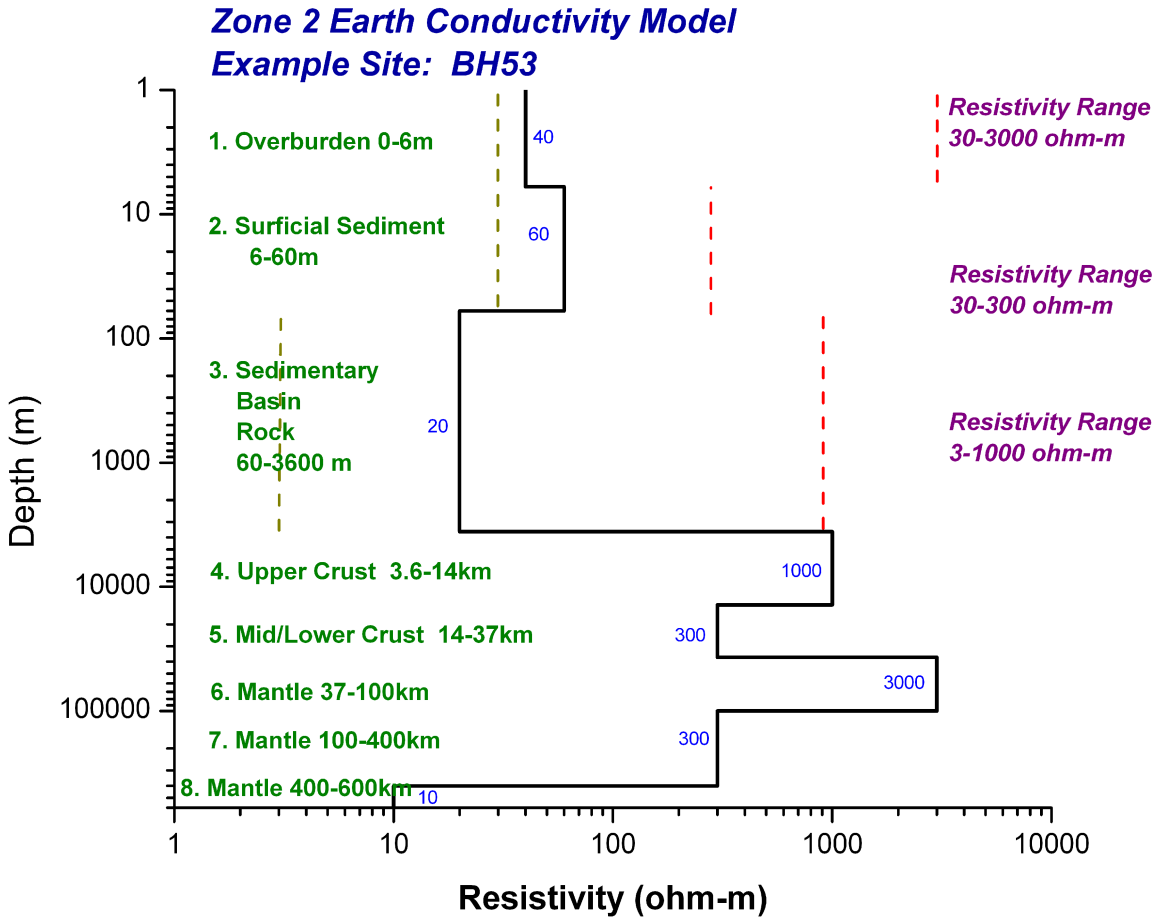

Figure 3.34. Earth conductivity model for Zone 2.
Refer to Table 3.6 for additional details.

TABLE 3.6: ZONE 2 EARTH CONDUCTIVITY MODEL

EXAMPLE BOREHOLE: **53 [geotechnical borehole, see Aylsworth et al., 2000]**
LAT / LONG: 68°, 36' / 133°, 33'

Geological Unit	Resistivity (Ωm) Avg	Range	Determination, Confidence	Resistivity Reference	Comments
1a. Overburden (silt, silty sand, clay), *frozen* *[ice layers, ice bonded]* (0 – 6 m)	>40 > 5,000 ice lenses	30-3,000	In-situ (laboratory), A for avg > 40 In-situ (laboratory), B, for range 30-3000 based on Ft.Simpson measurements Ex-situ (DC restv'y) B for >5000 for high-ice content silts	Assoc. Mining 2004, p.63 Todd & Dallimore 1998, Fig. 8 Assoc. Mining 2004, p.64	• unit source: Bull.547. Fig.1 BH53 • area of abundant massive ice; Irregular large ice masses likely • Depth from BH53 log
2.. Surficial Sediments (silt, sand, clay, pebbly till), *frozen* (6 – 60 m)	60	30-300	In-situ (laboratory), B, for average of typical frozen clay till Ex-situ (EM survey), A, for range of frozen unconsolidated local sediment	Scott, p.356, for avg Todd & Dallimore 1998 (abstract) for range	• unit source: Allen 1998 p.40 • Permafrost depth ~ 200m hand-scaled from Smith et al 2001, Fig.3 • Bedrock depth variable 60-70 m, reported in EIS reports, Kokelj 2003 p.49,
3. Sedimentary Basin Rock (~0 - ~3.6 km)	20 ---	3 – 1,000 5 – 500	Ex-situ (MT survey), C, for avg and range Ex-situ (MT survey, C, for range	Ferguson & Odwar for avg and range 3-1,000 in prairie prov Simpson & Bahr, p.11 for range 5-500 global	• 3.6 km depth hand-scaled from crustal seismic lines in O'Leary 1995, coincides with Parson Lake gas field geol. X-sec in EIS reports.
4. Upper Crust (~3.6 – 14 km)	> 1000 avg rge 1000-10,000		Ex-situ (MT survey), C	Wu et al 2005, p.25, p.31 p.71, for value Ferguson & Odwar for range	• 14 km depth hand-scaled from crustal x-section in Aspler et al 2004, O'Leary et al 1995 • Used Wu's average value from site 07 located 1100 km south of site 53 • Used Ferguson's range value from resistivity model for Prairie Provinces
5. Middle – Lower Crust (14 – 37 km)	300	10 - 200	Ex-situ (MT survey), C	Ferguson & Odwar for average Simpson & Bahr 2005, p.11 for range	• Used avg value from Ferguson's resistivity model for Prairie Provinces • Used Simpson's range value for mid-lower continental crust
6. Mantle (37 - 100 km)	3000	15 - 2000	Ex-situ (MT survey), C	Ferguson & Odwar for average Simpson & Bahr 2005, p.11 for range	• 37 km upper depth from gravity model by Stephenson et al 1994, p.385 • 100 km lower depth from Ferguson's resistivity model for Prairie Provinces • Used avg value from Ferguson's resistivity model for Prairie Provinces • Used Simpson's range value for mid-lower continental crust
7. Mantle (100 - 400 km)	300	---	Ex-situ (MT survey), C	Ferguson & Odwar for average	• Depth & restv'y values from Ferguson's resistivity model for Prairie Provinces
8. Mantle (400 - 600 km)	10	---	Ex-situ (MT survey), C	Ferguson & Odwar for average	• Depth & restv'y values from Ferguson's resistivity model for Prairie Provinces

Zone 3

Zone 3 extends from Zone 2 to just south of Norman Wells. In this region the permafrost is about 150 m deep. Below this the sedimentary basin that underlies Zones 1 and 2 continues to become shallower and a depth of 1600m is used in the model. In this model the decreased thickness of the sedimentary basin is replaced by a thicker crust. The higher resistivity (1000 ohm-m) of the upper crust gives a more resistive response to this model.

Zone 3 will be the site of KP 145 to KP 534 of the main pipeline.

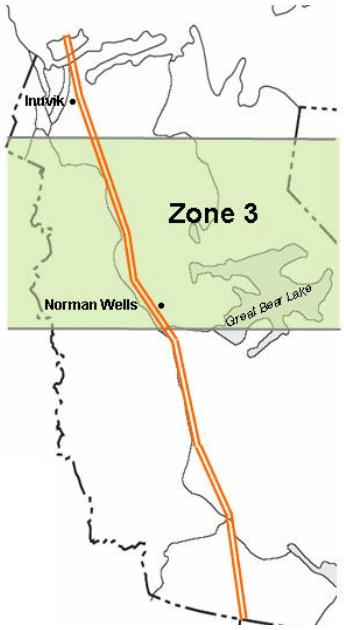

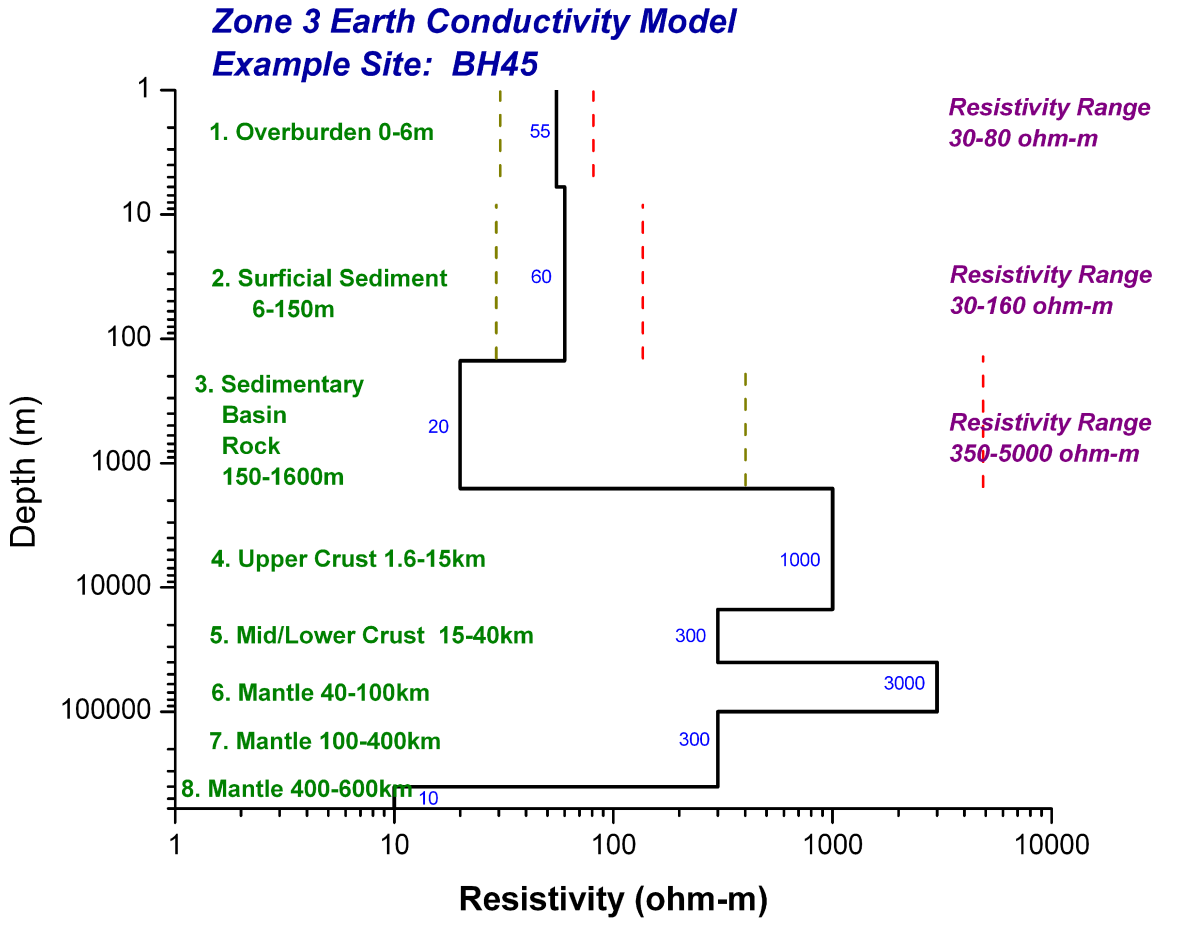

Figure 3.35. Earth conductivity model for Zone 3.
Refer to Table 3.7 for additional detail.

TABLE 3.7: ZONE 3 EARTH CONDUCTIVITY MODEL

EXAMPLE BOREHOLE: **45 [geotechnical borehole, see Aylsworth et al., 2000]**
LAT / LONG: 66°, 53' / 129°, 49'

Geological Unit	Resistivity (Ωm) Avg	Range	Determination, Confidence	Resistivity Reference	Comments
1a. Overburden (silty clay), *frozen* (0 – 6 m)	---	**30 - 80**	In-situ (Laboratory), B	Assoc. Mining 2004	• From previous compilation of resistivity values at Ft. Simpson
2a. Surficial Sediments *frozen* (6 - 150 m)	**60**	**30-160**	Ex-situ (MT survey), B, for value In-situ (lab), B, for range	Wu 2001, p.365 Wu et al 2005, p.20 for value Assoc Mining 2004, p.10 for range	• Permafrost depth (~140m) hand-scaled from Smith et al 2001, Fig 3. • Minimum 150m depth from well *Richfield Oil Corp et al Grandview Hills No.1* located 40 km NNW in the valley • Assume sediments mostly silt and clay - using Wu's value from site 07 located 800 km south of site 45
3. Sedimentary Basin Rocks (~ 0 - ~ 1600 m)	**20**	**350 - 5000**	Ex-situ (MT survey), C for value In-situ (lab), C for range	Ferguson & Odwar, for value Telford 1976, p.455 for range	• Minimum 1600m depth from preliminary cross-section (Williams 1990, Section E-F) • Avg value from resistivity model for Prairie Provinces • Range value is for dolostone – predominant sedimentary rock on cross-section
4. Upper Crust (~0 – 15 km)	**>1000**	**1000-10000**	Ex-situ (MT survey), C	Wu et al 2005, p.25, p.31 p.71, for value Ferguson & Odwar for range	• Using Wu's value from site 07 located 800 km south of site 45 • Range value from resistivity model for Prairie Provinces
5. Middle – Lower Crust (15 – 40 km)	**300**	**10 - 200**	Ex-situ (MT survey), C	Ferguson & Odwar for average Simpson & Bahr 2005, p.11 for range	• Depth from resistivity model for Prairie Provinces • Avg value from resistivity model for Prairie Provinces • Range value for mid-lower continental crust
6. Mantle (40 - 100 km)	**3000**	**15 - 2000**	Ex-situ (MT survey), C	Ferguson & Odwar for average Simpson & Bahr 2005 for range	• resistivity model for Prairie Provinces for average • upper continental mantle for range
7. Mantle (100 - 400 km)	**300**		Ex-situ (MT survey), C	Ferguson & Odwar	• resistivity model for Prairie Provinces
8. Mantle (400 - 600 km)	**10**	---	Ex-situ (MT survey), C	Ferguson & Odwar	• resistivity model for Prairie Provinces

Zone 4

In Zone 4 the permafrost extends to a total depth of about 70m. Sedimentary basin rock is thin, in contrast to the Zone 1 and 2 models, and its depth is based on exploration wells and therefore likely to be representative for this zone. For the upper crust, a resistivity of 1000 ohm-m was assigned, being the higher end of a previously interpreted resistivity range (Wu, 2001). The upper mantle is assigned the same resistivity value used for Zone 5 to the south assuming similar deep conductive structure, however, the 40 km depth to the upper mantle is a general value used for continental structure in western Canada.

Zone 4 will be the site of KP 534 to KP 803 of the main pipeline.

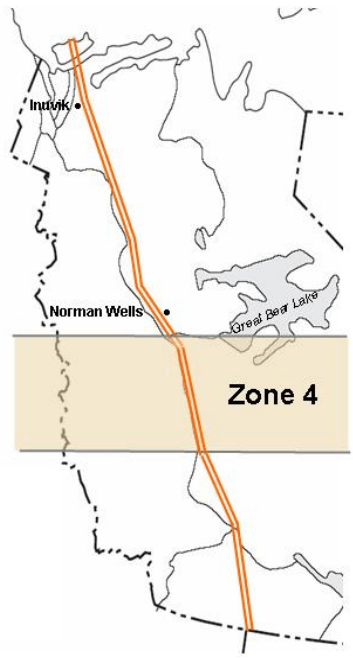

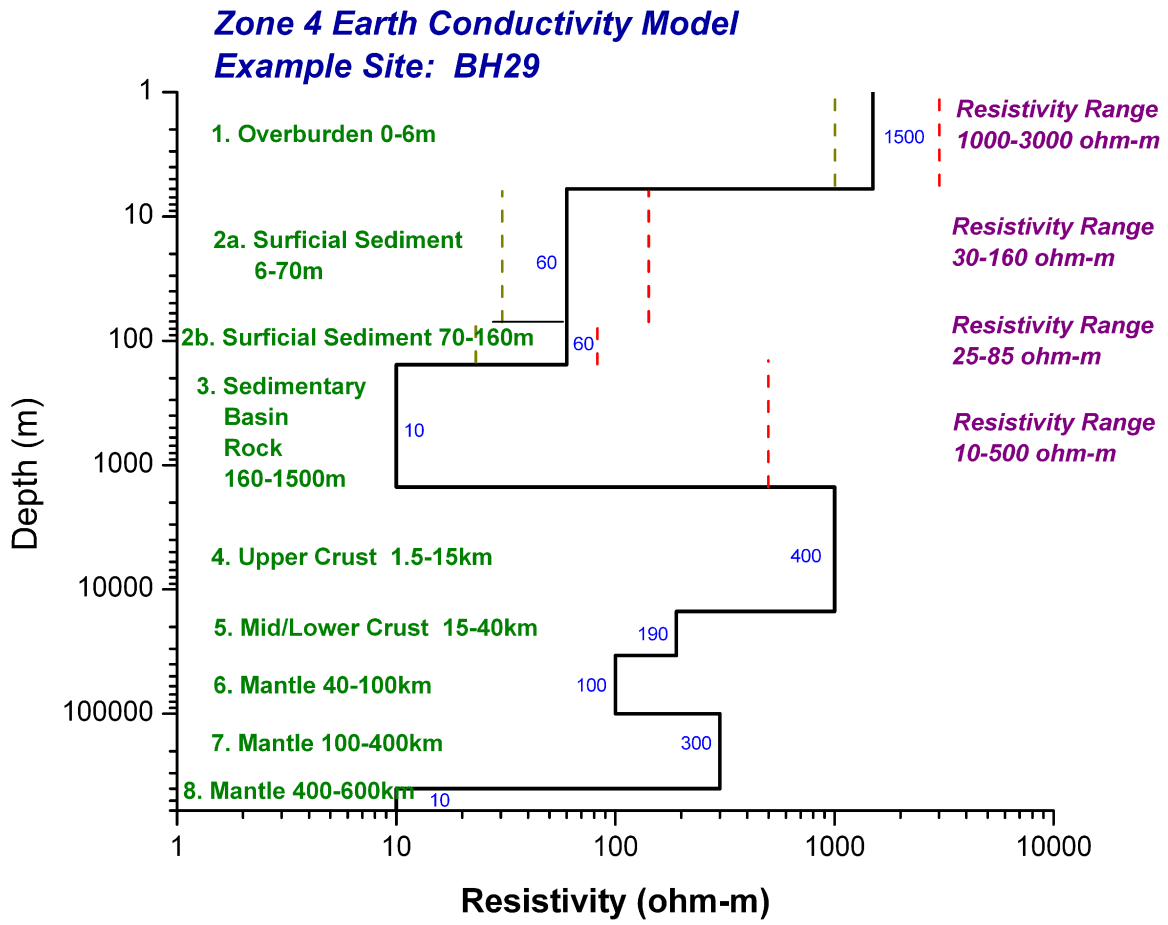

Figure 3.36. Earth conductivity model for Zone 4.
Refer to Table 3.8 for additional details.

TABLE 3.8: ZONE 4 EARTH CONDUCTIVITY MODEL

EXAMPLE BOREHOLE: **29** [geotechnical borehole, see Aylsworth et al., 2000]
LAT / LONG: 64°, 48' / 124°, 58'

Geological Unit	Resistivity (Ωm) Avg	Range	Determination, Confidence	Resistivity Reference	Comments
1a. Overburden (silty sand), ***frozen*** (0 – 6 m)		1000 - 3000	In-situ (Laboratory), B	Assoc. Mining 2004	• From previous compilation of resistivity values at Ft. Simpson
2a. Surficial Sediments ***frozen*** (6 - 70 m)	60	30 - 160	Ex-situ (MT survey), B, for value In-situ (lab), B, for range	Wu 2001, p.365 Wu et al 2005, p.20 for value Assoc Mining 2004, p.10 for range	• Permafrost depth hand-scaled from Smith et al 2001, Fig 3. • Depth from well Aquit Old Fort Point E-30 (Yorath & Cook 1981) • Assume sediments mostly silt and clay – used Wu's values from site 07 located 500 km south of site 29
2b. Surficial Sediments (70 - 156 m)	60	25 - 85	Ex-situ (MT survey), B, for value In-situ (lab), B, for range	Wu 2001, p.365 Wu et al 2005, p.20 Assoc Mining 2004, p.10 for range	• Depth from well Aquit Old Fort Point E-30 (Yorath & Cook 1981) • Uncertain if all is unconsolidated surficial sediments • Assume sediments mostly silt and clay - used Wu's value from site 07 located 500 km south of site 29
3. Sedimentary Basin Rocks (~ 0 - > 780 m to 1500 m) --- ***from geological well log*** (156 - 274 m, shale) (275 - 780 m, dolostone)	~ 10 --- 	10 - 500 --- 20 - 2000 350 - 5000	Ex-situ (MT survey), B --- In-situ (lab), C In-situ (lab), C	Wu 2001, p.365 Wu et al 2005, p.20 for average Simpson & Bahr 2005, p.11, for range Telford 1976, p.455 for well log values	• Minimum 780m depth from well Aquit Old Fort Point E-30 (Yorath & Cook 1981) • Minimum 1078m depth from well Imperial Canol Bluefish 1-A (Tassonyi 1968) • 1500m depth from DNAG 5, Fig 5.5 • Using Wu's value from site 07 located 500 km south of site 29
4. Upper Crust (~0 – 15 km)	>1000		Ex-situ (MT survey), C	Wu et al 2005, p.25, p.31 p.71	• Using Wu's value from site 07 located 500 km south of site 29
5. Middle – Lower Crust (15 – 40 km)	300	10 - 200	Ex-situ (MT survey), C	Ferguson & Odwar for average Simpson & Bahr 2005, p.11 for range	• Depth from resistivity model for Prairie Provinces • Avg value from resistivity model for Prairie Provinces • Range value for mid-lower continental crust
6. Mantle (40 - 100 km)	3000	15 - 2000	Ex-situ (MT survey), C	Ferguson & Odwar for average Simpson & Bahr 2005 for range	• resistivity model for Prairie Provinces for average • upper continental mantle for range
7. Mantle (100 - 400 km)	300		Ex-situ (MT survey), C	Ferguson & Odwar	• resistivity model for Prairie Provinces
8. Mantle (400 - 600 km)	10	---	Ex-situ (MT survey), C	Ferguson & Odwar	• resistivity model for Prairie Provinces

Zone 5

In Zone 5, surficial sediments extend to a depth of some 100m based on MT interpretation. Sedimentary basin rock is thin, in contrast to the Zone 1 and 2 models, however, this depth is also based on MT survey results and is in general agreement with exploration wells and therefore considered to be representative for Zone 5. For the upper crust, a resistivity of 400 ohm-m was assigned, being the lower end of a resistivity range interpreted by Wu (2001). A major difference in contrast to models of Zones 1 to 3, is the presence of a more conductive upper mantle, and that the crust to mantle boundary (Moho discontinuity) is higher (34 km deep) at Zone 5.

Zone 5 will be the site of KP 803 to KP 1221 of the main pipeline.

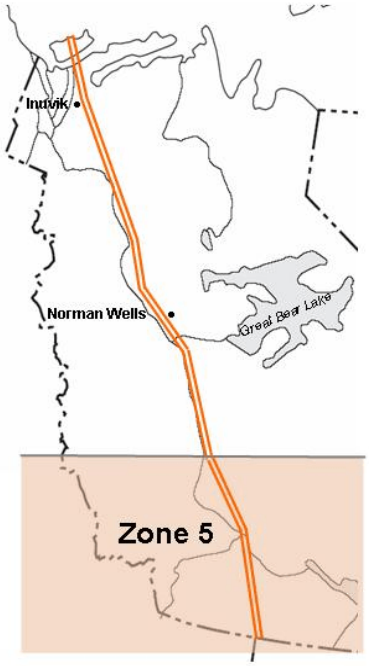

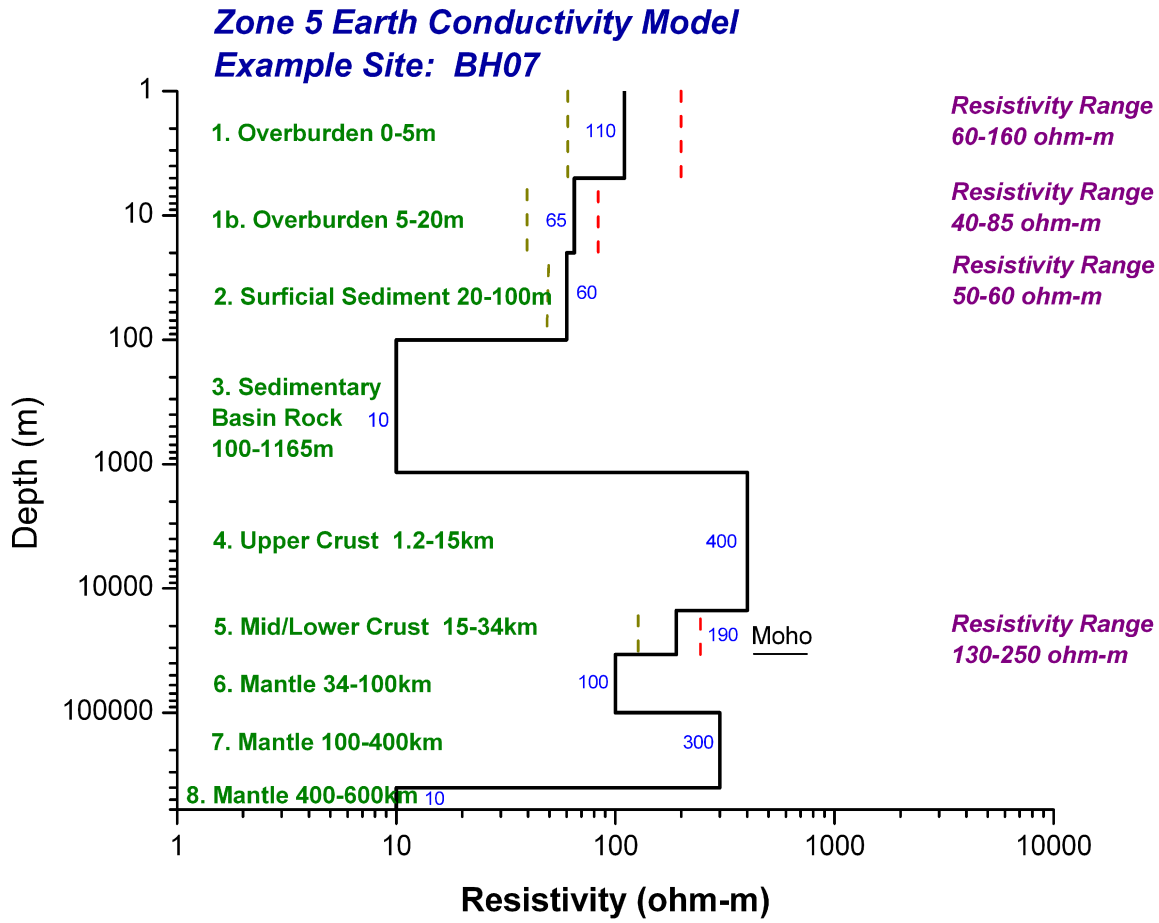

Figure 3.37. Earth conductivity model for Zone 5.
Refer to Table 3.9 for additional details.

TABLE 3.9: ZONE 5 EARTH CONDUCTIVITY MODEL

EXAMPLE BOREHOLE: **07** [geotechnical borehole, see Aylsworth et al., 2000]
LAT / LONG: 61°, 13' / 120°, 59'

Geological Unit	Resistivity (Ωm) Avg	Range	Resistivity Determination	Resistivity Reference	Comments
1. Overburden (silt) ***frozen*** (2 – 5 m)	---	60 - 160	In-situ (Laboratory), A	Assoc. Mining 2004	• From previous compilation of resistivity values at Ft. Simpson
2a. Overburden (silt), unfrozen (5 – 20 m)	---	40 - 85	In-situ (Laboratory), A	Assoc. Mining 2004	• From previous compilation of resistivity values at Ft. Simpson
2b. Surficial Sediments (20 - 100 m)	60	50 - 60	Ex-situ (MT survey), A	Wu 2001, p.365 Wu et al 2005, p.20	• Depth from MT survey near site
3. Sedimentary Basin Rocks (~ 0 - 1000 / 1165 m)	~ 10	---	Ex-situ (MT survey), A	Wu 2001, p.365 Wu et al 2005, p.20	• 1165 m depth from MT survey near site, generally coincident with petroleum exploration well Jean Marie E-7
from geological well log					
(0 – 215 m)	~ 50	lmst	In-situ (well log), A		
(215 – 810 m)	~ 8	shale, lmst	In-situ (well log), A	Wu 2001, p. 378	
(810 – 864 m)	~ 300	lmst	In-situ (well log), A	Wu 2001	
(864 – 907 m)	25	dolost, sst	In-situ (well log), A	Wu 2001	
(907 – 940 m)	> 500	lmst, dolost	In-situ (well log), A	Wu 2001	
4. Upper Crust (0 – 15 km)	> 400 - > 1000		Ex-situ (MT survey), B	Wu et al 2005, p.25, p.31 p.71	• Proterozoic (meta)sedimentary rocks • Conflicting values in reference
5. Middle – Lower Crust (15 – 34 km)	---	~130-250	Ex-situ (MT survey), B	Wu et al 2005, p.25	• Unusual conductive zone in upper crust near Ft. Simpson
6. Mantle (34 - ~ 100 km)	100	---	Ex-situ (MT survey), A	Wu et al 2005	• mantle depth from MT survey
7. Mantle (100 - 400 km)	300		Ex-situ (MT survey), C	Ferguson & Odwar	• resistivity model for Prairie Provinces
8. Mantle (400 - 600 km)	10	---	Ex-situ (MT survey), C	Ferguson & Odwar	• resistivity model for Prairie Provinces

TABLE 3.10: EXPLANATORY NOTES FOR TABLES 3.5 – 3.9

1. Determination – in-situ (laboratory) or ex-situ (geophysical) method used to determine the resistivity.
2. Confidence – judgment as to how representative is the value, based on following criteria;
    * A = best representative (measurements from site or nearby),
        - surficial sediments - value obtained by laboratory measurement, from local area
        - sedimentary basin - value obtained by MT survey near the site
        - crust – value obtained by MT survey near the site
        - mantle – value obtained by MT survey near the site

    * B = likely representative extrapolated
        - values extrapolated from previous measurements taken at some distance from the site

        - surficial sediments - value obtained by laboratory measurement or geophysical measurement
        - sedimentary basin - value obtained by regional MT survey
        - crust – value obtained by regional MT survey
        - mantle – value obtained by regional MT survey

    * C = possibly representative (measurements from general compilations)

ABBREVIATIONS

MT	magnetotelluric
Lmst	limestone
Dolost	dolostone, dolomite
Sst	sandstone

Appendix 3.1: Geologic Time Scale

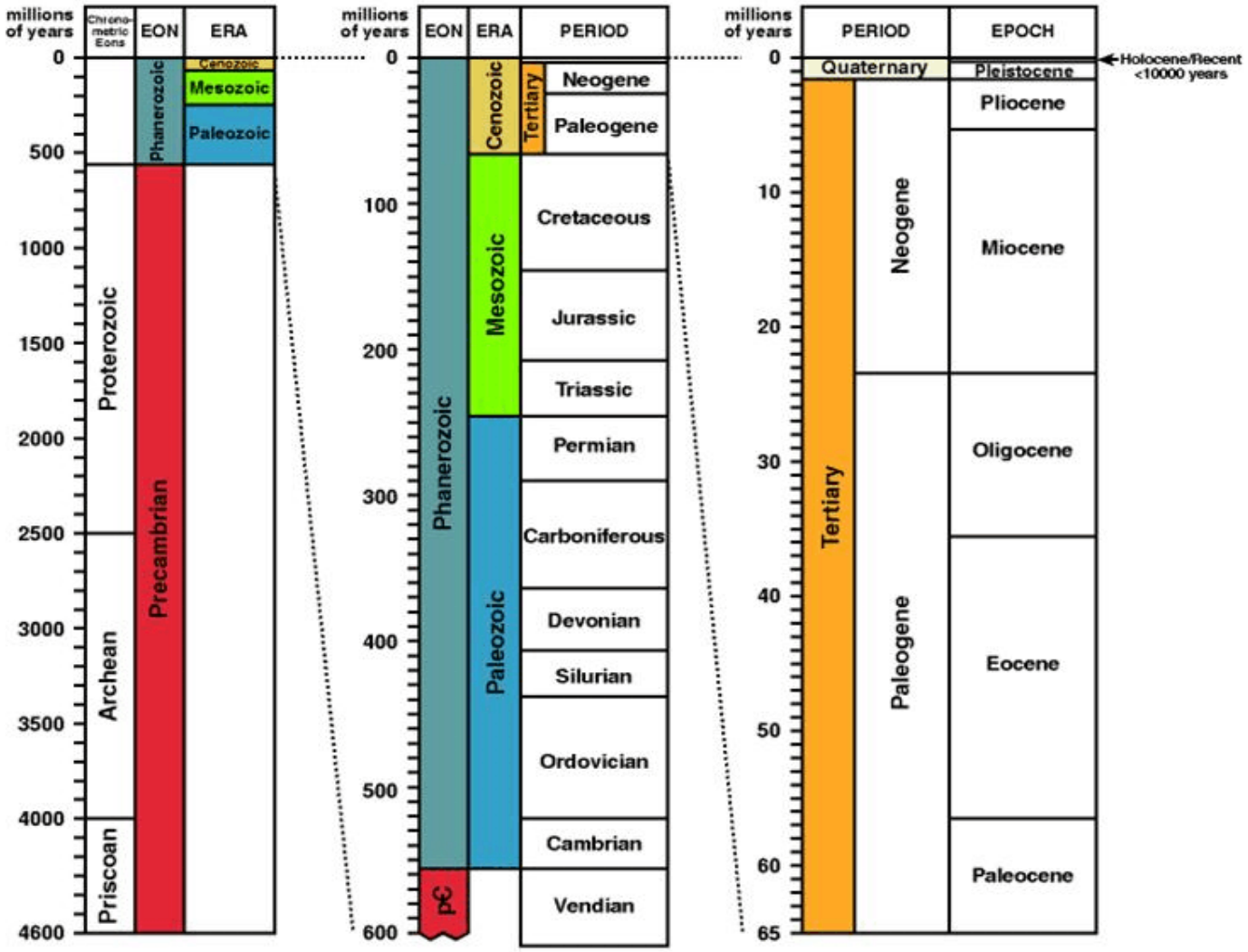

[Source: http://www.geo.ucalgary.ca/~macrae/timescale/time_scale.gif]

Appendix 3.2: Glossary of Talik Terminology

Talik - A layer or body of *unfrozen ground* occurring in a permafrost area due to a local anomaly in thermal, hydrological, hydrogeological, or hydrochemical conditions.

Taliks may have temperatures above 0°C (noncryotic) or below 0°C (cryotic, forming part of the permafrost). Some taliks may be affected by seasonal freezing. Several types of taliks can be distinguished on the basis of their relationship to the permafrost (closed, open, lateral, isolated and transient taliks), and on the basis of the mechanism responsible for their unfrozen condition (hydrochemical, hydrothermal and thermal taliks):

1. *closed talik* - a noncryotic talik occupying a depression in the *permafrost table* below a lake or river (also called "*lake talik*" and "*river talik*"); its temperature remains above 0°C because of the heat storage effect of the surface water;

2. *hydrochemical talik* - a cryotic talik in which freezing is prevented by mineralized groundwater flowing through the talik.

3. *hydrothermal talik* - a noncryotic talik, the temperature of which is maintained above 0°C by the heat supplied by groundwater flowing through the talik;

4. *isolated talik* - a talik entirely surrounded by perennially *frozen ground*; usually cryotic (see *isolated cryopeg*), but may be noncryotic (see transient talik);

5. *lateral talik* - a talik overlain and underlain by perennially *frozen ground*; can be noncryotic or cryotic;

6. *open talik* - a talik that penetrates the permafrost completely, connecting *suprapermafrost* and *subpermafrost water*, (e.g., below large rivers and lakes). It may be noncryotic (see *hydrothermal talik*) or cryotic (see hydrochemical talik).

SYNONYMS: (not recommended) through talik, penetrating talik, perforating talik, piercing talik;

7. *thermal talik* - a noncryotic talik, the temperature of which is above 0°C due to the local *thermal regime of the ground*;

8. *transient talik* - a talik that is gradually being eliminated by freezing, e.g., the initially noncryotic closed talik below a small lake which, upon draining of the lake, is turned into a transient isolated talik by *permafrost aggradation* (see also *closed-system pingo*).

[Source: Glossary, Frozen Ground Data Centre, National Snow and Ice Data Centre http://nsidc.org/fgdc/glossary/english.html#T]

3.6. References

Arcone, S.A., Chacho, E.F. and Delaney, A.J., 1998: Seasonal structure of taliks beneath arctic streams determined with ground-penetrating radar; in Seventh International Conference (Proceedings). Yellowknife (Canada), Collection Nordicana No. 55, p. 19-24.

Associated Mining Consultants Ltd. 2004: Report on the application of electrical and electromagnetic techniques in the design and construction of northern pipelines; Geological Survey of Canada, Open File Report.

Aspler, L.W, Pilkington, M. and Miles, W.F., 2003: Interpretations of Precambrian basement based on recent aeromagnetic data, Mackenzie Valley, Northwest Territories., Geol. Surv Can, Current Research 2003-C2

Aylsworth, J.M, Burgess, M.M., Desrochers, D.T., Duk-Rodkin, A., Roberston, T. and Traynor, J.E., 2000: Surficial geology, subsurface materials, and thaw sensitivity of sediments; *in* The Physical Environment of the Mackenzie Valley, Northwest Territories: a Base Line for the Assessment of Environmental Change, (ed.) L.D. Dyke and G.R. Brooks; Geological Survey of Canada, Bulletin 547, p. 41 – 48.

Aylsworth, J.M, and Kettles, I.M., 2000: Distribution of peatlands; *in* The Physical Environment of the Mackenzie Valley, Northwest Territories: a Base Line for the Assessment of Environmental Change, (ed.) L.D. Dyke and G.R. Brooks; Geological Survey of Canada, Bulletin 547, p. 49 – 55.

Bradford, J.H., McNamara, J.P., Bowden, W. and Gooseff, M.N., 2005: Measuring thaw depth beneath peat-lined arctic streams using ground-penetrating radar, Hydrological Processes (published on-line http://www3.interscience.wiley.com/cgi-bin/abstract/110471861/ABSTRACT retrieved July 2005)

Bobrov, N.Y., Krylov, S.S. and Soroka, I.V., 1998: Statistical investigations of shallow permafrost by electromagnetic profiling; in Seventh International Conference (Proceedings). Yellowknife (Canada), Collection Nordicana No. 55, p. 51-55.

Burn, C.R., 2002: Tundra lakes and permafrost, Richards Island, western Arctic Coast, Canada., Canadian Journal Earth Science, 39, p. 1291-1298.

Burgess, M.M. and Smith, S.L**.,** 2000: Shallow ground temperatures; *in* The Physical Environment of the Mackenzie Valley, Northwest Territories: a Base Line for the Assessment of Environmental Change, (ed.) L.D. Dyke and G.R. Brooks; Geological Survey of Canada, Bulletin 547, p. 89 – 103.

Burgess, M.M. and Smith, S.L. 2003. 17 years of thaw penetration and surface settlement observations in permafrost terrain along the Norman Wells pipeline, Northwest Territories, Canada; Proceedings of 8th International Conference on Permafrost, July 2003, Zurich Switzerland, p. 107-112.

Campbell, W.H., 1997: Introduction to Geomagnetic Fields; Cambridge University Press.

Collett, T.S., and Dallimore, S.R., 2002: Integrated well log and reflection seismic analysis of gas hydrate accumulations on Richards Island in the Mackenzie Delta, NWT, Canada, CSEG Recorder, Oct 2002, p.30-39.

Cook, F.A., van der Velden, A.J., Hall, K. W., and Roberts, B.J., 1999: Frozen subduction in Canada's Northwest Territories: Lithoprobe deep lithospheric reflection profiling of the western Canadian Shield., Tectonics 18, p.1-24.

Cumberland Resources Ltd., 2004: _Meadowbank Gold Project, Draft Environmental Impact Statement (Executive Summary), December 2004., http://www.cumberlandresources.com/mdb/ExecutiveSummary.pdf Retrieved July 2005.

Delaney, A.J., Peapples, P.R. and Arcone, S.A., 2001: Electrical resistivity of frozen and petroleum-contaminated fine-grained soil, Cold Regions Science and Technology 32, p.107-119.

Dixon, J., Dietrich, J.R., McNeil, D.H., and Lane, L.S., 2001: Geological framework of the Beaufort-Mackenzie Basin (abstract), Rock the Foundation, June 18-22, Canadian Society of Petroleum Geologists.

Dyke, L.D., 2000: Shoreline permafrost along the Mackenzie River; *in* The Physical Environment of the Mackenzie Valley, Northwest Territories: a Base Line for the Assessment of Environmental Change, (ed.) L.D. Dyke and G.R. Brooks; Geological Survey of Canada, Bulletin 547, p. 143-151.

Ebasco Services Incorporated, 1974: Cathodic_protection system for the Arctic Gas Pipeline, prepared for Alaskan Arctic Gas Study Company and Canadian Arctic Gas Study Limited through Northern Engineering Services Company Ltd.

Ferguson, I.J. and Odwar, H.D., 1997: Appendix 4: Review of conductivity soundings in Canada; *in* Geomagnetically Induced Currents: Geomagnetic hazard Assessment Phase II, Final Report, Volume 3; Geological Survey of Canada, Open File Report xxx, p. A3-1 – A3-121.

Ferguson, I., 2005: Web page, Faculty and Their Research, Dept. Geological Sciences, University of Manitoba. http://www.umanitoba.ca/geoscience/faculty/ferguson/iferguson.htm Retrieved July 2005.

French, H.M., 1996: The Periglacial Environment, Addison Wesley Longman Limited.

Hewes, F.W., 1973: Electrical properties of soils, Caproco Corrosion Prevention Ltd.

Imperial Oil Resources Ventures Limited, 2005: Permafrost – Taliks, Response 1.21WP (INAC-0021WP).

Jones A.G. and Ferguson, I.J., 2001: The electric moho, Nature 409, January 2001, p.331 – 333.

Kokelji, S.V., 2003: Near-surface ground ice in sediments of the Mackenzie Delta region, Northwest Territories, Unpub. Thesis, Carleton University, Ottawa.

Lane, L.S., 2002: Tectonic Evolution of the Canadian Beaufort Sea – Mackenzie Delta region: a brief overview, CSEG Recorder, Feb 2002, p.49-54

Mackenzie Gas Producer Group, 2003: Various reports; http:// www.mackenziegas project.com/theProject/overview/index.html Retrieved March 2005

Mackenzie Gas Project, Joint Review Panel Intervenor Information Request Response, pp. 60 http://www.ngps.nt.ca/Upload/IORVL_IR_Round_1_Responses_to_INAC.pdf Retrieved July 2005

Mackay, D.K., 1970: Electrical resistivity measurements in frozen ground, Mackenzie Delta area, Northwest Territories, *in* Hydrology of Deltas, Proceeding of the Bucharest Symposium, Vol. 2, p.363-375.

Mackay, J.R and Burn, C.R., 2002: The first 20 years (1978-1979 to 1998-1999) of active-layer development, Illisarvik experimental drained lake site, western Arctic coast, Canada., Canadian Journal Earth Science, 39, p. 1657-1674.

Mussett, A.E. and Khan, M.A., 2000: Looking into the earth; an introduction to geological geophysics, Cambridge Univ. Press, Cambridge, UK.

Nixon, F.M., 2000: Thaw-depth monitoring; *in* The Physical Environment of the Mackenzie Valley, Northwest Territories: a Base Line for the Assessment of Environmental Change, (ed.) L.D. Dyke and G.R. Brooks; Geological Survey of Canada, Bulletin 547, p. 119 – 126.

Nixon, M., Tarnocai, C. and Kutny, L. 2003. Long-term active layer monitoring: Macknezie Valley, northwest Canada. Proceedings of the 8th International Conference on Permafrost, July 2003, Zurich Switzerland. M. Phillips, S.M. Springman and L.U. Arenson (eds.), A.A. Balkema, Lisse, the Netherlands, p. 821-826

Northern Engineering Services Company Limited, 1972: Cathodic protection tests at the Arctic Test Facility, prepared for Canadian Arctic Gas Study Limited.

Northern Engineering Services Company Limited, 1976: Geophysical Investigations on the rivers of the Arctic Coastal Plain in Alaska, prepared for Canadian Arctic Gas Study Limited,

Northern Engineering Services Company Limited, 1977: Geotechnical data report permafrost distribution: Willowlake River, NWT to Zama Lake, Alberta

Northwest Territories Cumulative Impact Monitoring Program, 2005: *Valued Component – Snow, Ground Ice and Permafrost (Update November 2004),* Snow, Ground Ice and Permafrost Excerpt http://www.nwtcimp.ca/reports_water/snow_ice_permafrost_nov2004.pdf . Retrieved June 2005.

O'Leary, D.D., Ellis, R.M., Stephenson, R.A., Lane, L.S., and Zelt, C.A.,1995: Crustal structure of the northern Yukon and Mackenzie Delta, northwestern Canada., Journal of Geophysical Research 100, no.B7, p.9905-9920.

Parkhemenko, E.I., 1967: Electrical properties of rock, New York, Plenum Press.

Pidwirny, M., 2005: Chapter 10: Introduction to the Lithosphere, Periglacial Processes and Landforms, *in* Phys.Geog..Net. http://www.geog.ouc.bc.ca/physgeog/contents/11q.html Retrieved July 2005.

Pole, D.F. and Lawton, D.C., 1991: A model study of multichannel reflection seismic imaging over shallow permafrost in the Beaufort sea continental shelf, Canadian Journal of Exploration Geophysics, 27, No. 1, p. 34-42.

Redman, D. and Bauman, P., 2004: Draft - Applications of geophysical methods to permafrost, review of literature; Geological Survey of Canada, Open File Report

Scott, W.J., Sellmann, P.V., and Hunter, J.A., 1990: Geophysics in the study of permafrost; *in*, (ed.) S. H. Ward; Geotechnical and Environmental Geophysics, Vol 1: Review and Tutorial, Societey of Exploration Geophysicists, p. 355 – 384.

Shell Canada Limited, 2004: Section 5.1, Design Criteria, Application for Approval of the Development Plan for Niglinkgak Field Description, NDPA-1 August 2004, p. 5-9., http://www2.ngps.nt.ca/applicationsubmission/Documents/MGP_Nig_DPA_Section_5.pdf Retrieved July 2005

Sheriff, R.E., 2002: Encyclopedic dictionary of applied geophysics, 4 ed, Tulsa; Society of Exploration Geophysics

Simpson, F. and Bahr, K., 2005: Practical Magnetotellurics; New York; Cambridge University Press, p. 11

Smith, S.L., Burgess, M.M., and Heginbottom, J.A., 2001: Permafrost in Canada, a challenge to northern development; *in* A Synthesis of Geological Hazards in Canada, (ed.) G.R. Brooks; Geological Survey of Canada, Bulletin 548, p. 241 – 264.

Smith, S.L., Burgess, M.M. and Nixon, F.M., 2001. Response of active-layer and permafrost temperatures to warming during 1998 in the Mackenzie Delta, Northwest Territories and at Canadian Forces Station Alert and Baker Lake, Nunavut; Geological Survey of Canada Current Research 2001-E5, 8 p.

Stephenson, R.A., Coflin, K.C., Lane, L.S. and Dietrich, J.R., 1994: Crustal structure and tectonics of the southeastern Beaufort Sea continental margin, Tectonics, Vol, 13, No.2, p.389-400.

Stott, D.F. and Klassen, R.W., 1993: Geomorphic divisions; Subchapter 2C in Sedimentary Cover of the Craton in Canada, D.F. Stott and J.D. Atkin, Geol. Surv Can, Geology of Canada, no. 5, p.31-44.

Taylor, A.E., Burgess, M.M. Judge, A.S. and Allen, V.S., 2000: Deep ground temperatures; *in* The Physical Environment of the Mackenzie Valley, Northwest Territories: a Base Line for the Assessment of Environmental Change, (ed.) L.D. Dyke and G.R. Brooks; Geological Survey of Canada, Bulletin 547, p. 105 – 109.

Terrain Science Division, 2005: Regional Studies; Geological Survey of Canada, web posting; http://sts.nrcan.gc.ca/permafrost/regional.html Retrieved April 2005.

Trenhaile, A.S., 1998: Geomorphology: A Canadian Perspective, Oxford University Press.

University of Alaska Water and Environmental Research Centre, 2005: Prospectus, Kuparuk River watershed, proposed long term hydrologic observatory, north slope, Alaska. http://www.uaf.edu/water/ArcticCUAHSI.pdf Retrieved July 2005.

Walker, H.H., 1983: Guidebook 2, Guidebook to Permafrost and Related Features of the Colville river Delta, Alaska, Fourth International Conference on Permafrost, University of Alaska, Fairbanks, Alaska, July 18-22, 1983 http://wwwdggs.dnr.state.ak.us/scan1/gb/text/GB2.PDF Retrieved July 2005.

Wawruck, W.A., 1971: Soil resistivity measurements along routes, Gas Arctic Service.

Wu, X., 2001: Determination of near-surface, crustal and lithospheric structures in the Canadian Precambrian Shield using time-domain electromagnetic and magnetotelluric methods, Ph.D thesis, University of Manitoba

Wu, X., Ferguson I.J. and Jones, A.G., 2005: Geoelectrical structure of the Proterozoic Wopmay Orogen and adjacent terranes, Northwest Territories, Canada (in preparation).

Viejo, G.F., and Clowes, R.M., 2003: Lithospheric structure beneath the Archaean Slave province and Proterozoic Wopmay origin, northwestern Canada, from a Litho probe refraction/wide-angle reflection survey., Geophysics. J. Int. 153, p.1-19.

Yershov, E.D., 1998: General Geocryology, Cambridge University Press.

Chapter 4

Assessment of Telluric Activity

4.1. Introduction

The geomagnetic field fluctuations are accompanied by the geo-electric (telluric) field and telluric currents at the surface of the Earth and in the pipelines. These telluric currents disturb pipeline cathodic protection levels, creating pipe-to-soil potential (PSP) fluctuations with different amplitudes. Amplitudes of PSP fluctuations directly depend on the telluric activity in the area of the pipeline location. This chapter contains description of telluric activity in the Mackenzie Valley area.

Two parameters define telluric activity in the particular area, one is the geomagnetic field variations, and other is the deep ground conductivity structure. The basic theory of the relations between geomagnetic field and telluric currents are presented in Part 4. 2. This theory allows us to find the geo-electric (telluric) field at the Earth surface if the geomagnetic field and the Earth conductivity profile are known.

This theory was applied in order to calculate geo-electric (telluric) field variations in the Mackenzie Valley area. Magnetic data from Yellowknife Geomagnetic Observatory (chapter 2) were used with surface impedance, derived from one-dimensional Earth conductivity models for five different zones based on the geological surveys (Chapter 3). Frequency characteristics of the surface impedance and effect of the surficial active layer are discussed in Part 4.3.

In Part 4.4 we present examples of 1-minute electric field variations for days with different geomagnetic activity for all 5 zones along the pipeline route. These daily variations were used later (Chapter 6) with the pipeline model to show the sizes of the pipe-to-soil variations for days with different geomagnetic activity levels.

To properly evaluate effects of telluric activity on the scale of years, statistical study is needed. For the statistical analysis of telluric activity in Mackenzie Valley, we established two types of indices of telluric electric field: hourly maximum of the absolute value of the electric field and hourly standard deviation of the electric field. For evaluation of the electric fields (and pipeline voltages) during different geomagnetic conditions, a linear regression analysis has been performed. It gives the relationship between hourly electric field indices and hourly ranges of magnetic field (X-component). Linear fit gives simple formulas to infer telluric indices from local geomagnetic index for Yellowknife (Part 4.5) for different zones along the pipeline route.

To develop a quantitative scale for different telluric activity levels, hourly telluric indices were calculated for two different areas, low latitude (Ottawa) and area of interest (Yellowknife). Ottawa results were used to establish the normal quiet value of telluric indices, which occurred 95% of the year. For other values of the telluric activity scale, Yellowknife statistical evaluation has been used (Part 4.6).

More complete statistical study has been made for each of 5 zones of the conductivities structures along the pipeline route (Part 4.7).It shows, that 5 zones can be reduced to 3 larger areas according to the hours in the year when indices were above established threshold levels of telluric activity.

From statistical geomagnetic results (chapter 2) for almost three complete solar cycles, the most active (2003) and the most quiet (1996) years for Yellowknife magnetic observatory were chosen for electric field calculations and production of statistical plots for telluric activity (Part 4.8).

4.2. Theoretical Background

The electric fields produced by geomagnetic disturbances drive electric currents within the earth. These induced currents have the effect of shielding the interior of the earth from the geomagnetic disturbance. The decrease of the magnetic and electric fields within the earth is dependent on frequency and on the conductivity structure of the earth. At the frequencies of geomagnetic field variations, the skin depths within the earth extend to hundreds of kilometers, and the conductivity of the earth down to these depths has to be taken into account in calculating the relation between the electric and magnetic fields at the surface.

The variation of conductivity with depth within the earth can be modeled using multiple horizontal layers with a different uniform conductivity as shown in Chapter 3, with the last layer as an uniform half-space. For the calculation of the geo-electric field an assumption needs also to be made about the spatial structure of the source of geomagnetic fluctuations. Here we assumed the simplest case of a plane wave, propagating down the Earth.

We use the geomagnetic coordinate system with axis *x* north, *y* east, and *z* vertically downwards. For the frequency range of 1sec- 24 hours and earth conductivities 1-1000 Ohm-m, displacement currents are small in comparison with conductivity currents. Therefore, electric and magnetic fields in the frequency domain can be given by diffusion equations.

$$\frac{d^2E}{dz^2} = i\omega\mu\sigma E \tag{4.1}$$

$$\frac{d^2H}{dz^2} = i\omega\mu\sigma H \tag{4.2}$$

Solutions for each layer have the form

$$E = A(e^{-kz} + Re^{kz}) \tag{4.3}$$

and

$$H = A(\frac{e^{-kz}}{Z_0} - \frac{Re^{kz}}{Z_0}) \tag{4.4}$$

where A and R are the amplitude and reflection coefficient, $k=\sqrt{i\omega\mu\sigma}$ is the propagation constant, $Z_0=\frac{i\omega\mu}{k} = \sqrt{\frac{i\omega\mu}{\sigma}}$ is the characteristic impedance (ratio of the electric and magnetic fields for the uniform medium).

For our case, when the magnetic field at the surface of the earth (1st layer) is known from the magnetic observations, the electric field can be obtained from the ratio (impedance) of magnetic and electric fields

$$E_s = Z_1 H_s \tag{4.5}$$

The impedance at any layer can be found by applying the recursion relation for the impedance of an N - layered half-space (Weaver, 1994).

$$Z_n = i\omega\mu \left(\frac{1 - r_n e^{-2k_n l_n}}{k_n (1 + r_n e^{-2k_n l_n})} \right) \tag{4.6}$$

where $\mathbf{l_n}$, $\mathbf{k_n}$ are the thickness and propagation constant of the layer n,

$$r_n = \frac{1 - k_n \frac{Z_{n+1}}{i\omega\mu}}{1 + k_n \frac{Z_{n+1}}{i\omega\mu}} \tag{4.7}$$

and for the last layer

$$Z_N = \frac{i\omega\mu}{k_N} \tag{4.8}$$

To obtain geo-electric field at the earth surface from known geomagnetic field data, the following sequence of operations was performed:

1 Conversion of the geomagnetic data (time into frequency domain by using Fast Fourier Transformation (FFT).
2. Multiplication by the surface impedance, obtained from one-dimensional conductivity profile of particular area.
3. Inverse transform into time domain by using inverse FFT.

The Fourier transformation routine is available as built-in procedure in ORIGIN 6 and available as FORTRAN code in (Press et al, 1992).

4.3. Surface Impedance Models

The earth conductivity profiles for different zones, described in Chapter 3, were used as an input to the recursion relation (4.6) to produce surface impedance values for 5 zones along the pipeline route. This surface impedance represents transfer function between geomagnetic variations and geo-electric (telluric) field at the Earth surface and used with known geomagnetic data from Yellowknife observatory to obtain 1-minute electric field variations

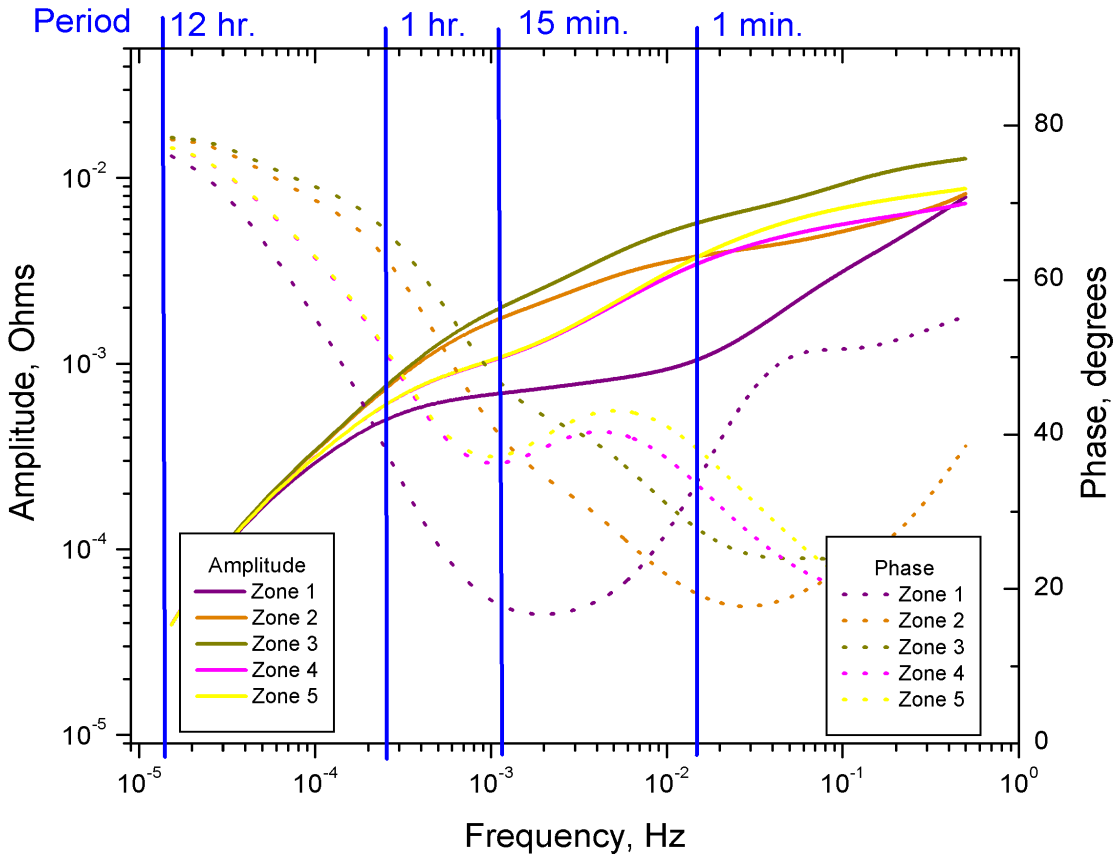

Fig. 4.1. Surface impedance for the earth models, Zones 1-5.
Solid lines - amplitudes, dotted lines - phases.

As shown in Fig.4.1, surface impedances are different for different zones. They depend on the frequency as well as on the conductivities of the different layers. This dependence can be explained in terms of "skin depth" of conductors with respect to the electromagnetic waves. When the electromagnetic waves of different frequencies propagate down the Earth, they partially penetrate conductive layers and decay at different depths, depending on their frequency and particular conductivity of the layer. In our study we are using 1-minute data, which defined the highest frequency we are concerned with as 0.015 Hz. Variations with more than 12 hours period or about 0.01 mHz, characterize the lower part of studied frequency spectrum. Natural electromagnetic waves

of this frequency range (0.01 Hz-0.01 mHz) penetrate deep into the Earth and are not affected by the surficial geology.

Because in the Mackenzie Valley area the surface of the ground changes from frozen to thawed during the season, we performed the additional modeling of frozen-thawed top active layer of maximum 2 meters depth on top of the layered earth model of Zone 5.The results for two extreme cases of the resistivities of the top active layer of 2000 Ohm-m (frozen) and 2 Ohm-m (thawed) are shown in Fig. 4.2

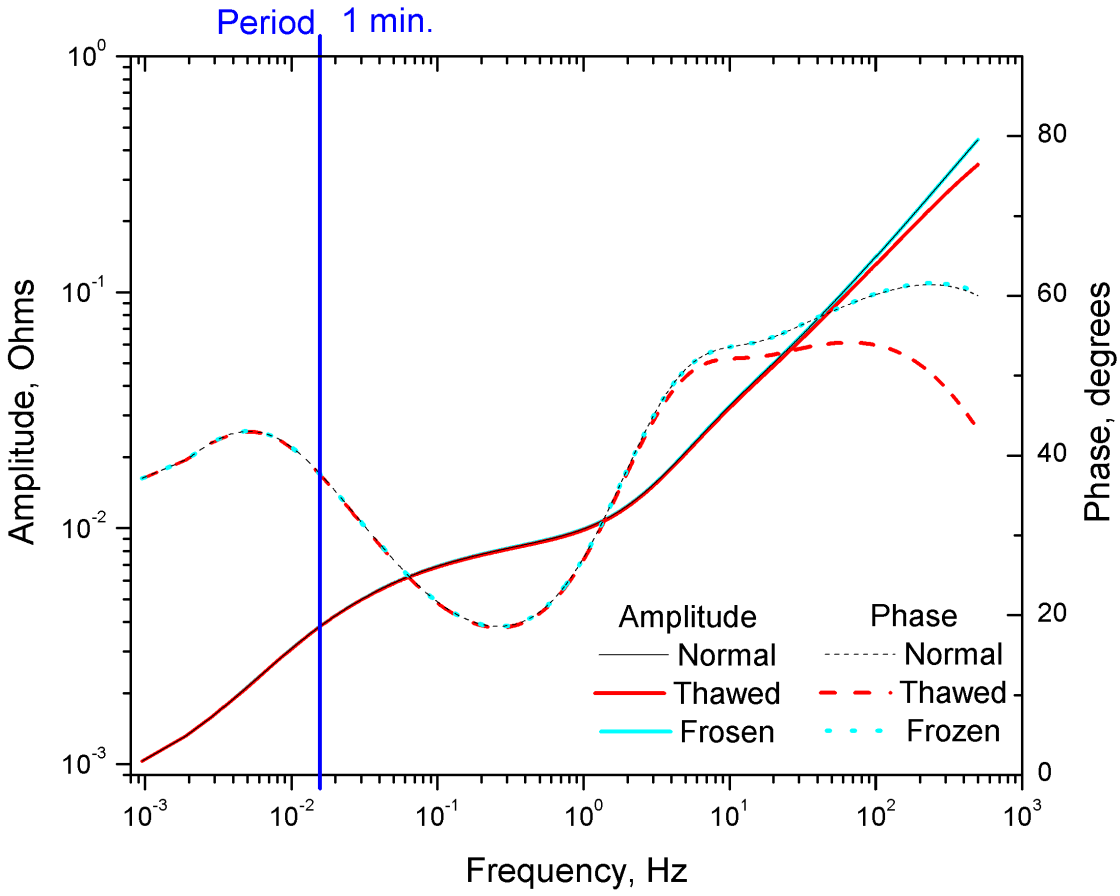

Fig. 4.2. Surface impedance with and without top active layer.
Solid lines - amplitudes, dotted lines - phases.

From the results demonstrated in Fig. 4.2., we can conclude that the existence of the active layer at the top of the layered earth structure started to have effect on the impedance values (phase) at frequencies of more than 1 Hz. Therefore, active layer will not be included in the further surface impedance models for the telluric electric field calculations.

4.4. Daily Variations of Geo-Electric Field

From the investigation of magnetic activity in 2004, specific days were chosen as representative of the different classes of magnetic activity. To choose these days, we applied the following procedure to the geomagnetic hourly range index from Yellowknife geomagnetic observatory data.

When the certain predefined hourly range limits of the geomagnetic activity occurred for most of the day, this day has been chosen as representative. These hourly range limits represent scale of the geomagnetic activity in the Mackenzie Valley area and were described in Chapter 2.

For example, there were some days with 24 HRX values below 40 nT quiet limit, from which the day with the lowest HRX values was chosen. There were no days when HRX>600 nT for all 24 hours, so the day with largest number of this highest level of activity has been chosen.

Dates for the electric field calculations were:

Quiet days with HRX< 40 nT : November 6.

Unsettled days with 40 nT <HRX< 300 nT: January 17.

Active days with 300 nT <HRX< 600 nT : January 16.

Special transitional from quiet to stormy day : November 7

Stormy days with HRX>600 nT : November 8

Geomagnetic data for these days were used to calculate electric field X (northward) and Y(eastward) components with 5 different models of the surface impedance, representing 5 different zones along the pipeline route. The results are shown in Figs 4.3 - 4.12. It can be seen, that amplitude of electric field fluctuations are below 20 mV/km for quiet day, below 200 mV/km for unsettled day (even larger in Y-component), around 400 mV/km in active day and above 600 mV/km for geomagnetic storm.

Comparisons between the different zones for the same day show, that, not only geomagnetic activity, but also earth conductivity model affect the amplitude of electric field variations.

Comparison of the electric fields for different zones shows, that zone 1 produced the lowest electric field values, while zone 3 produce the largest. These preliminary results will be then undergo more extended statistical studies.

The Ex and Ey components of the electric field later has been used to produce the time variations of the electric field in the direction of the pipeline and serve as an input to a pipeline model (Chapter 6).

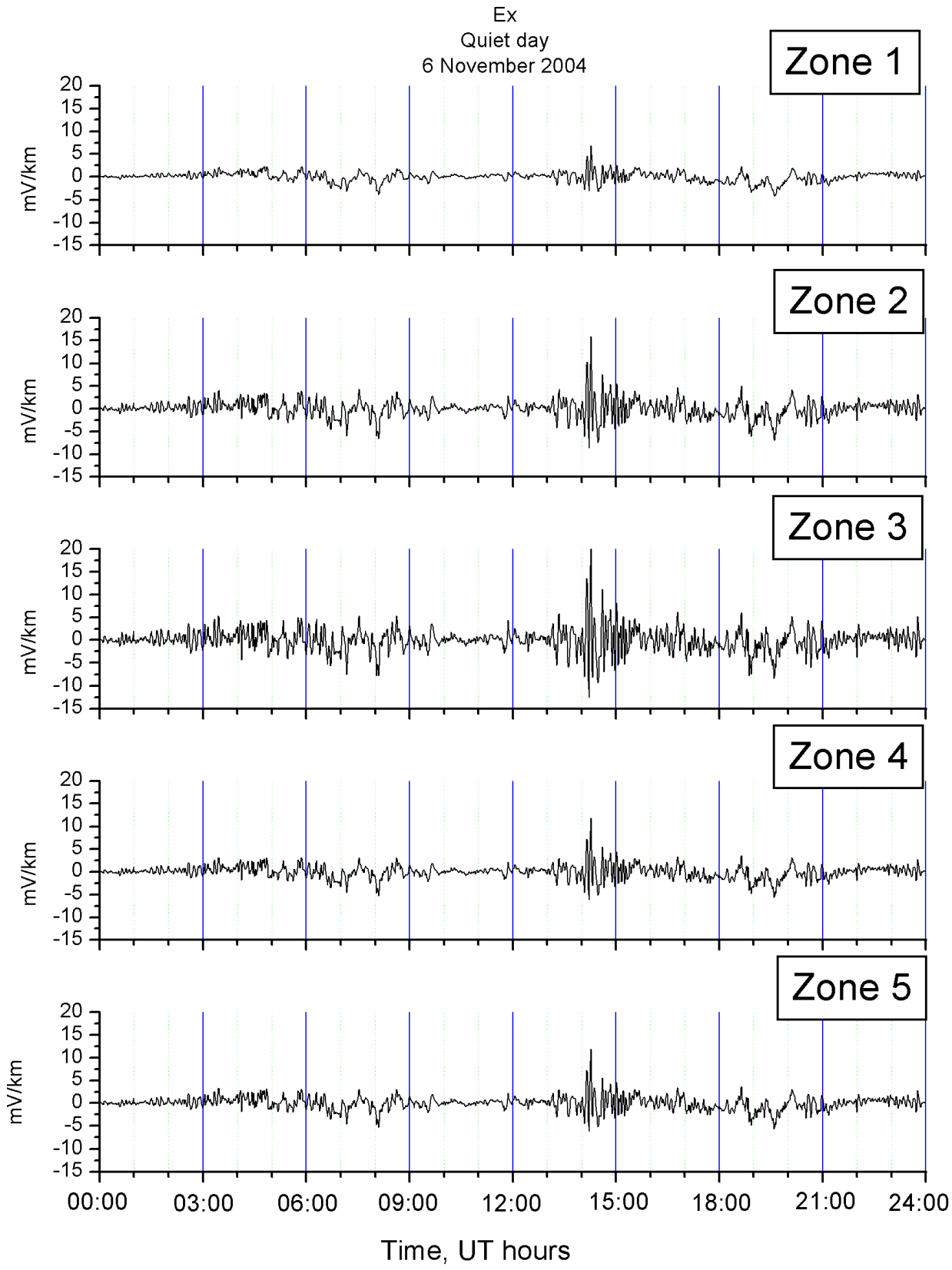

Fig. 4.3 Northward (Ex) electric field variations on a quiet day

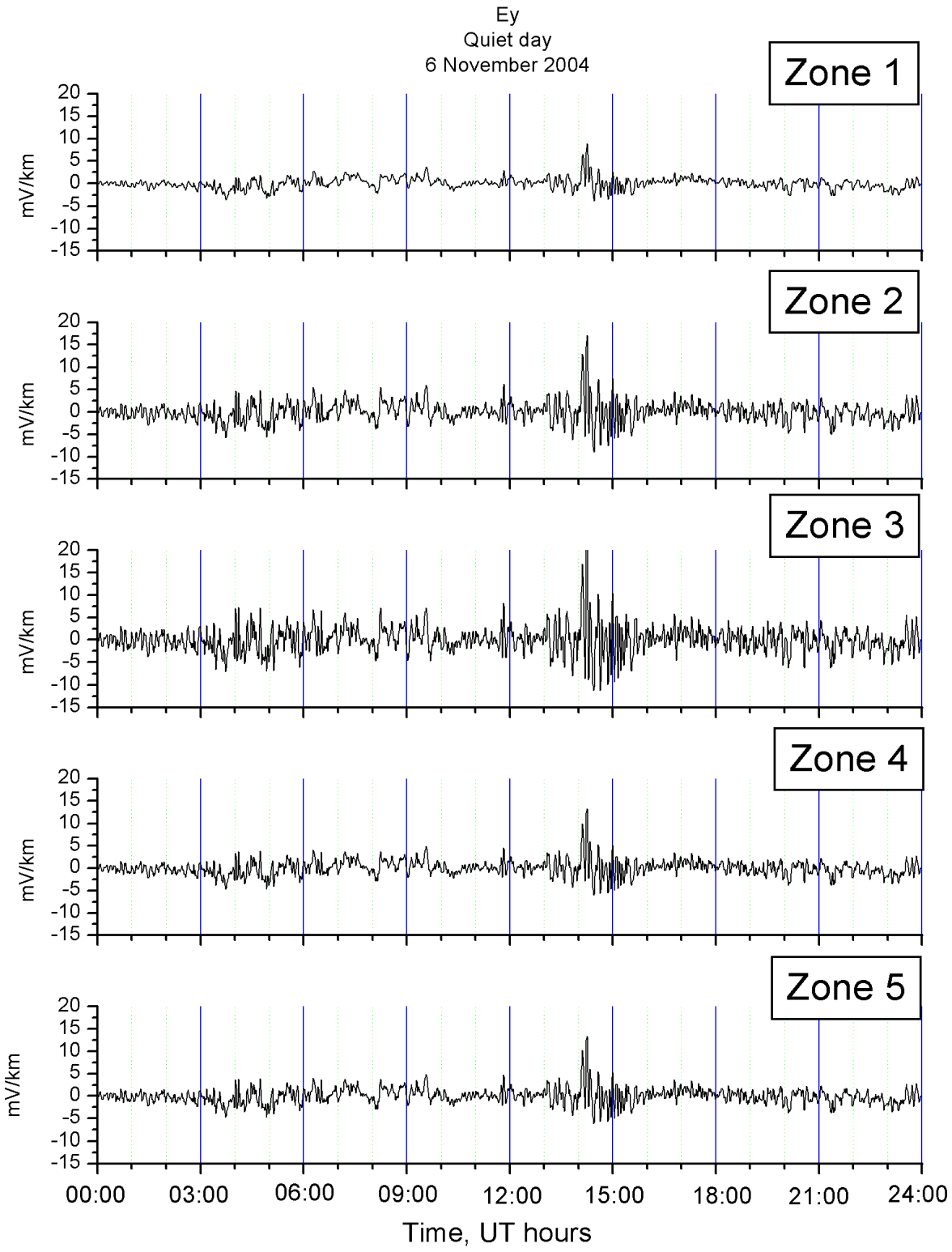

Fig. 4.4 Eastward (Ey) electric field variations on a quiet day

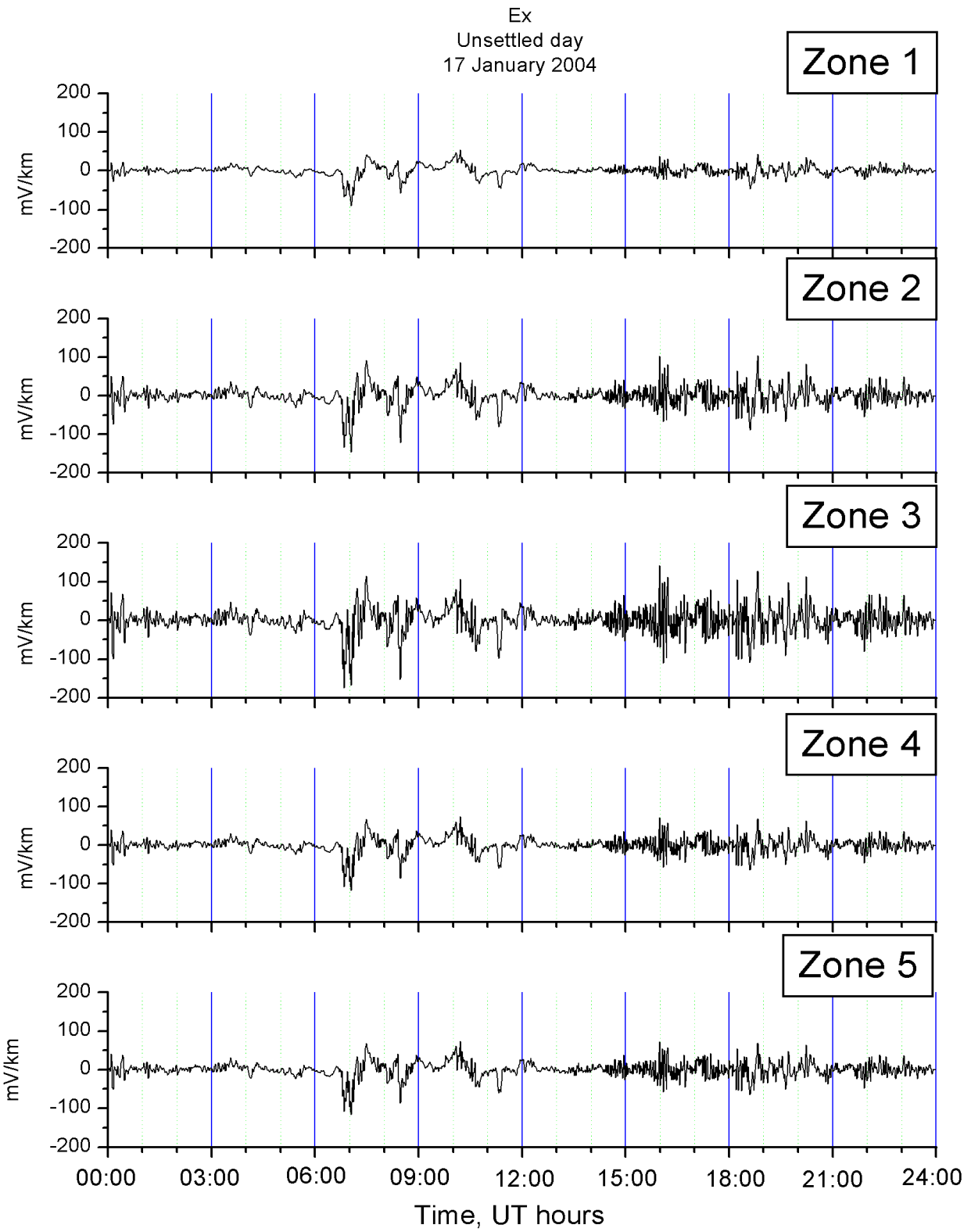

Fig. 4.5 Northward (Ex) electric field variations on an unsettled day

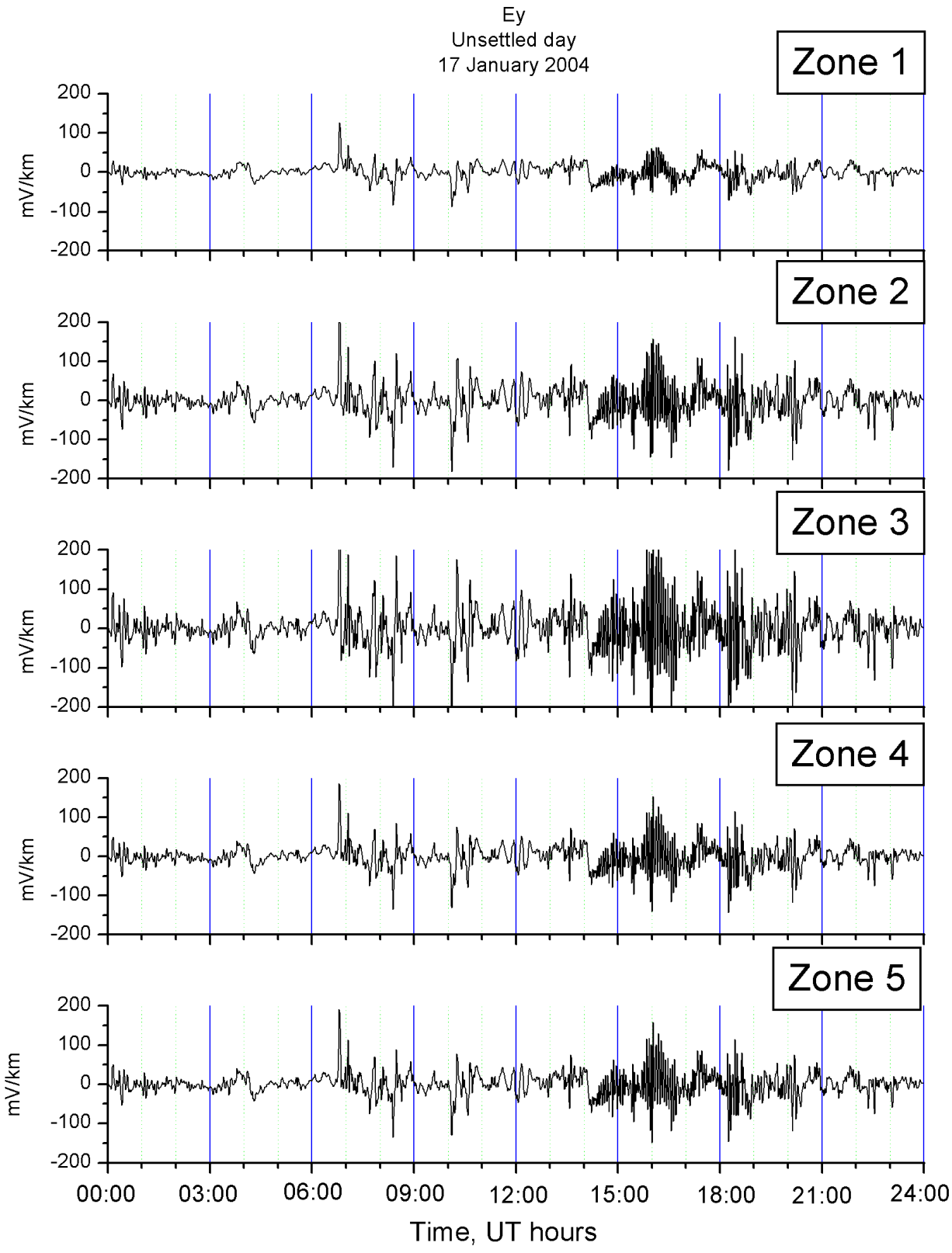

Fig. 4.6 Eastward (Ey) electric field variations on an unsettled day

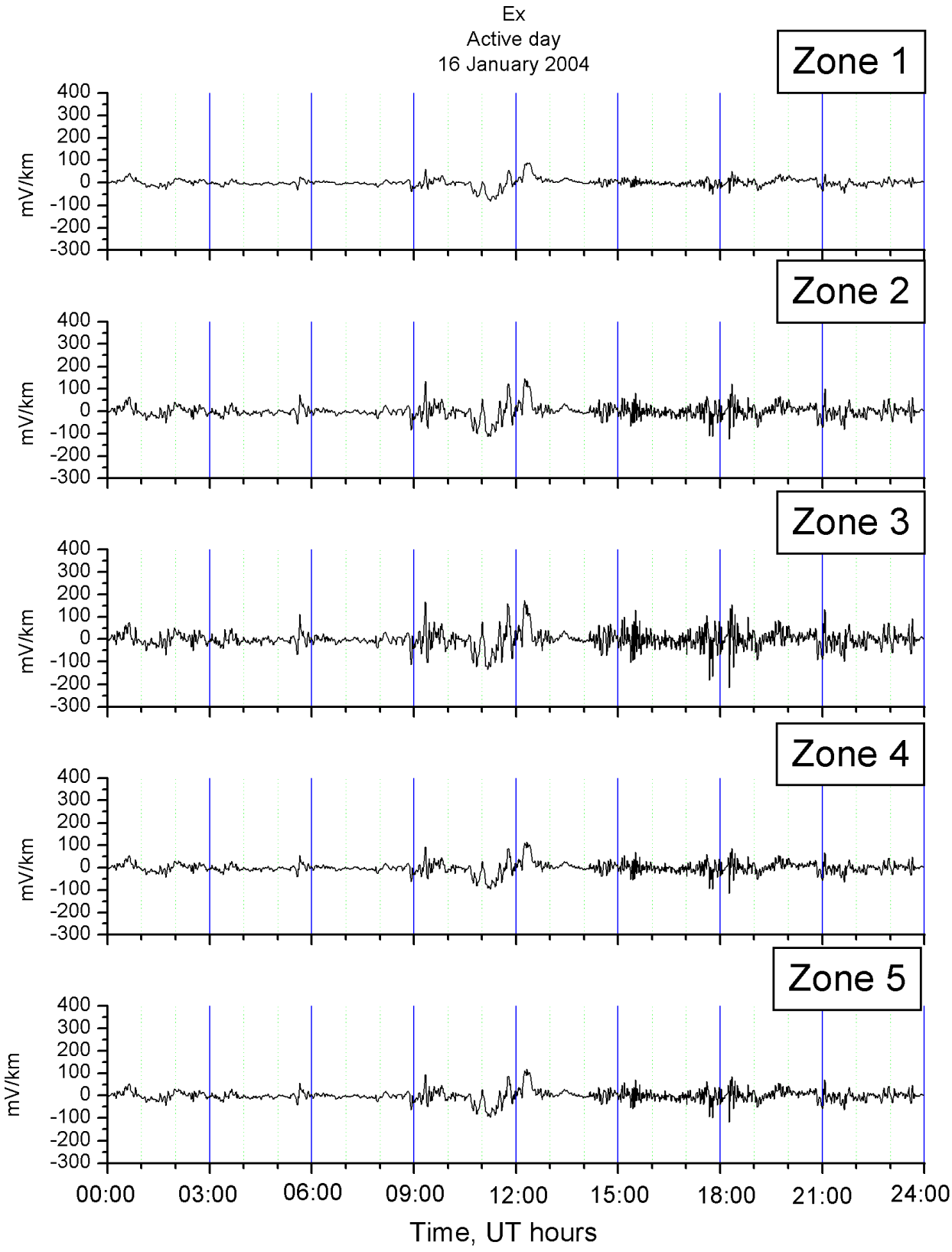

Fig. 4.7 Northward (Ex) electric field variations on an active day

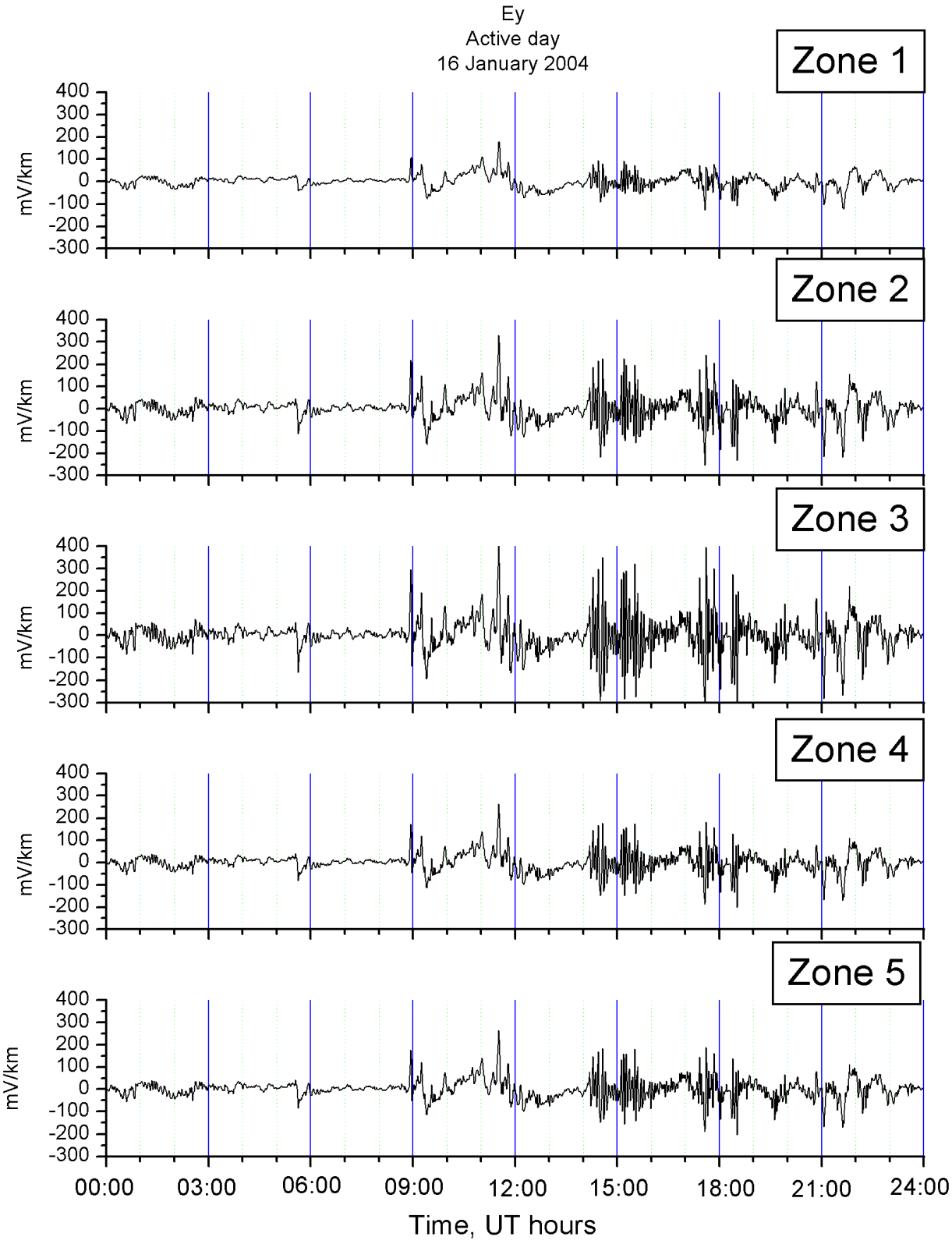

Fig. 4.8 Eastward (Ey) electric field variations on an active day

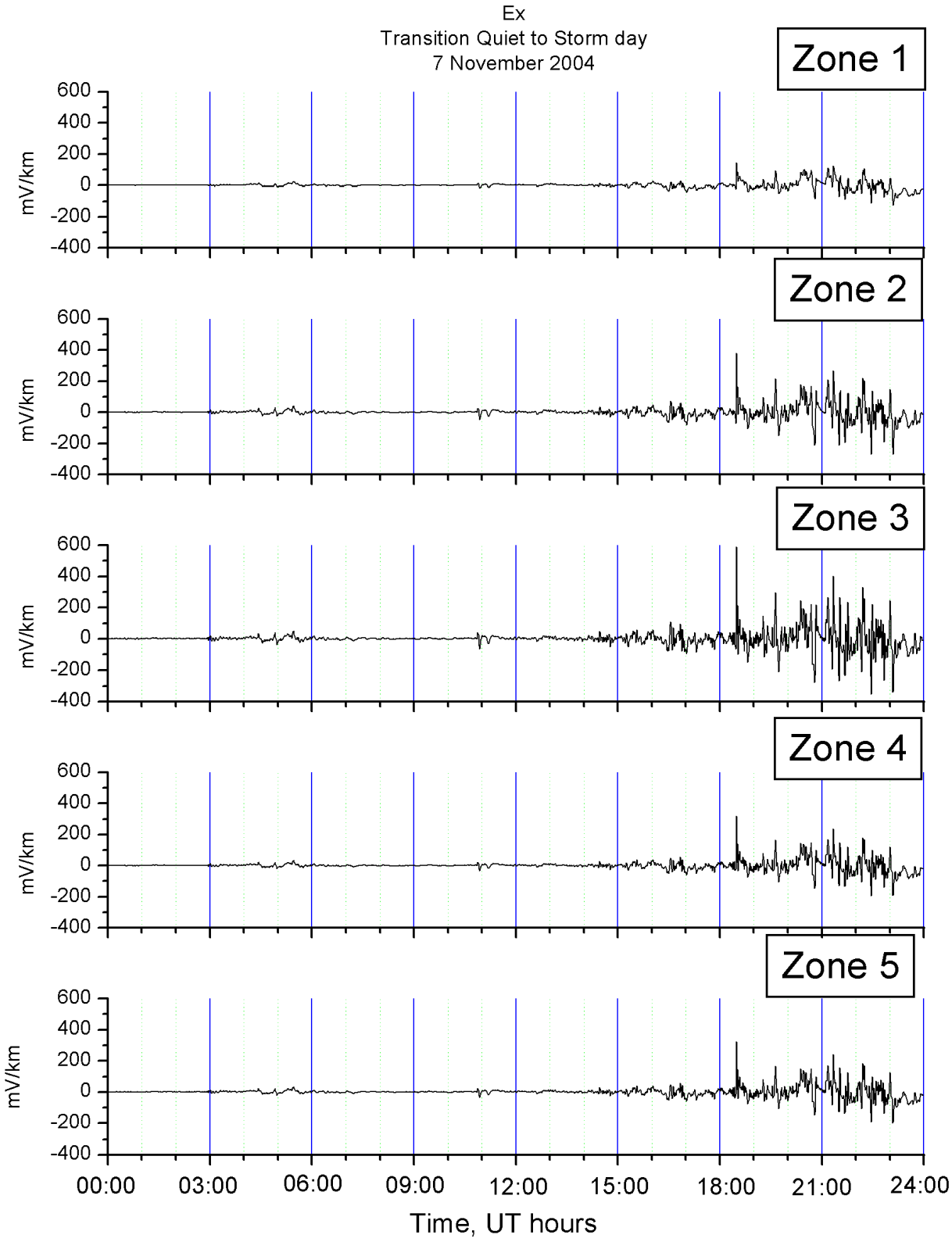

Fig. 4.9 Northward (Ex) electric field variations on a day showing a transition from quiet to storm

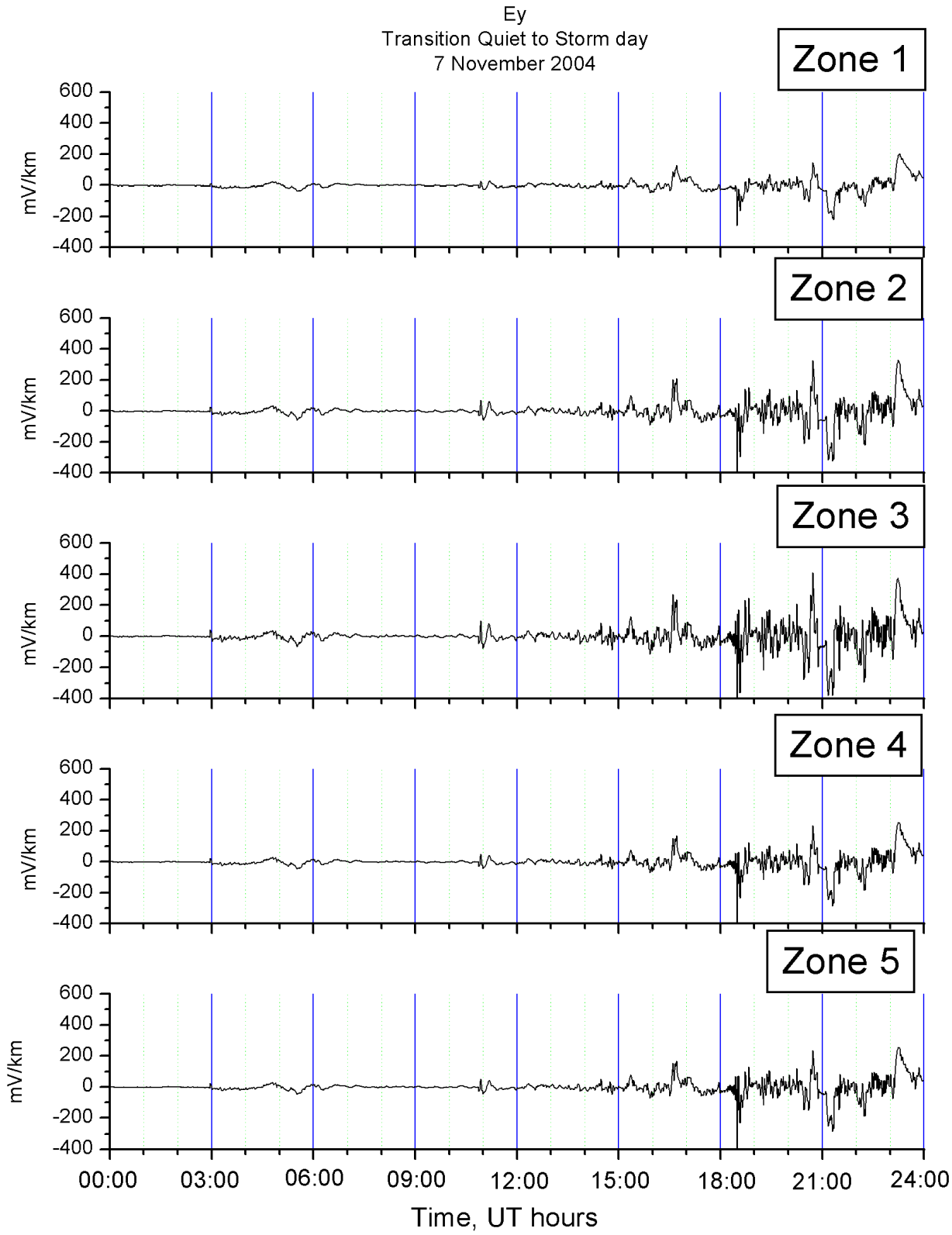

Fig. 4.10 Eastward (Ey) electric field variations on a day showing transition from quiet to storm

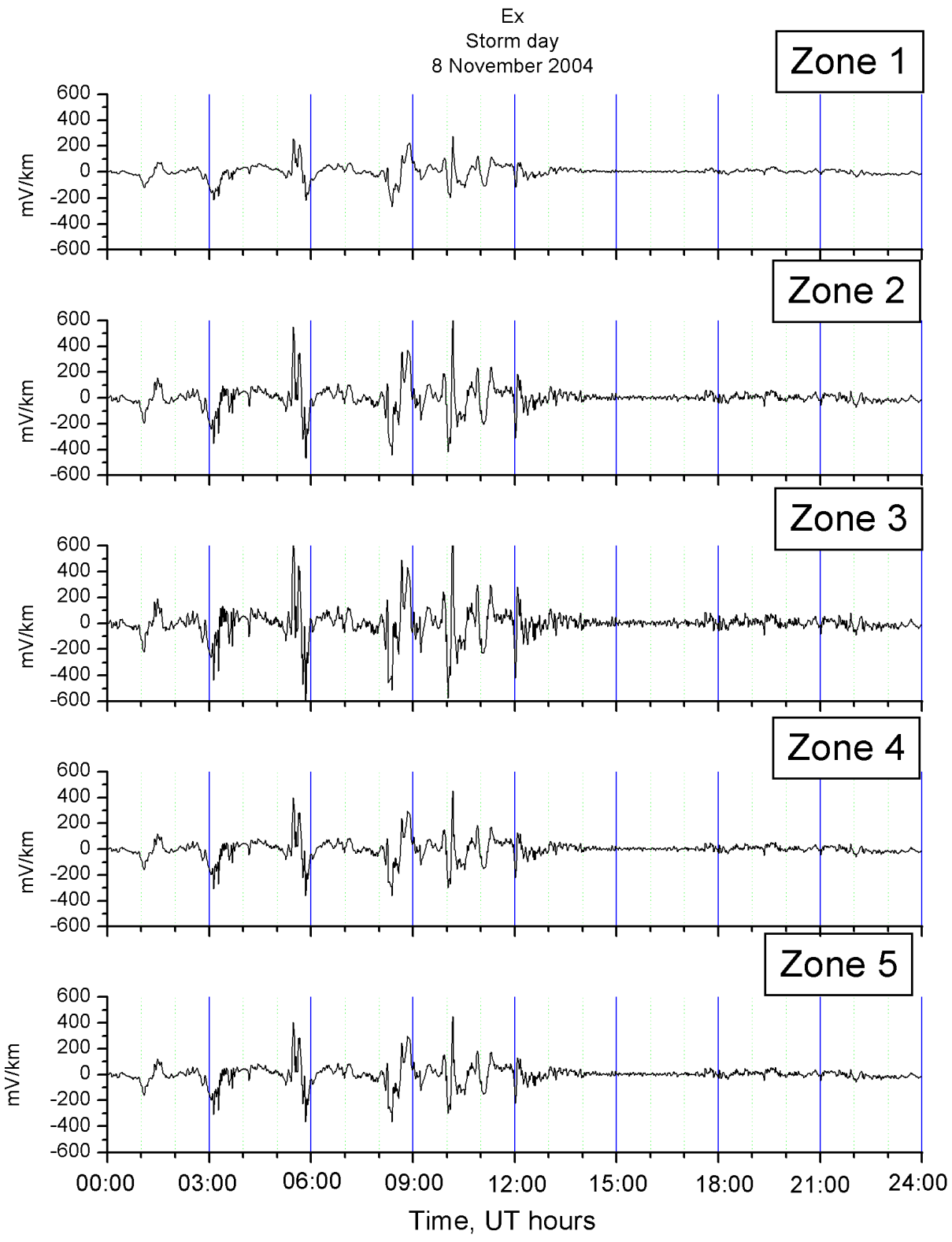

Fig. 4.11 Northward (Ex) electric field variations on a storm day

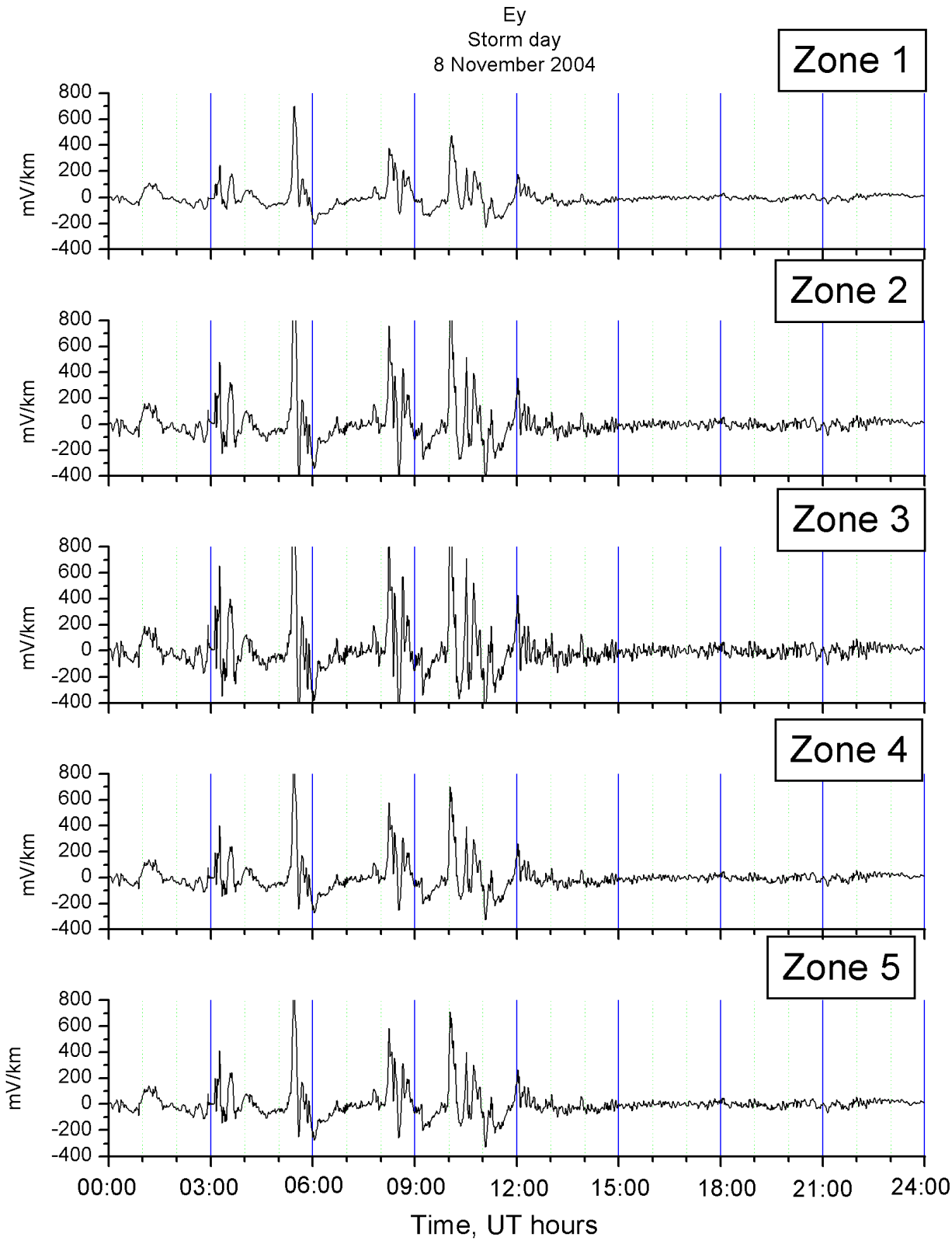

Fig. 4.12 Eastward (Ey) electric field variations on a storm day

4.5. Indices of Telluric Activity

In order to get statistical description of telluric activity, we have to establish some descriptive indices, which will characterize general pattern, rather than minute by minute fluctuations. Similar to the indices of the geomagnetic activity, the indices of telluric activity should have few typical levels of electric field variations in Mackenzie Valley area. Characteristic time for the indices stays one hour, this allows to use hourly range geomagnetic field index to be used in establishing the relations between telluric and geomagnetic activities.

In order to give the most general characteristics of telluric currents and field, we establish two types of the electric field indices. One looks after the extreme maximum electric field values in one hour, by using maximum amplitude of the electric field in one hour (Hourly Maximum Amplitude, HMA).Second index characterizes the distribution of the fluctuations in one hour, which is hourly standard deviation of the electric field (Hourly Standard Deviation, HSD).

The simplest way to model the correspondence of the geomagnetic hourly ranges (HRX) and telluric hourly indices is to apply liner regression analysis and produce linear fit relations between two characteristics. For the geoelectric-to-geomagnetic expressions it is better to use logarithms of their indices, such as

$$\log_{10}(HMA) = A + B \cdot \log_{10}(HRX) \qquad (4.9)$$

or

$$\log_{10}(HSD) = A + B \cdot \log_{10}(HSD) \qquad (4.10)$$

This has been done for the electric field in the general direction of the pipeline for the entire year 2004 and for each conductivity zone and the results are presented in Figs. 4.13.-4.17.

In these plots the red line is the linear fit, coefficients A and B placed in the tables on the same plot. Statistical characteristics of the linear fit, such as correlation coefficient R, standard deviation SD, number of points N and probability that R is zero P, have also been placed in the same tables.

Inter-comparison of these statistical plots gives some initial information about the effects of the different conductivity zones on telluric activity. In Zone 1 both indices of telluric activity are the lowest, in Zone 3 are the highest, in Zone 2 are similarly high as in Zone 3, while telluric indices in Zones 4 and 5 are in the same middle range. Further this preliminary conclusion will be supported by investigations, presented in Part 4.6 and 4.7.

Correlations of the geoelectric-to-geomagnetic linear fits are above 90% and standard deviations are below 0.2 for all five cases. This allows us to use the established linear relationships for the further studies of pipeline parameters for design considerations (Chapters 6/7).

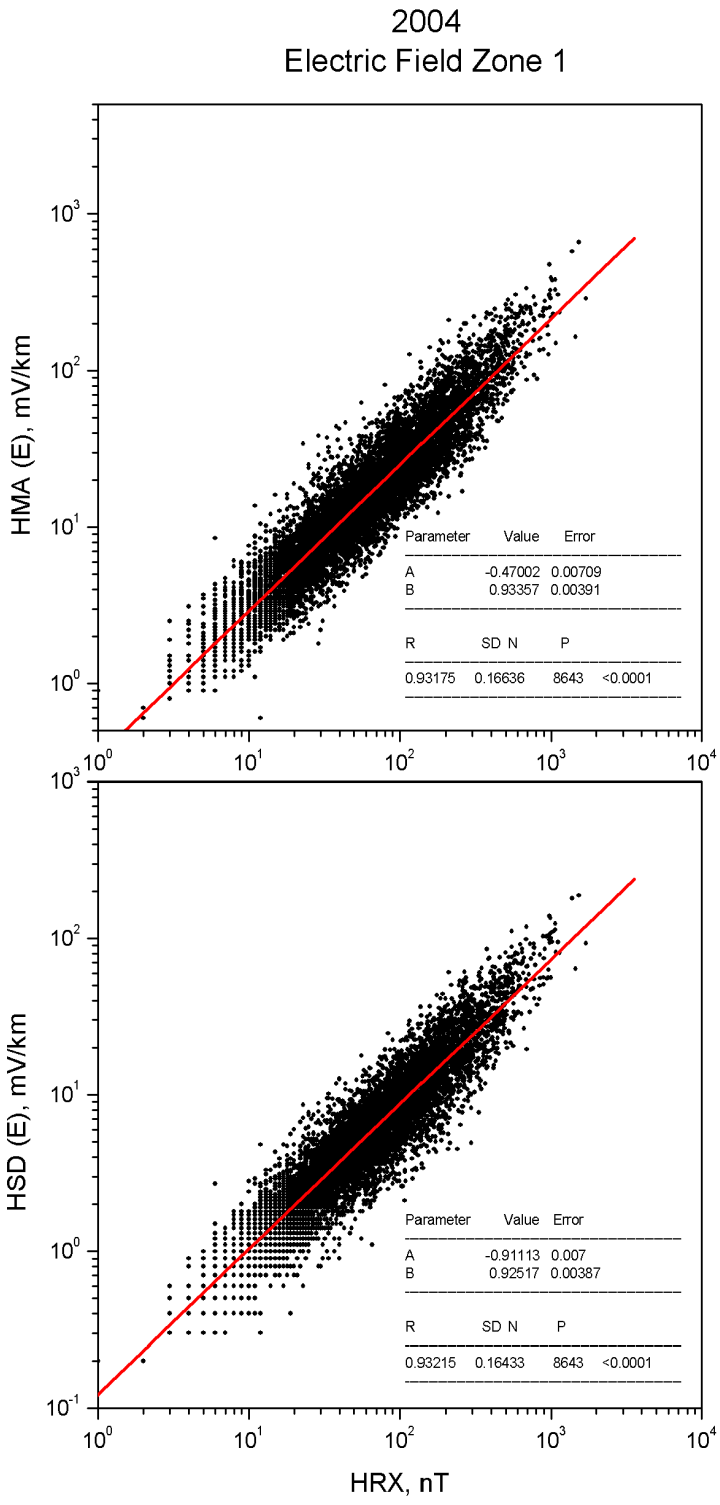

Fig. 4.13 Scatter plot of telluric indices vs. geomagnetic index for Zone 1 with linear fit (red line)

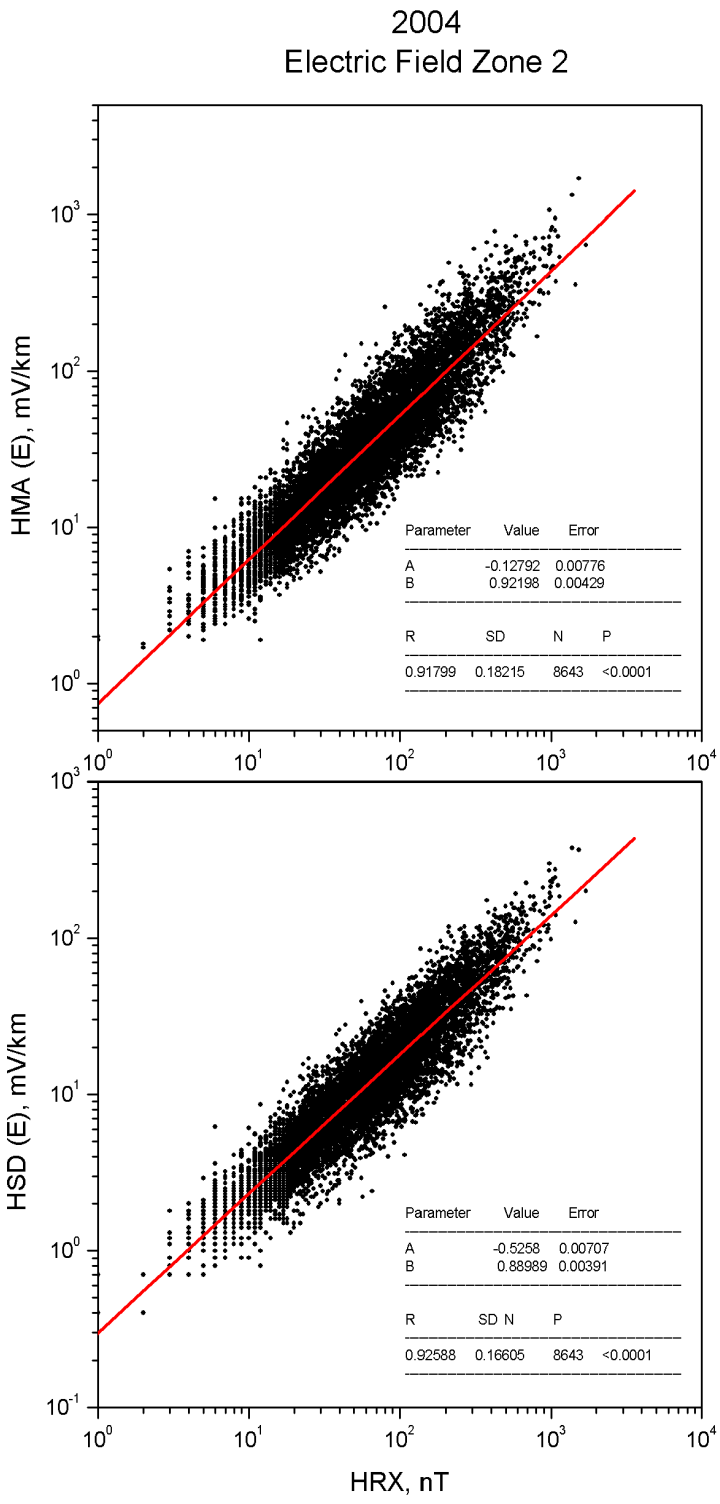

Fig. 4.14 Scatter plot of telluric indices vs. geomagnetic index for Zone 2 with linear fit (red line)

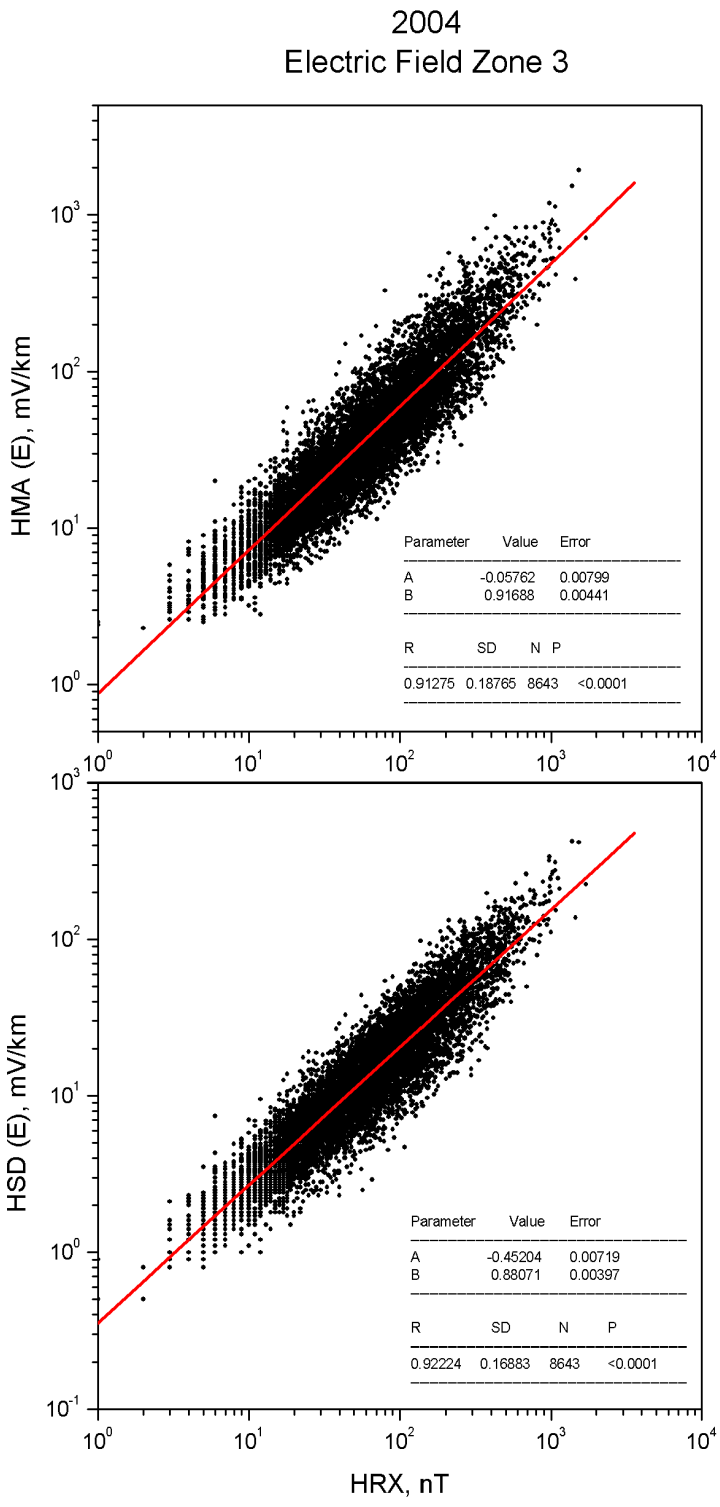

Fig. 4.15 Scatter plot of telluric indices vs. geomagnetic index for Zone 3 with linear fit (red line)

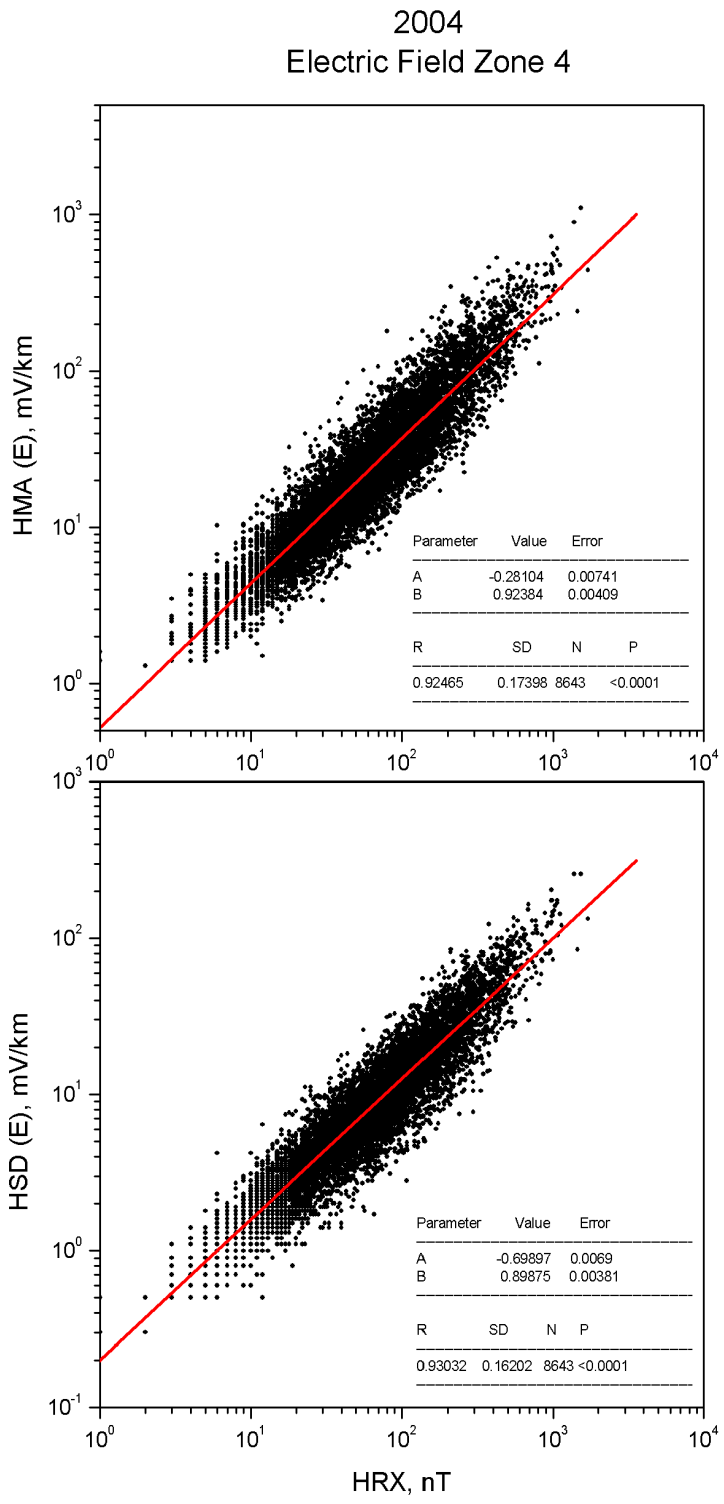

Fig. 4.16 Scatter plot of telluric indices vs. geomagnetic index for Zone 4 with linear fit (red line)

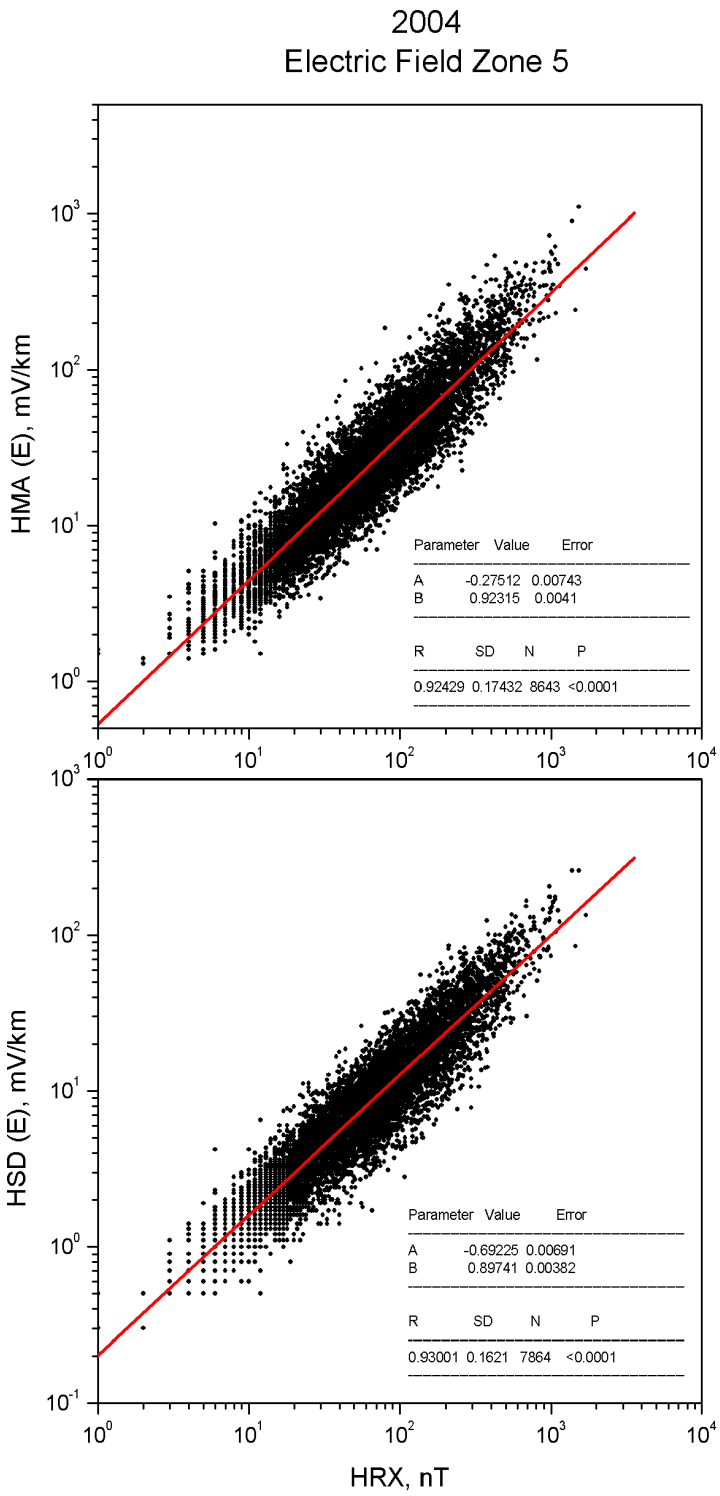

Fig. 4.17 Scatter plot of telluric indices vs. geomagnetic index for Zone 5 with linear fit (red line)

4.5. Scale of Telluric Activity for the Mackenzie Valley area

To describe quantitatively levels of telluric activity, we have to establish quiet level first. Analogous to the same procedure for the geomagnetic activity, we produced statistical plot of HMA telluric index for the normal quiet area, such as low-latitude area of Ottawa, and took 95 % occurrence as a quiet level. This plot is shown in Fig. 4.18. for sample year 2004 and conductivity model as for the southmost Zone 5. Thus, level of 20 mV/km can be named as absolute quiet or normal telluric activity for HMA index.

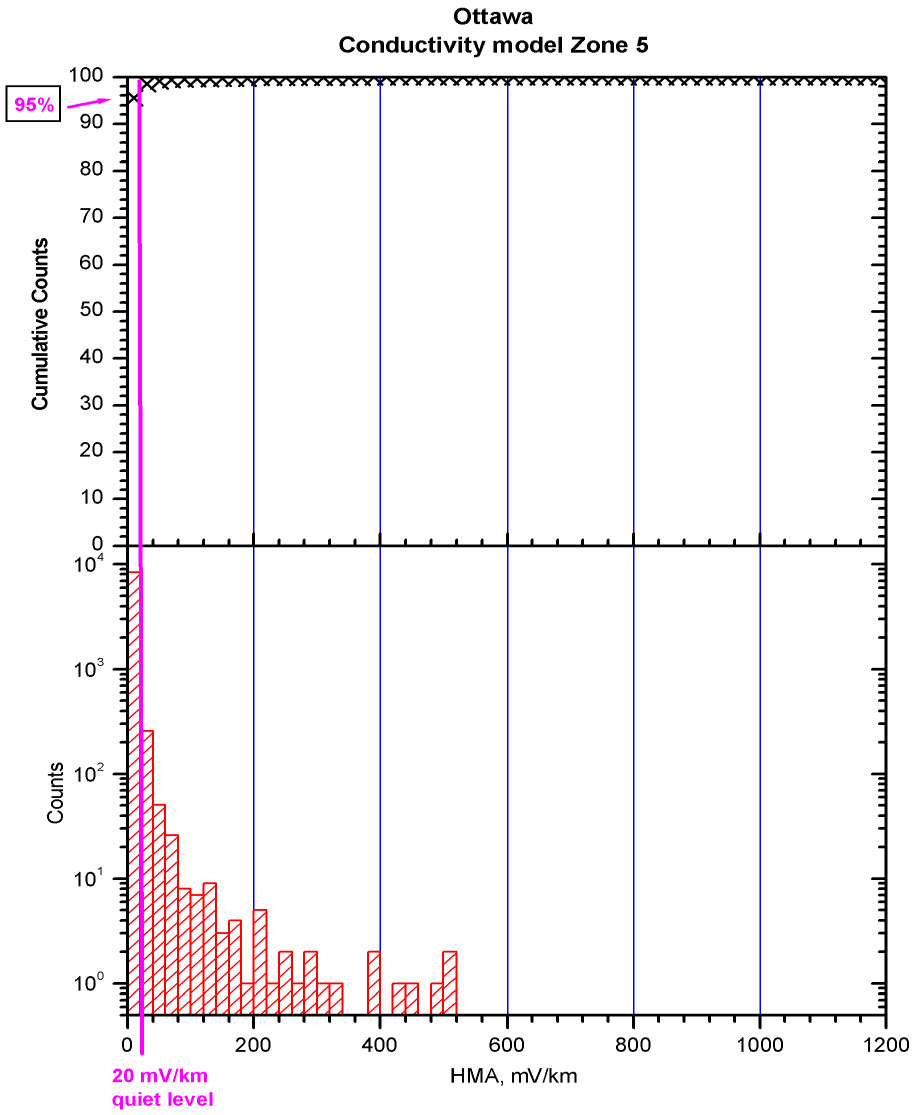

Fig. 4.18 Telluric activity at low latitude with absolute quiet level.

Statistical distribution of the same telluric index for the same year for Mackenzie Valley area, based on the Yellowknife data, is presented in Fig. 4.19. This distribution gives 95% of HMA index at the level of 140 mV/km (normal auroral level), which is 7 times more than normal quiet level.

To cover almost all distribution, the 99.5% level for Mackenzie valley area at HMA= 360mV/km has been defined as the active auroral level, which is 18 times larger than normal quiet level. These simple statistical evaluations give the possibility to infer the following scale of telluric activity of Mackenzie Valley area: Normal quiet level < 20 mV/km, Normal auroral level < 140 mV/km and Active auroral level < 360 mV/km.

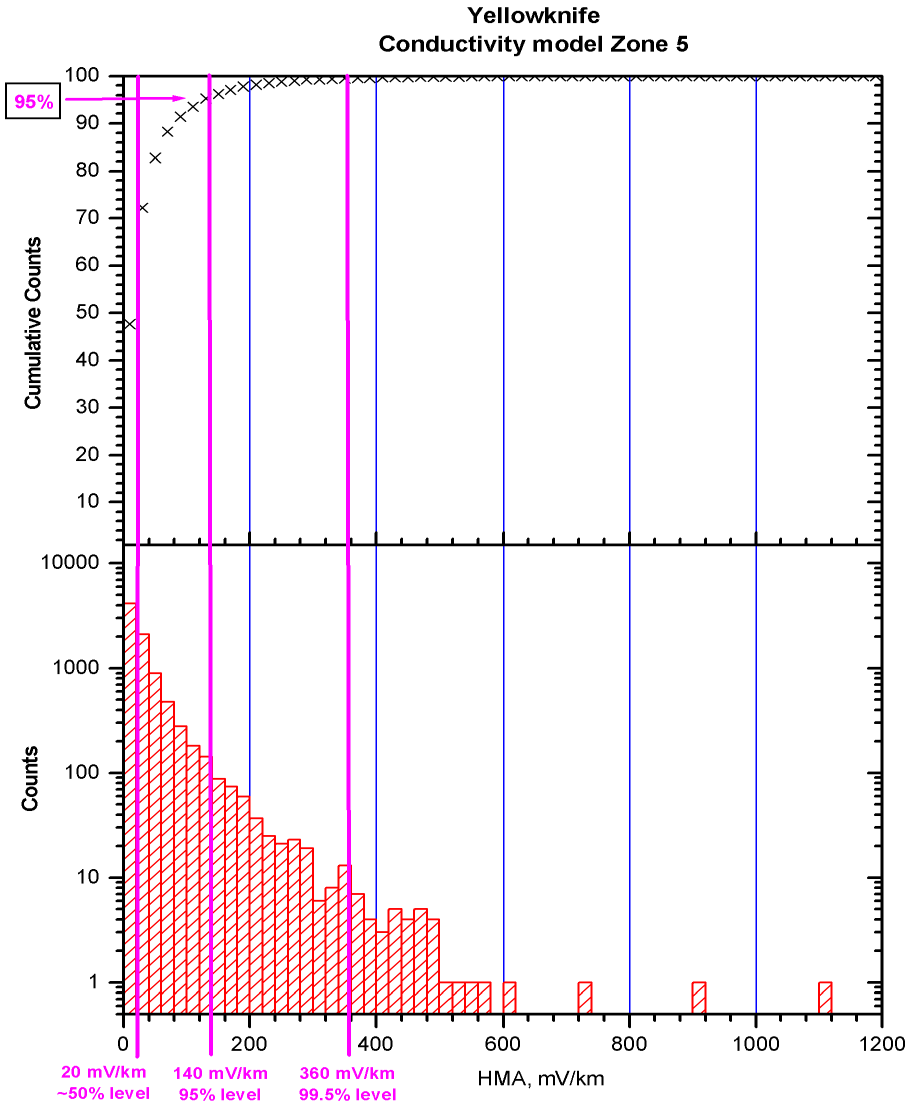

Fig. 4.19 Telluric activity at Mackenzie valley area with major activity levels.

From the statistical evaluations it follows that protection against telluric currents addressed to withstand mostly 20 mV/km, would work only for 50% of the time in the auroral zone but 95% of the time in low latitude areas.. To be able to equally protect pipeline against telluric activity in auroral zone, seven times larger telluric currents should be taken into the consideration.

4.6. Telluric Activity along the Pipeline Route

To provide more details on the influence of the ground conductivity profiles on telluric activity, statistical analysis of telluric activity indices for representative year 2004 has been done separately for each of the five conductivity zones along the pipeline route.

We use the same statistical parameters, as for the geomagnetic activity. Values of telluric activity hourly indices were split into 20mV/km bins and their distribution per year was plotted (in hours and in percentage per year). To characterize statistically the unfavorable (extreme) conditions, we plotted the number of hours/percentage per year with the hourly indices above each of binned levels. These plots for amplitude index (HMA) are presented in figs 4.20a-4.24 a and for standard deviation index (HSD) in figs. 4.20b-4.24 b.

As an example, from fig. 4.20 a , which represents Zone 1 telluric activity, it can be inferred, that there were 3200 hours or 35% of the year with HMA index more than 20mV/km, but only one day with HMA>600mV/km.

The HSD index, which characterizes the width of the distribution of telluric fluctuation in one hour, shows less variability and only 12% of the year is above 20 mV/km with only one day above 140 mV/km.

In order to get the percentage in a year (***P%)*** with hourly telluric indices above any level of interest, we produce the simple second-order fit of plots, which can be described as

$$P\% = A + B \cdot HMA + C \cdot (HMA)^2 \quad (4.11)$$

or for HSD-index

$$P\% = A + B \cdot HSD + C \cdot (HSD)^2 \quad (4.12)$$

Results are presented in Table 4.1 (HMA-index) and Table 4.2 (HSD-index) for the different conductivity zones.

Zone	A	B	C
1	1.84	-1.13×10^{-2}	8.65×10^{-6}
2	1.68	-0.47×10^{-2}	1.51×10^{-6}
3	1.68	-0.40×10^{-2}	1.13×10^{-6}
4	1.76	-0.71×10^{-2}	3.41×10^{-6}
5	1.76	-0.70×10^{-2}	3.37×10^{-6}

Table 4.1 Second order fit coefficients of HMA telluric index for 5 conductivity zones

Zone	A	B	C
1	2.26	-4.00×10^{-2}	1.01×10^{-4}
2	1.98	-1.85×10^{-2}	2.25×10^{-5}
3	1.92	-1.55×10^{-2}	1.60×10^{-5}
4	2.1	-2.69×10^{-2}	4.74×10^{-5}
5	2.1	-2.66×10^{-2}	4.62×10^{-5}

Table 4.2 Second order fit coefficients of HSD telluric index for 5 conductivity zones

All of these approximate formulas produce fit with the very high correlation coefficients (R-square) of 0.99.

Comparisons between different zones give the following results.

For the low activity (less than the size of the bin, i.e. <20 mV/km), formulas gives the percentage in the year, which can be described by the first coefficient, value A. Results from plots and formulas give the highest values of occurrences for Zone 1 and the lowest for Zone 2 and 3 in both indices, with Zones 2 and 3 being very similar. The occurrences values for Zones 4 and 5 are also very similar and are in the middle range between Zone 1 and Zones 2-3.

The rate of decrease (first derivative, B-coefficient) is fastest for the Zone 1 and slowest for zones 2-3 with zones 4-5 having the middle value. The rate of decrease characterize the speed of fall off of the percentage with increasing activity levels.

More detailed version of the comparisons for all 5 zones is presented in Fig. 4.25 for exact values, which supports conclusions made on the basis of the approximate formulas.

For the further analysis, therefore, we can suggest reducing number of telluric activity zones to three, North (former Zone1), Middle (former Zones 2 and 3) and South (former Zones 4 and 5), see the next part.

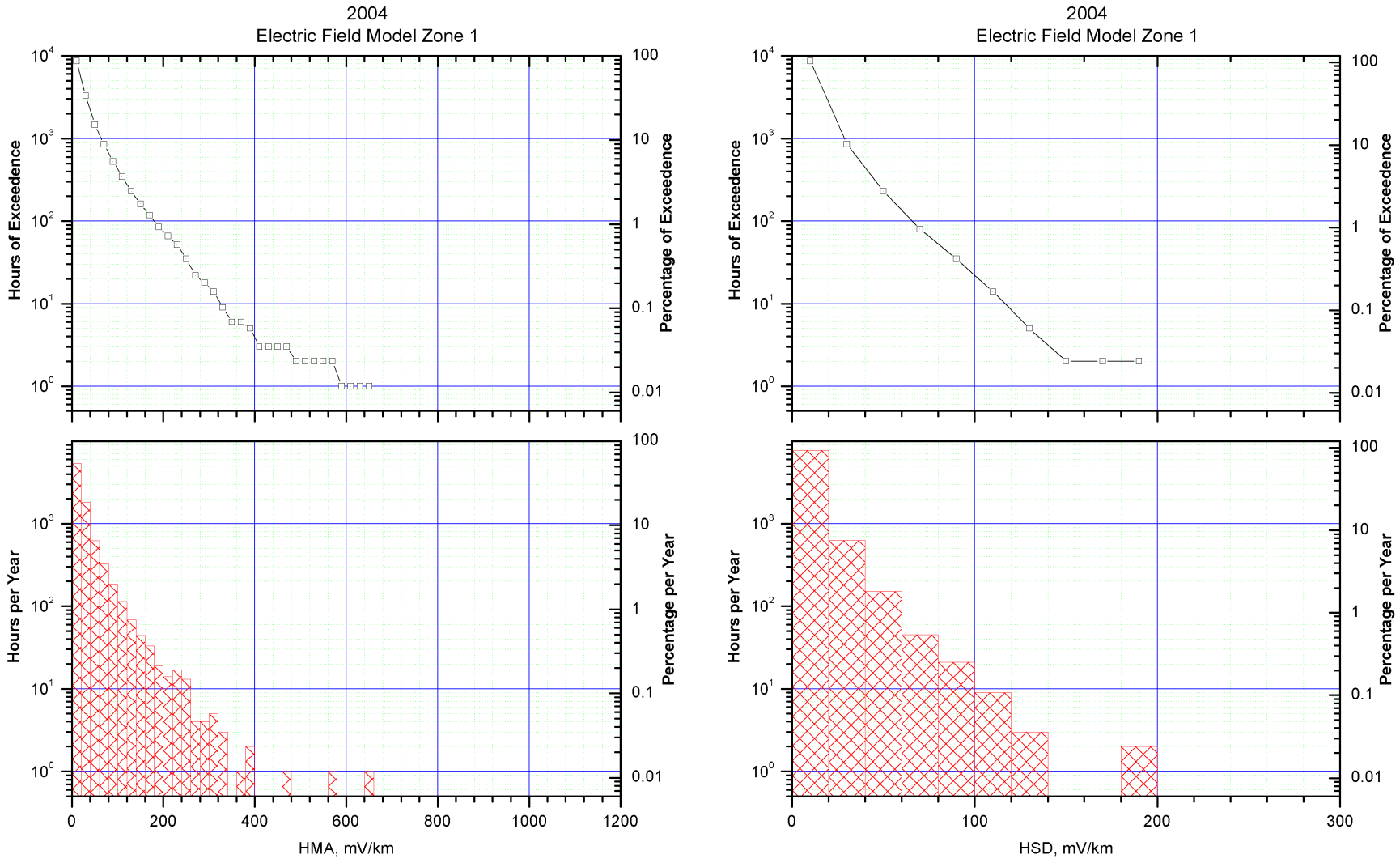

Figure 4.20. Histograms of telluric activity indices distribution (bottom) and exceedence of activity levels (top) in 2004 for Zone 1
a) hourly maximum amplitude index, b) hourly standard deviation index

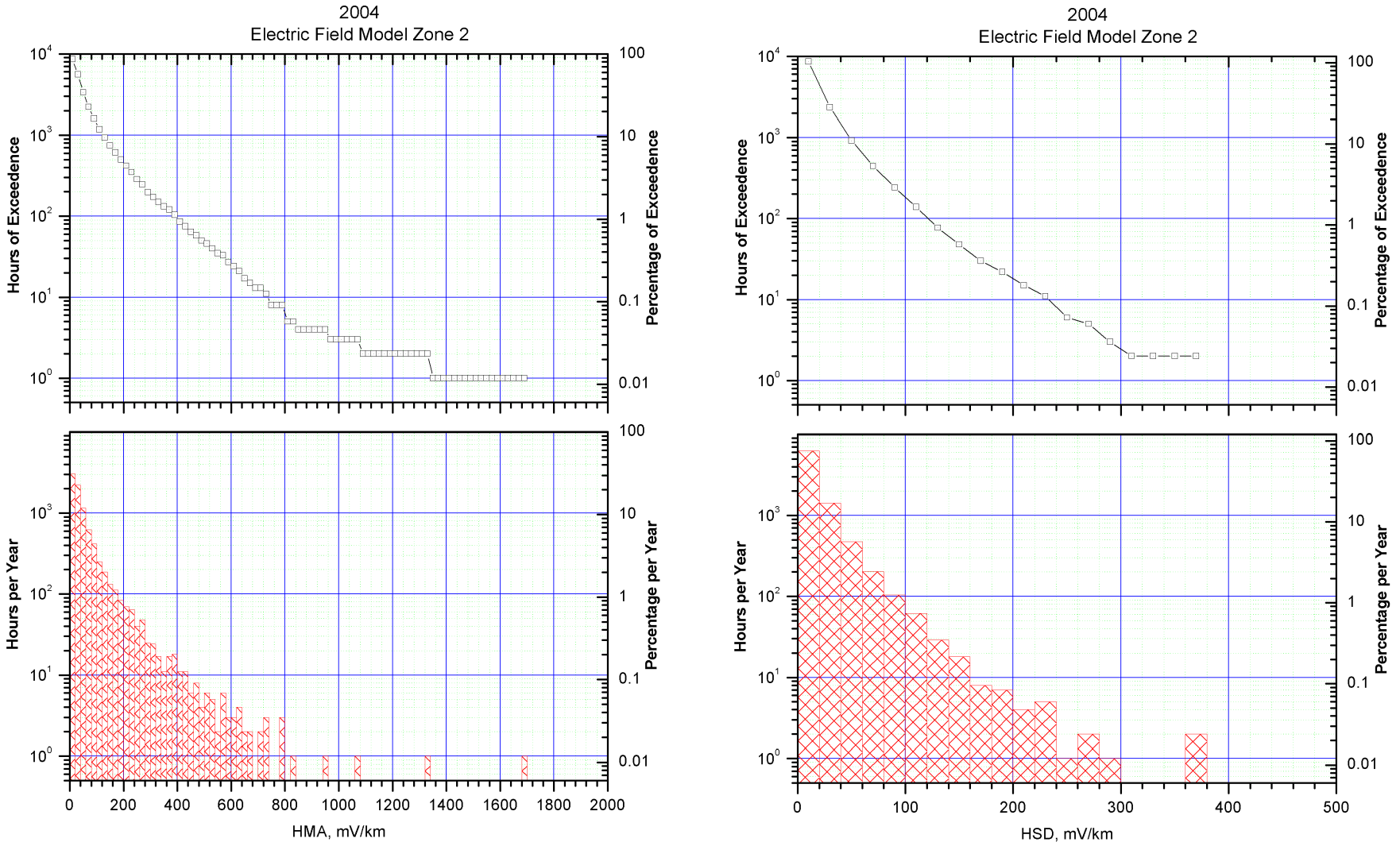

Figure 4.21. Histograms of telluric activity indices distribution (bottom) and exceedence of activity levels (top) in 2004 for Zone 2
a) hourly maximum amplitude index, b) hourly standard deviation index

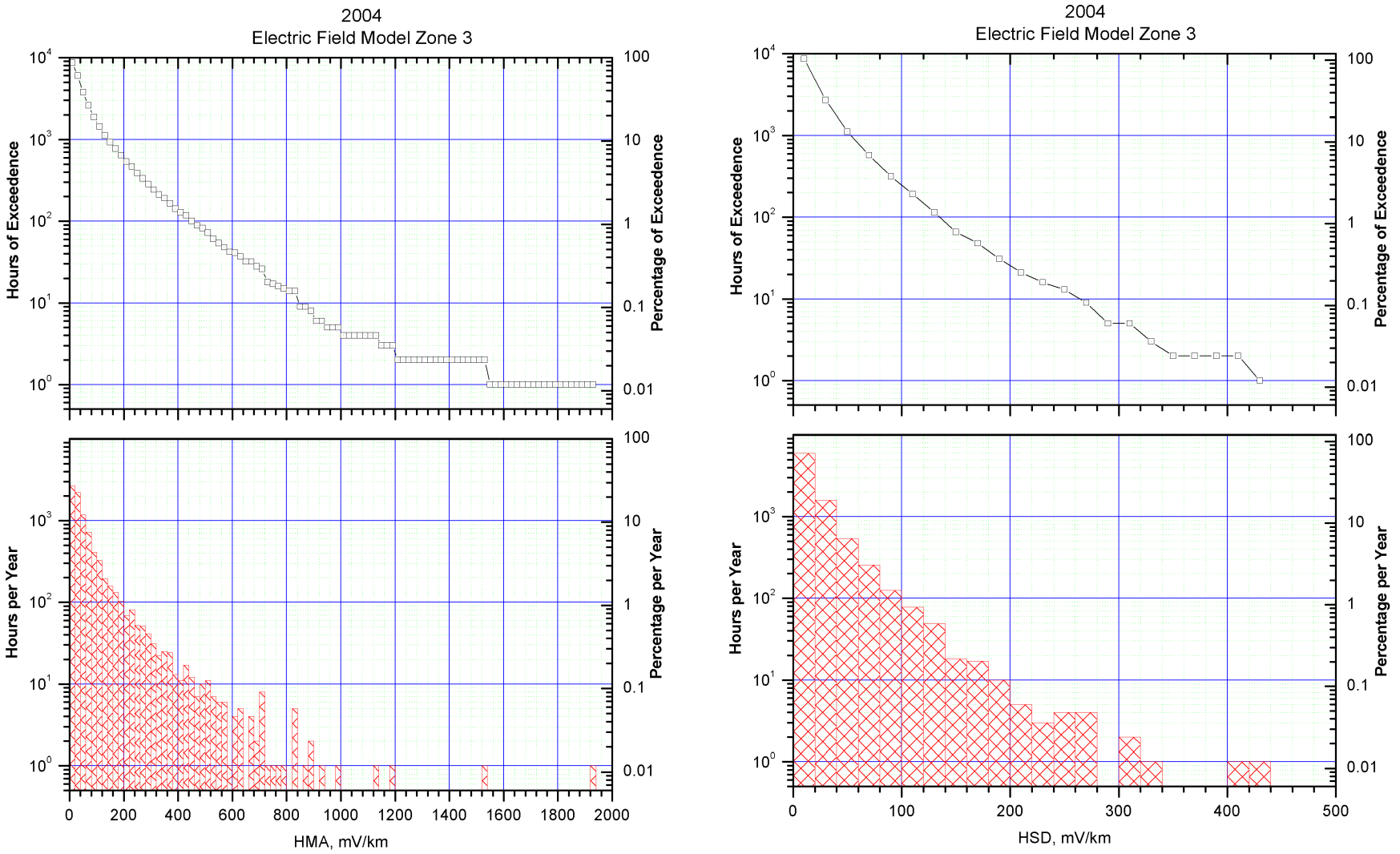

Figure 4.22. Histograms of telluric activity indices distribution (bottom) and exceedence of activity levels (top) in 2004 for Zone 3
a) hourly maximum amplitude index, b) hourly standard deviation index

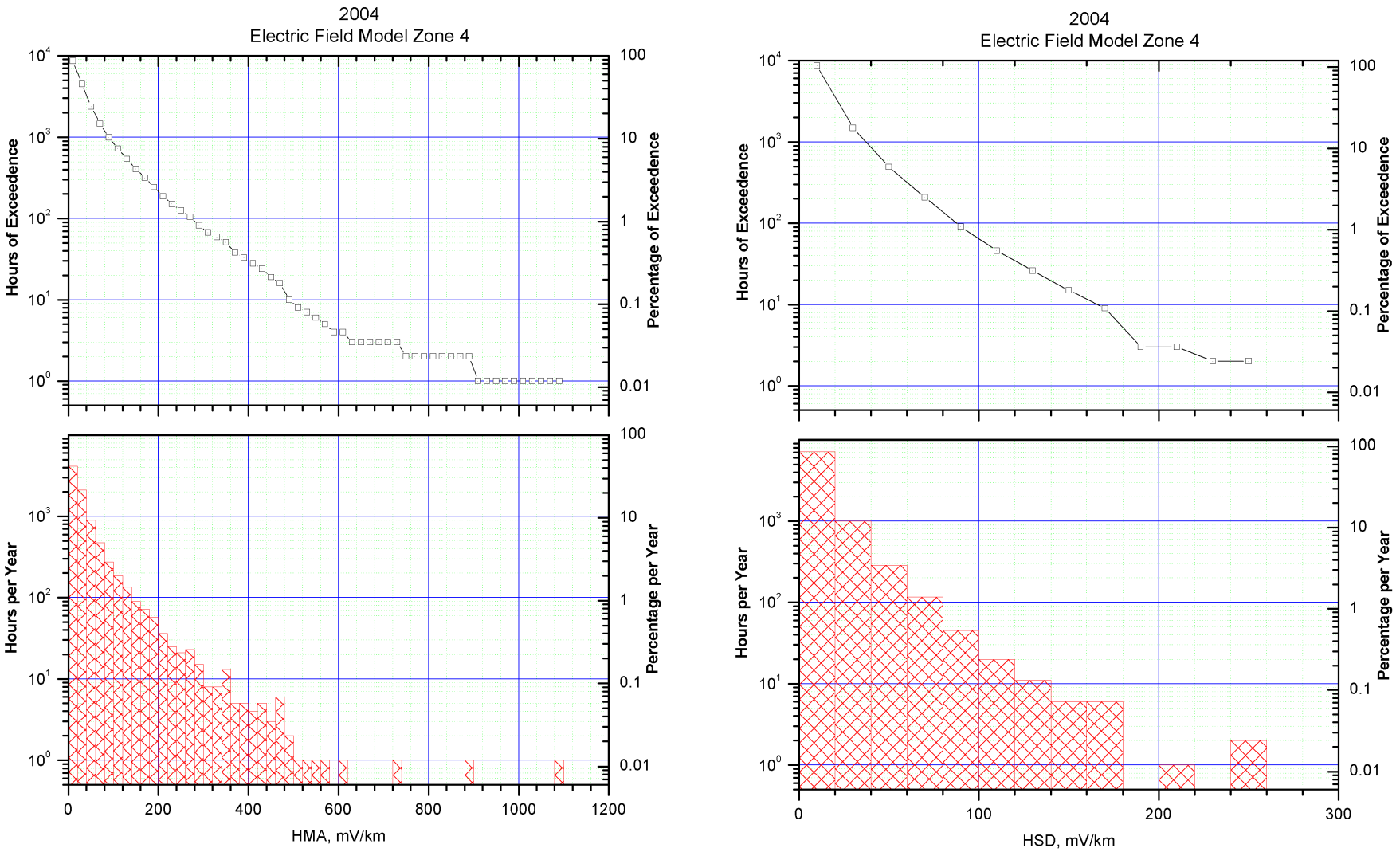

Figure 4.23. Histograms of telluric activity indices distribution (bottom) and exceedence of activity levels (top) in 2004 for Zone 4
a) hourly maximum amplitude index, b) hourly standard deviation index

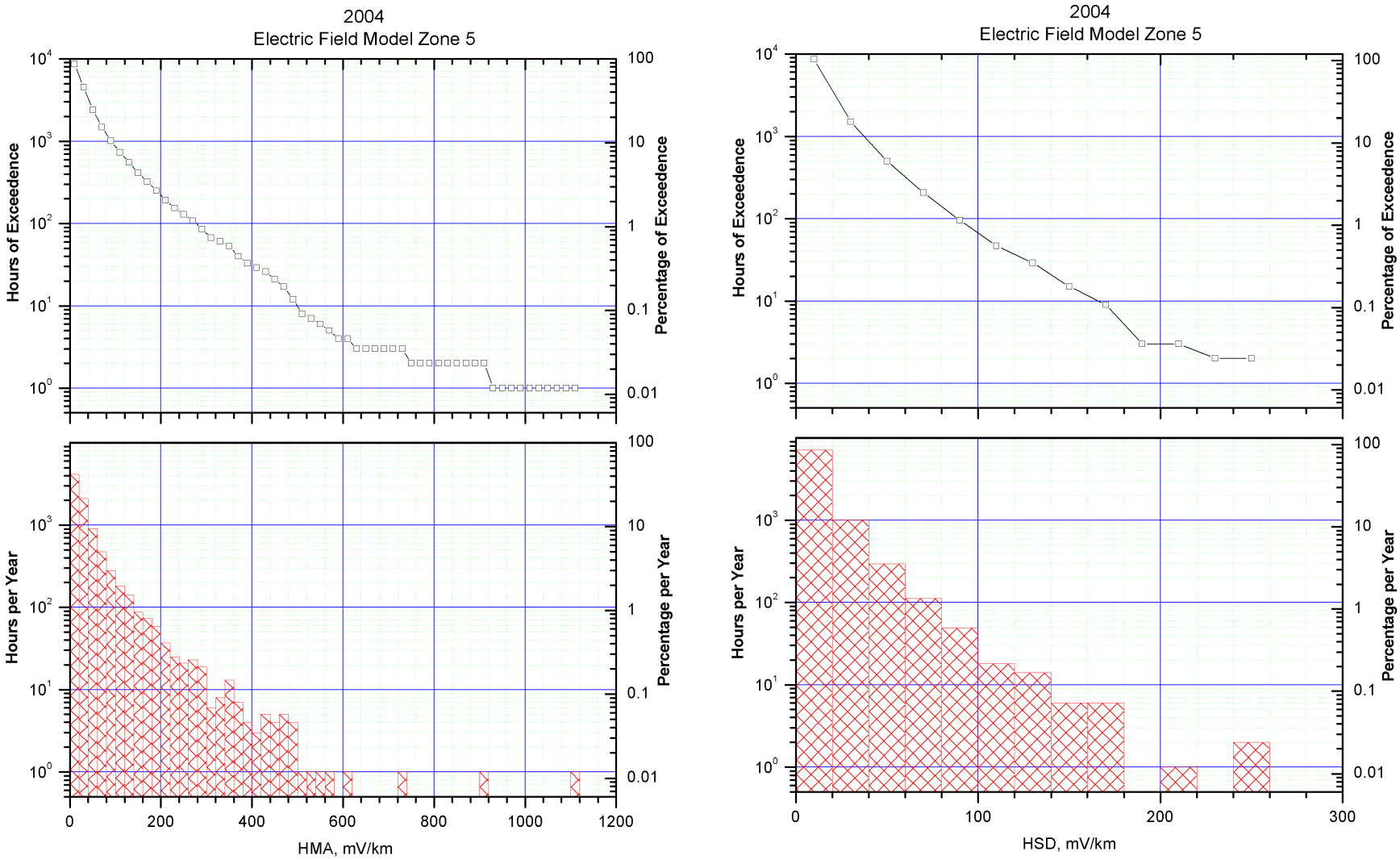

Figure 4.24. Histograms of telluric activity indices distribution (bottom) and exceedence of activity levels (top) in 2004 for Zone 5
a) hourly maximum amplitude index, b) hourly standard deviation index

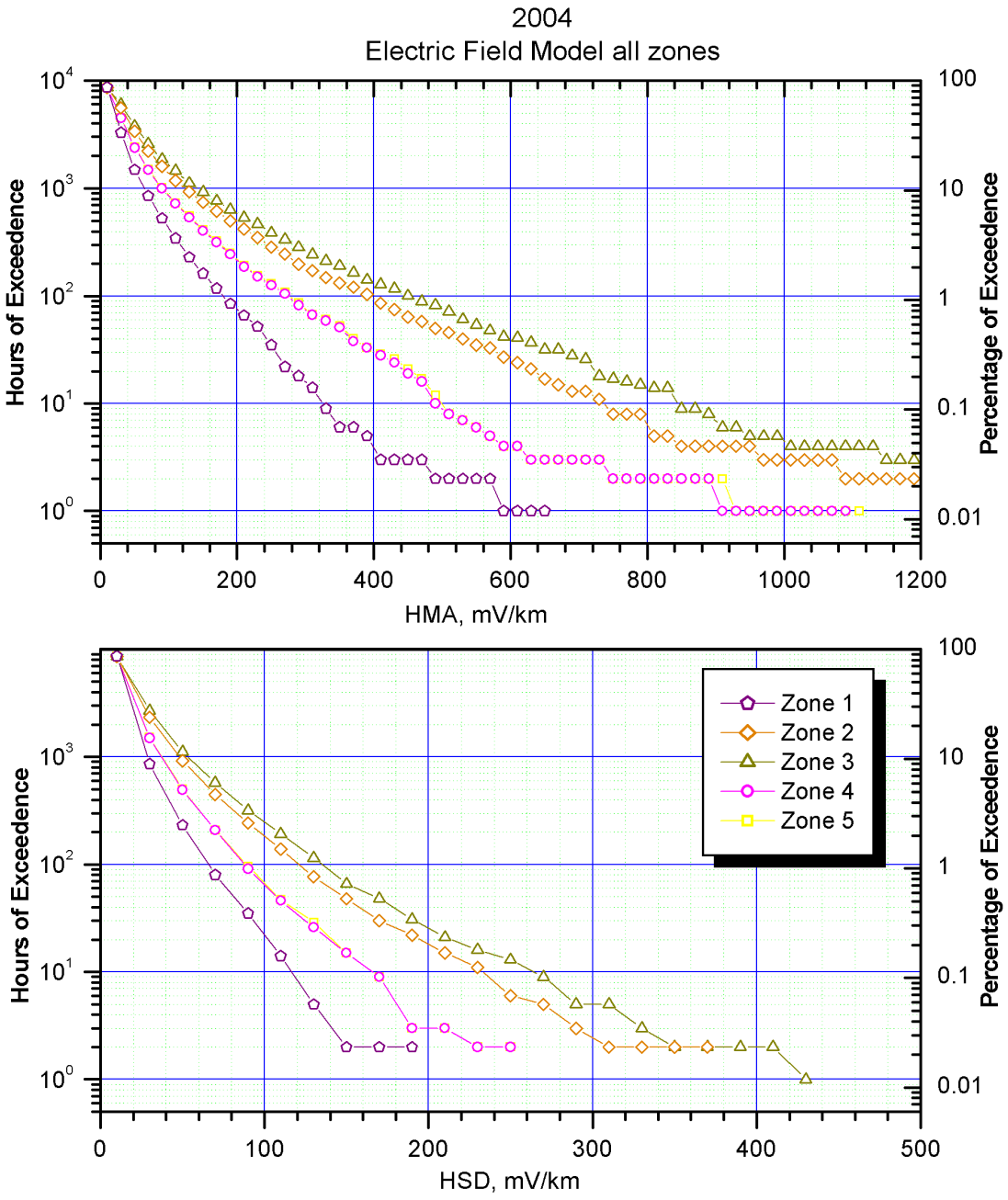

Fig. 4.25. Statistical characteristics of telluric activity indices HMA (top) and HSD (bottom) for all zones in Mackenzie Valley

4.7. Long-Term (solar cycle) Variations of Telluric Activity

Previous analysis of telluric activity in the Mackenzie Valley area dealt with the year 2004 as a representative year in terms of typical geomagnetic activity in the area. The long-term study of the geomagnetic activity, based on the data of Yellowknife observatory (Chapter 2), allows us to extend telluric analysis to include the most active year, which was 2003, close to the last solar maximum, as well as to the year of the lowest activity, 1996, during solar minimum.

Statistical study has been done to produce distribution plots for the HMA and HSD indices, as for the year 2004, for three areas of telluric activity along the pipeline route. Results are presented in Figs. 4.27-4.28, with HMA index plotted in Figs 4.27a, 4.28a and HSD index plotted in Figs. 4.27b, 4.28b.

The approximate formulas were derived to present the percentage of hours with activity indices above the certain level by the second order polynomial function (as in the previous part).
Results for the HMA and HSD indices for 3 areas are given in Tables 4.3 and 4.4 for year 2003 and Tables 4.5 and 4.6 for year 1996.

Area	A	B	C
North	1.87	-0.97×10^{-2}	5.88×10^{-6}
Middle	1.77	-0.37×10^{-2}	8.56×10^{-7}
South	1.81	-0.61×10^{-2}	2.36×10^{-6}

Table 4.3 Second order fit coefficients of HMA telluric index of solar maximum year for 3 areas

Area	A	B	C
North	2.27	-3.42×10^{-2}	6.87×10^{-5}
Middle	2.04	-1.43×10^{-2}	1.26×10^{-5}
South	2.16	-2.36×10^{-2}	3.34×10^{-5}

Table 4.4 Second order fit coefficients of HSD telluric index of solar maximum year for 3 areas

Area	A	B	C
North	1.89	-1.36×10^{-2}	1.15×10^{-5}
Middle	1.69	-0.46×10^{-2}	1.28×10^{-6}
South	1.77	-0.80×10^{-2}	4.06×10^{-6}

Table 4.5 Second order fit coefficients of HMA telluric index of solar minimum year for 3 areas

Area	A	B	C
North	2.47	-5.52×10^{-2}	2.03×10^{-4}
Middle	1.98	-1.81×10^{-2}	1.39×10^{-5}
South	2.15	-3.09×10^{-2}	4.60×10^{-5}

Table 4.6 Second order fit coefficients of HSD telluric index of solar minimum year for 3 areas

All these formulas give fit with correlation (R-square) of 98% and higher and standard deviations of lower than 0.15. They can be used for the telluric impact assessment for evaluations of the minimum and maximum percentage of occurrence for any level of telluric activity indices.

References

Weaver, J.T., *Mathematical methods for geo-electromagnetic induction*, Research Studies Press LTD, Taunton,Somerset, England, 1994.

Press, W.H., S.A.Teukolsky, W.T.Vettering, B.P.Flannery, *Numerical Recipes in FORTRAN: The Art of Scientific Computing, second edition*, Cambridge University Press, 1992.

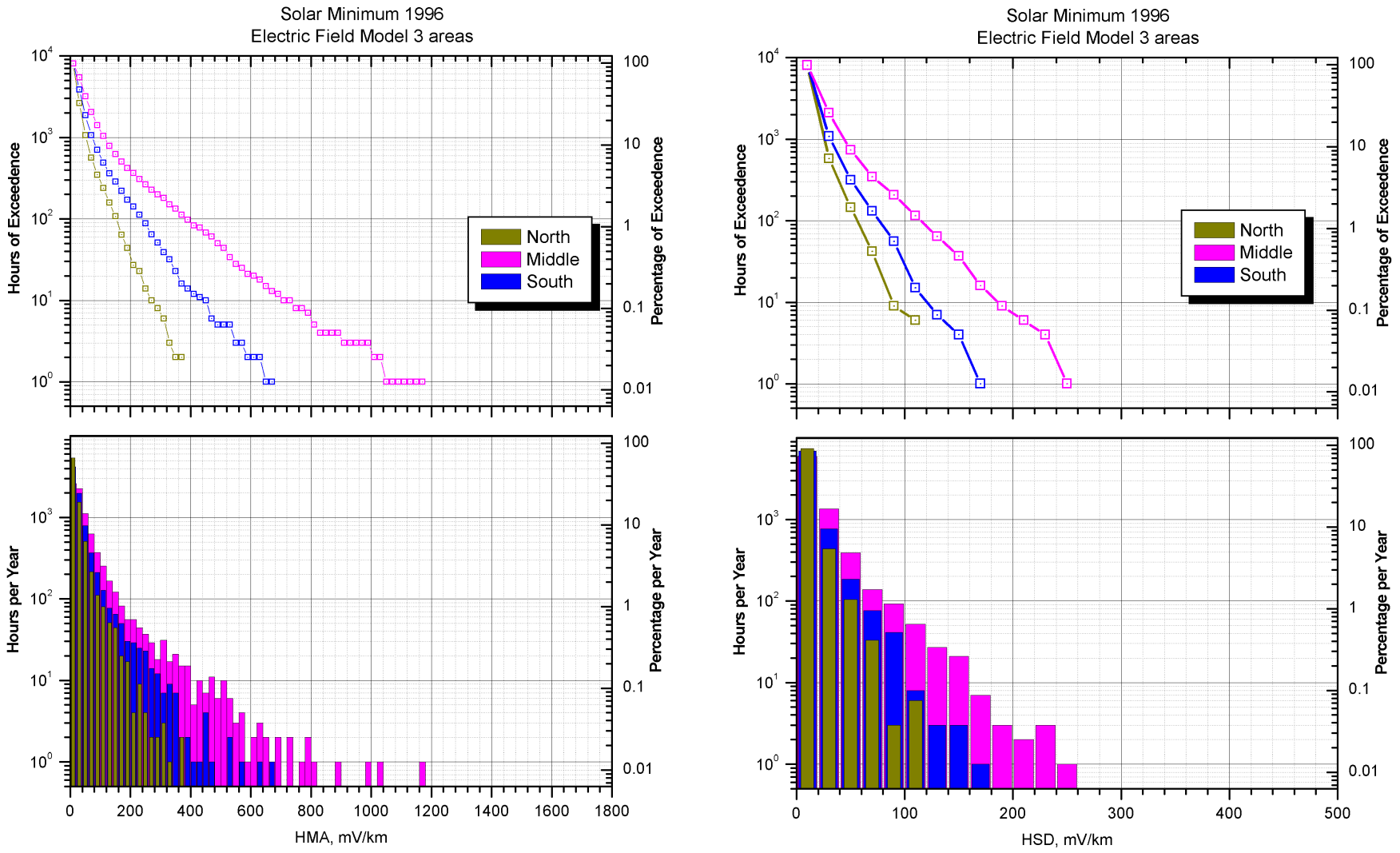

Figure 4.26. Histograms of telluric activity indices distribution (bottom) and exceedence of activity levels (top) in 1996 for three geographic areas of telluric activity: a) hourly maximum amplitude index, b) hourly standard deviation index

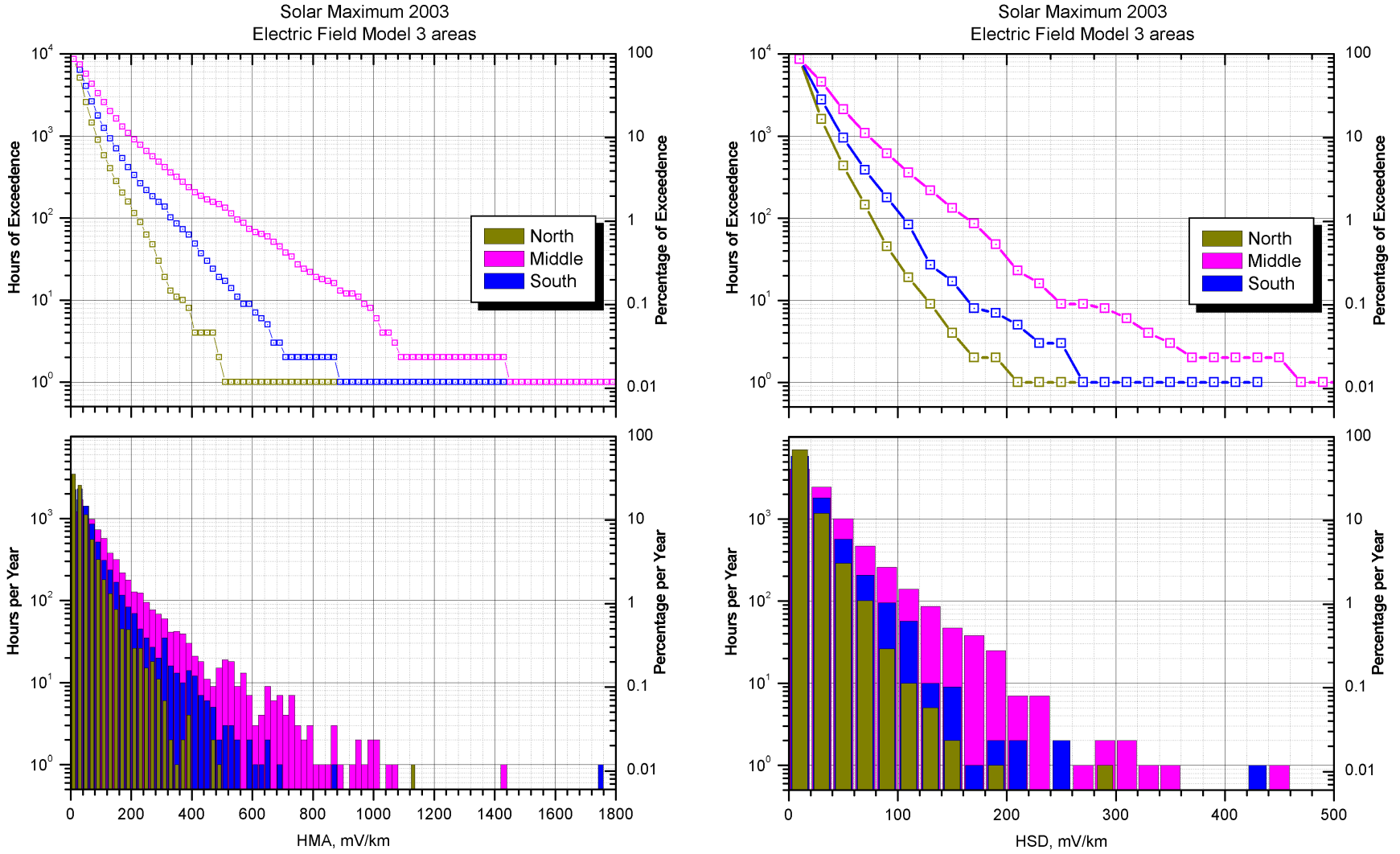

Figure 4.27. Histograms of telluric activity indices distribution (bottom) and exceedence of activity levels (top) in 2003 for three geographic areas of telluric activity: a) hourly maximum amplitude index, b) hourly standard deviation index